

AD-A152 582

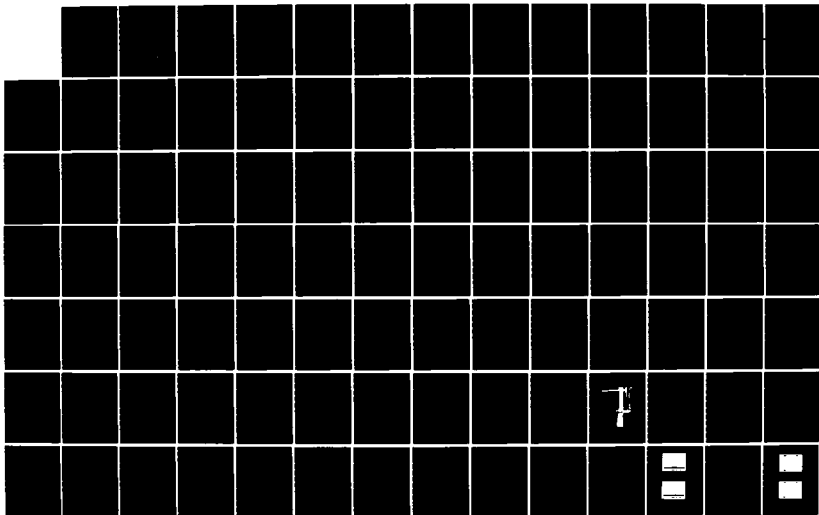
ADAPTIVE NULLING AT HF USING A COMPACT ARRAY OF ACTIVE  
PARASITIC ANTENNAS(U) ZEGAR-ABRAMS INC GLENSIDE PA  
T E JONES ET AL. MAR 85 R85-NRL-1 N00173-78-C-0265

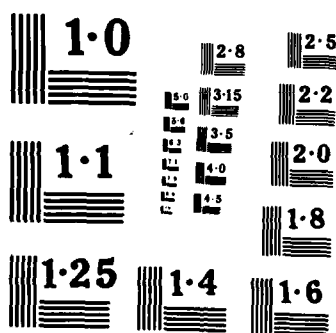
1/2

UNCLASSIFIED

F/G 9/5

NL





27 March 1985

R85-NRL-1

ZA

2

AD-A152 582

ADAPTIVE NULLING AT HF  
USING A  
COMPACT ARRAY OF ACTIVE PARASITIC ANTENNAS

Final Report

Thomas E. Jones

Andrew E. Zeger

Zeger-Abrams Incorporated

29 E. Glenside Ave.

Glenside, PA 19038-4669

DTIC FILE COPY

Prepared For  
U.S. Naval Research Laboratory  
Washington, DC 20375  
Contract N00173-78-C-0265  
(CDRL Sequence No. A003)

DTIC  
ELECTE  
APR 18 1985  
S  
A E

UNCLASSIFIED

REPORT DOCUMENTATION PAGE		READ INSTRUCTIONS BEFORE COMPLETING FORM
1. REPORT NUMBER	2. GOVT ACCESSION NO.	3. RECIPIENT'S CATALOG NUMBER
	AD-A152582	
4. TITLE (and Subtitle)		5. TYPE OF REPORT & PERIOD COVERED
ADAPTIVE NULLING AT HF USING A COMPACT ARRAY OF ACTIVE PARASITIC ANTENNAS		Final Technical Report SEPT 1978 to MARCH 1984
		6. PERFORMING ORG. REPORT NUMBER
		R85-NRL-1
7. AUTHOR(s)		8. CONTRACT OR GRANT NUMBER(s)
Thomas E. Jones Andrew E. Zeger		N00173-78-C-0265
9. PERFORMING ORGANIZATION NAME AND ADDRESS		10. PROGRAM ELEMENT, PROJECT, TASK AREA & WORK UNIT NUMBERS
Zeger-Abrams Incorporated 29 East Glenside Avenue Glenside, PA 19038		
11. CONTROLLING OFFICE NAME AND ADDRESS		12. REPORT DATE
U.S. Naval Research Laboratory 4555 Overlook Ave., S.W. Washington, DC 20375		March 1985
		13. NUMBER OF PAGES
		159
14. MONITORING AGENCY NAME & ADDRESS (if different from Controlling Office)		15. SECURITY CLASS. (of this report)
Same		UNCLASSIFIED
		15a. DECLASSIFICATION/DOWNGRADING SCHEDULE
		N/A
16. DISTRIBUTION STATEMENT (of this Report)		
<div style="border: 1px solid black; padding: 5px; width: fit-content;">             This report is available for distribution           </div>		
17. DISTRIBUTION STATEMENT (of the abstract entered in Block 20, if different from Report)		
18. SUPPLEMENTARY NOTES		
19. KEY WORDS (Continue on reverse side if necessary and identify by block number)		
Active Parasitic Antennas ) Adaptive Array ) Complex Gradients , ECCM	Gradient Control HF Interference Cancellation Nonlinear Control	- Nulling Array Parasitic Array Scattering Parameters Spatial Interference Cancellation
20. ABSTRACT (Continue on reverse side if necessary and identify by block number)		
<p>The parasitic array is a promising method of building an adaptive array in a tiny aperture. This is particularly attractive for HF. Both theory and experimental results are presented. The theory is established with respect to two models of a compact array, an impedance model and a transmission line model. The relationship between the models is derived. The models are then used to explore the issues of null forming and adaptive control, with an emphasis on active terminations. Zeger-Abrams designed an electronically</p>		

DD FORM 1473

EDITION OF 1 NOV 65 IS OBSOLETE

UNCLASSIFIED

SECURITY CLASSIFICATION OF THIS PAGE (When Data Entered)

UNCLASSIFIED

SECURITY CLASSIFICATION OF THIS PAGE(When Data Entered)

20. variable active termination. Experimental results were obtained from an array both with passive and active terminations. Empirical results with active complex-valued terminations demonstrated the feasibility of simultaneously nulling multiple HF jammers with an adaptively controlled compact array having parasitic auxilliary elements and an unweighted main antenna. Finally, an algorithm to adaptively control the active terminations is derived.

UNCLASSIFIED

SECURITY CLASSIFICATION OF THIS PAGE(When Data Entered)

# Abstract

The parasitic array is a promising method of building an adaptive array in a tiny aperture. This is particularly attractive for HF. Both theory and experimental results are presented. The theory is established with respect to two models of a compact array, an impedance model and a transmission line model. The relationship between the models is derived. The models are then used to explore the issues of null forming and adaptive control, with an emphasis on active terminations. Zeger-Abrams designed an electronically variable active termination. Experimental results were obtained from an array both with passive and active terminations. Empirical results with active complex-valued terminations demonstrated the feasibility of simultaneously nulling multiple HF jammers with an adaptively controlled compact array having parasitic auxiliary elements and an unweighted main antenna. Finally, an algorithm to adaptively control the active terminations is derived.

ORIGINATOR - SUPPLIED KEY WORDS INCLUDE:

Accession For	
NTIS GRA&I	<input checked="" type="checkbox"/>
DTIC TAB	<input type="checkbox"/>
Unannounced	<input type="checkbox"/>
Justification	
By	
Distribution/	
Availability Codes	
Dist	Avail and/or Special
A-1	



## TABLE OF CONTENTS

<u>Section</u>	<u>Page</u>
1.0 INTRODUCTION AND BACKGROUND	1-1
1.1 Introduction	1-1
1.2 Background	1-1
1.3 Scope	1-4
1.4 Glossary of Notation	1-4
2.0 CHARACTERIZATION OF PARASITIC ANTENNA ARRAYS	2-1
2.1 Transmission Line Model	2-1
2.2 Impedance Model	2-8
2.3 Properties of Compact Parasitic Arrays	2-10
3.0 RELATIONSHIPS BETWEEN TRANSMISSION LINE AND IMPEDANCE MODELS OF A PARASITIC ARRAY	3-1
3.1 Single Antenna Transmitting	3-1
3.2 Single Antenna Receiving	3-7
3.3 Multiple Element Array Transmitting	3-11
3.4 Multiple Element Array Receiving	3-17
4.0 NULL FORMING CAPABILITY OF AN ACTIVELY TERMINATED PARASITIC ARRAY	4-1
4.1 Forming N Nulls on N Simultaneous Signals	4-1
4.2 Stability of a Parasitic Array With Active Complex Terminations	4-6
5.0 ADAPTIVE CONTROL OF PARASITIC ARRAY NULLS	5-1
5.1 Least Mean Square Control of Active, Complex Terminations	5-1
5.2 Gradient Control	5-2
5.3 Dither Algorithms	5-11
5.4 Search Algorithms	5-12
6.0 EXPERIMENTAL RESULTS WITH A PASSIVE REACTIVELY TERMINATED PARASITIC ARRAY	6-1
6.1 Experimental Parasitic Array	6-1
6.2 Experimental Measurements	6-5

## TABLE OF CONTENTS (Continued)

<u>Section</u>	<u>Page</u>
7.0 DEVELOPMENT BY ZA OF ACTIVE CONTROLLABLE COMPLEX TERMINATIONS	7-1
7.1 Design	7-1
7.2 Laboratory Experimental Data	7-7
7.3 Experimental Results of Parasitic Array with Active Complex Terminations	7-15
8.0 DEVELOPMENT OF A CONTROL ALGORITHM FOR ACTIVE TERMINATIONS	8-1
8.1 Oscillation Detector (Unstable States)	8-1
8.2 Modified Univariate Search Algorithm	8-3
9.0 DEVELOPMENT OF AN IMPROVED PERFORMANCE ASSESSMENT INDICATOR (PAI)	9-1
10.0 SUMMARY AND CONCLUSIONS	10-1
REFERENCES	R-1
APPENDIX A: MATRIX IDENTITIES AND DIFFERENTIATION FORMULAE	A-1
APPENDIX B: RELATING S-PARAMETERS TO Z-PARAMETERS	B-1
APPENDIX C: SCATTERING PARAMETERS IN TERMINATED TRANSMISSION LINES	C-1
C.1 Single Transmission Line	C-1
C.2 Multiple Transmission Lines	C-5
APPENDIX D: EQUIVALENCE OF EQUATIONS (3.16) AND (3.21)	D-1
APPENDIX E: SUFFICIENCY OF STABILITY CONDITION WITH NARROWBAND FILTER IN REFLECTIVITIES	E-1
APPENDIX F: A STABILITY ANALYSIS EXAMPLE	F-1



TABLE OF CONTENTS (Continued)

<u>Section</u>	<u>Page</u>
APPENDIX G: GRADIENTS OF PSUEDO-ANALYTIC FUNCTIONS AND APPLICATIONS TO COMPLEX GRADIENT CONTROL	G-1
G.1 Theory of Psuedo-Analytic Functions	G-1
G.2 Complex Gradient Control	G-5
G.3 Gradient Control of Active Complex Parasitic Terminations	G-7
APPENDIX H: DERIVATION OF GRADIENT CONTROL WITH PILOT	H-1

## List of Figures

<u>Figure Number</u>	<u>Title</u>	<u>Page Number</u>
1	Adaptive Beamformers	1-3
2	Definition of Transmission Line Model Parameters	2-3
3	Measurement of Transmission Line Model Parameters	2-4
4	Illustration of Fundamental Equation of the Transmission Line Model	2-6
5	Harrington's Impedance Model of a Parasitic Array	2-9
6	Impedance Model of Single Element Array Transmitting	3-2
7	Transmission Line Model of Single Element Array Transmitting	3-6
8	Impedance Model of Single Element Array Receiving	3-8
9	Impedance Model of Multiple Element Array Transmitting	3-12
10	Voltage Traveling Wave Relationships for Multiple Transmission Lines	3-13
11	Transmission Line Model of Multiple Element Array Transmitting	3-16
12	Impedance Model of Multiple Element Array Receiving	3-19
13	Scenario Which Removes a Degree of Freedom in Conventional Array	4-4
14	Single Element Array Model for Stability Analysis	4-8
15	Basic Gradient Control Implementation	5-4
16	Design for SIC with Pilot and Polar Reflectivities	5-6
17	Design for SIC with Dither Driven Gradient Algorithm	5-9
18	Main Antenna Dither Signal Canceler	5-10
19	Experimental Antenna Array	6-2
20	Variable Reactance Termination Mounted at Base of Parasitic Elements	6-3
21	Antenna Array Test Setup	6-4
22	Antenna Pattern After Nulling an Interference Source	6-6
23	Antenna Pattern After Manual Adaptation to a Desired Signal $S$ and Two Interferers $I_1$ and $I_2$	6-6
24	Antenna Pattern After Manual Adaptation to a Desired Signal $S$ and an Interferer $I$	6-8
25	Block Diagram of Active Termination	7-2
26	Schematic of Active Termination	7-3
27	Signal Level Analysis for Active Termination	7-6
28	Dynamic Range Test Setup	7-8

# List of Figures (con'd)

<u>Figure Number</u>	<u>Title</u>	<u>Page Number</u>
29	Dynamic Range Test Results	7-9
30	Phase Control Test Setup	7-10
31	Phase Control Test Results	7-11
32	Amplitude Control Bandwidth Test Setup	7-12
33	Amplitude Control Bandwidth Test Results with 1 KHz Control Signal	7-13
34	Amplitude Control Bandwidth Test Results with 40 KHz Control Signal	7-14
35	Adaptive Pattern for a Single-Jammer Threat; Small, Actively Terminated, Two Element Array	7-16
36	Oscillation Detector	8-2
37	Basic PAI Design	9-2
38	Recommended Signal-Interference Discriminator	9-5
39	Recommended PAI Design	9-7
B1	Network Model for Calculating Scattering Parameters	B-2
C1	Model for Terminated Transmission Line	C-3
C2	Model for Multiple Terminated Transmission Lines	C-6
E1	Reflectivity with Narrowband Filter	E-2
F1	Array with an Unstable Element	F-2
H1	Pilot Signal Injection	H-2

## 1.0 INTRODUCTION AND BACKGROUND

### 1.1 Introduction

A parasitic array consists of a main element directly connected to a receiver plus additional parasitic elements coupled to the receiving element by the mutual impedance between the antennas. The array antenna pattern is controlled by adjusting the values of the complex impedances that terminate the parasitic elements. The value of each terminating impedance determines the phase and amplitude of the signals reflected from that parasitic element to the receiving element. Thus, the main antenna element receives the sum of the various reflected signals to form an array output. The use of such an array for directional beam forming has been studied by Harrington, [6-10].

A spatial interference canceller (SIC) uses a parasitic array with complex terminations for directional null forming. In addition, an adaptive SIC would require an automatic control algorithm for controlling the complex terminations, such as: least mean square (LMS), gradient control, univariate search, dither, etc.

Zeger-Abrams Incorporated (ZAI) has performed an analysis of the use of a parasitic array for adaptive nulling [1,2]. Below, the "transmission-line" model therein presented is refined, and an extended analysis of the methods of implementation and the performance of using a parasitic array for adaptive nulling is given.

The goal of the SIC program is to develop a compact adaptive array (an order of magnitude or more smaller than a conventional array) using parasitic elements with variable complex terminations. Such an array would provide anti-jamming (AJ) capabilities in a very tiny aperture, using less electronic hardware and fewer RF cables.

### 1.2 Background

Many present and future receivers (for radio communications, radar, navigation, IFF, Dr', ELINT, etc.) will be required to operate in a severe electromagnetic interference (EMI) environment that includes unintentional local and deliberate remote sources of EMI.

A common problem in Navy HF communications is the presence of strong intentional and unintentional sources of interference. Usually these sources have unpredictable azimuthal directions of arrival which are different than the desired signal azimuths. One technique for reducing

the interference is to use an adaptive array (AA) that is capable of placing nulls in the directions of interferers and a main lobe in the direction of the required signal.

Adaptive array hardware has been demonstrated at various frequencies from VLF to C-band. Previous AA designs for remotely generated interferences (e.g., ECM) have employed an array of antennas spaced greater than a half wavelength in order to minimize inter-element coupling. Interference cancellation has traditionally taken place in a physical device (directional coupler, transformer, hybrid summer) functioning as a phasor subtractor.

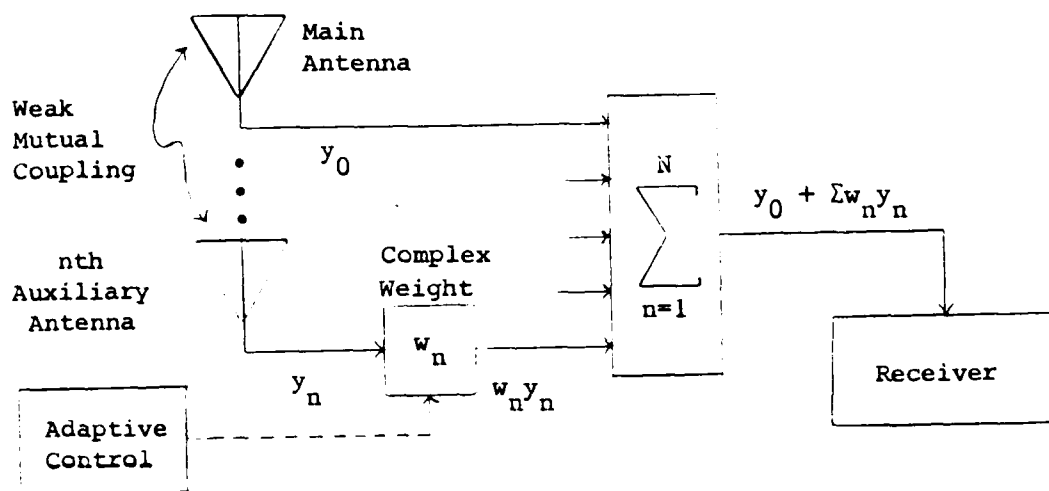
Prior AA designs suffer from costly installation of coaxial cables to elements, poor nulling performance due to inter-element coupling effects, and great consumption of available space on aircraft surfaces and ship masts by antennas.

These drawbacks of prior designs can be reduced or eliminated by using the linear superposition property of free space (for electromagnetic fields) to accomplish spatial interference cancellation (SIC).

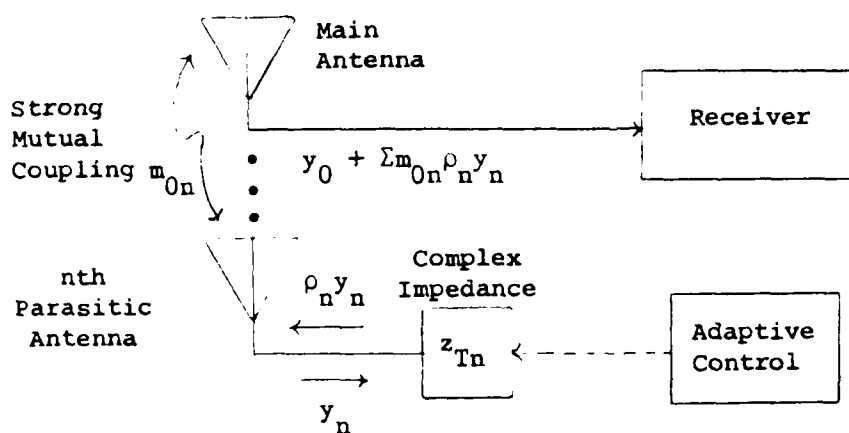
An antenna array and a conventional beamformer are illustrated in Figure 1a. The complex signal envelope  $y_n$  incident upon the nth antenna is weighted (complex multiplication) by the complex weight  $w_n$ . With an unweighted main antenna, the array output equals  $y_0 + \sum w_n y_n$ , which is the input to the receiver. Antenna element spacing is typically  $\lambda/2$ , and inter-element coupling is small and is usually neglected.

In a spacial beamformer, illustrated in Figure 1b, a main antenna is connected directly to the receiver, and a compact array of parasitic elements is terminated in complex impedances. The value of the terminating impedance  $z_{Tn}$  of the nth parasitic element is controlled to adjust its complex reflectivity  $\rho_n$ . In this way, the signal  $y_n$  incident upon  $z_{Tn}$  is weighted before being coupled to the main antenna, where it is spacially summed with contributions from the other parasitic elements. The input to the receiver is equal to  $y_0 + \sum m_{0n} \rho_n y_n$ , where  $m_{0n}$  is the dimensionless complex coupling coefficient between the nth parasitic element and the main antenna. The similarity of receiver inputs for the conventional and parasitic arrays is evident if one substitutes  $m_{0n} \rho_n$  for  $w_n$ .

Array pattern control in the conventional array is achieved by adjusting the  $w_n$ . In the parasitic array one can adjust the  $\rho_n$  or the  $z_{Tn}$ . If the complex impedance of the transmission line (between the nth antenna



a) Conventional Beamformer



b) Spatial Beamformer

Figure 1 Adaptive Beamformers

By combining Equations (2.6) and (2.7), we obtain  $\underline{v}_T$  in terms of  $\underline{v}_{oc}$ .

$$\underline{v}_T = Z_T(Z_T + Z_A)^{-1} \underline{v}_{oc} \quad (2.8)$$

Thus we can completely characterize the array during reception knowing the open circuit mutual impedance matrices of the antenna and the load networks and the vector of array open circuit voltages,  $\underline{v}_{oc}$ , due to an incident plane wave. Harrington gives computer programs which will calculate  $Z_A$  and  $\underline{v}_{oc}$  for an array of wire dipole antennas [10,12].

The impedance model has been briefly introduced here to allow the reader to become acquainted with it. The impedance model is fairly well defined in the literature. In the next chapter, the transmission line model that Zeger-Abrams Incorporated has developed shall be related to the impedance model. This relationship is based on the theory of scattering parameters, of which a derivation is given in Appendix B.

### 2.3 Properties of Compact Parasitic Arrays

The compact parasitic array has many differences with the conventional antenna array. These differences will be pointed out and discussed in this section.

The most important difference is that the compact parasitic array has strong mutual coupling. In the conventional array, mutual coupling is undesired and efforts are made to keep it minimal. The principal manner in which this is done, is to keep the antennas far apart. In the parasitic arrays, strong mutual coupling is necessary for operation. A small compact array (dimensions on the order of  $0.1\lambda$  or less) are needed to ensure strong mutual coupling.

Because the array is small, many features of the array will be broadband and broadbeamed. High directivity will not be possible as the main lobe will always be somewhat broad. Similarly, when nulls are formed, the null widths will be slightly wider than those obtained in conventional arrays. For details, see the experimental results reported in Chapters 6 and 8.

The frequency characteristics of the array, particularly with active terminations, are difficult to determine. The reflections off the parasitic element terminations and the mutual coupling create very complex feedback that is difficult to analyze. Even more funda-

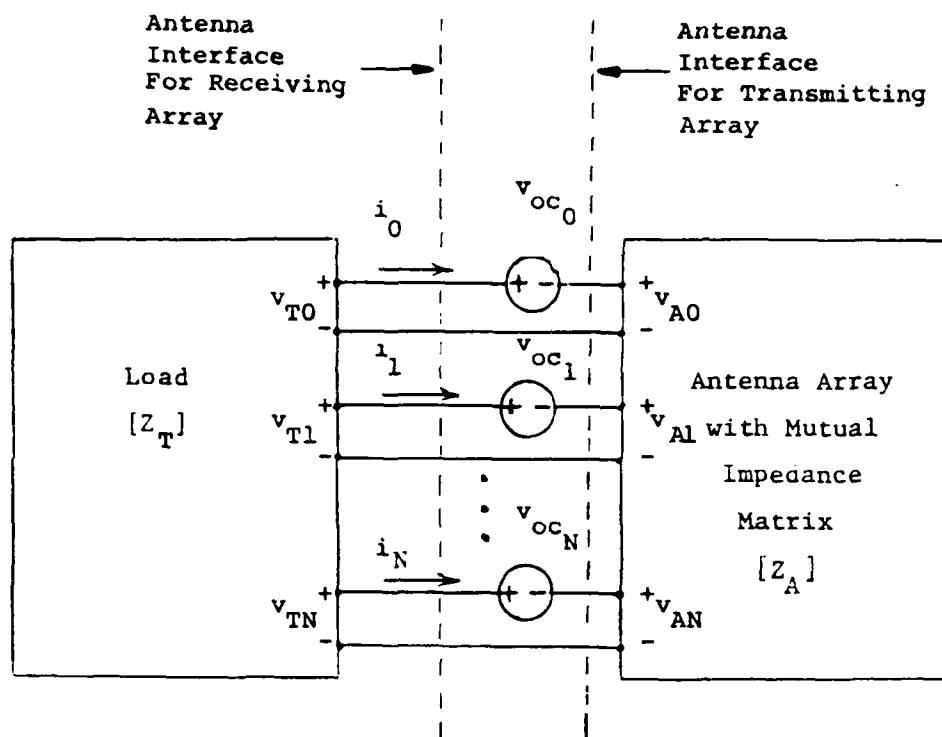


Figure 5 Harrington's Impedance Model of a Parasitic Array



The process of nulling a signal is one of finding the  $\rho_n$ 's such that  $y_0 = 0$  in Equation (2.3a). This is done in Section 4.1. The resulting  $\rho_n$ 's turn out to be independent of  $\rho_0$ . This results from the fact when there is no incident voltage to reflect at the termination (receiver) of the main antenna, it doesn't matter to the rest of the system what  $\rho_0$  is.

A final comment, for the transmission line model presented here it has been assumed that there are transmission lines between the antennas and the terminations. It turns out that this is not necessary (or more specifically, one can assume transmission lines of zero length). This is shown in Appendices C.1 and C.2.

## 2.2 Impedance Model

The impedance model has been used by Harrington in several papers to describe a parasitic array for various purposes [6-10]. This model of an array while receiving is illustrated in Figure 5.  $Z_A$  is the open circuit mutual impedance matrix of the antenna array looking directly into the antenna ports.  $Z_T$  is the open circuit mutual impedance matrix looking at the terminations through the transmission lines. In our array  $Z_T$  is diagonal, but the main results are valid for a general terminating network. The open circuit voltage,  $v_{ocn}$ , is the terminal voltage at the nth port due to a plane wave incident on the array with all antenna ports open circuited. As with  $y_{st}$  of the transmission line model,  $v_{oc}$  will depend on the field strength and wave vector,  $\underline{k}$ , of the incident plane wave. For convenience, the model used here assumes there are no transmission lines in between the terminations and the array (or at least the effect of these transmission lines are included in the impedance parameters).

To compute the vector of voltages across the load terminals,  $\underline{v}_T$ , we must first find the current vector,  $\underline{i}$ .

$$\underline{v}_{oc} = -(Z_T + Z_A)\underline{i}$$

therefore

$$\underline{i} = -(Z_T + Z_A)^{-1} \underline{v}_{oc} \quad (2.6)$$

But we know that  $\underline{i}$  is related to  $\underline{v}_T$  by the load matrix  $Z_T$ .

$$\underline{v}_T = -Z_T \underline{i} \quad (2.7)$$

If the input impedance of the receiver attached to the main antenna matches the line impedance =  $z_0$ , then  $\rho_0 = 0$ . The Equations (2.3) reduce to

$$y_0 = y_{s0} + \underline{m}_0^T P y \quad (2.4a)$$

$$y = y_s + M P y \quad (2.4b)$$

(with  $\rho_0 = 0$ )

Equation (2.4b) can be solved for the incident voltage vector of the auxiliaries,  $y$ .

$$y = (I - MP)^{-1} y_s$$

Thus Equations (2.4) can be rewritten as

$$y_0 = y_{s0} + \underline{m}_0^T P Q^{-1} y_s \quad (2.5a)$$

$$y = Q^{-1} y_s \quad (2.5b)$$

(with  $\rho_0 = 0$  and  $Q = I - MP$ )

Equations (2.5) could have been obtained directly from Equation (2.2) using matrix identity (A.9) from Appendix A with the fact  $\rho_0 = 0$ .

$$Q_+ (\rho_0 = 0) = \begin{pmatrix} 1 & \vdots & -\underline{m}_0^T P \\ \dots & \dots & \dots \\ 0 & \vdots & I - MP \end{pmatrix} = \begin{pmatrix} 1 & \vdots & -\underline{m}_0^T P \\ \dots & \dots & \dots \\ 0 & \vdots & Q \end{pmatrix}$$

From identity A.9 we can compute

$$Q_+^{-1} (\rho_0 = 0) = \begin{pmatrix} 1 & \vdots & \underline{m}_0^T P Q^{-1} \\ \dots & \dots & \dots \\ 0 & \vdots & Q^{-1} \end{pmatrix}$$

thus

$$\begin{pmatrix} y_0 \\ \dots \\ y \end{pmatrix} = \begin{pmatrix} 1 & \vdots & \underline{m}_0^T P Q^{-1} \\ \dots & \dots & \dots \\ 0 & \vdots & Q^{-1} \end{pmatrix} \begin{pmatrix} y_{s0} \\ \dots \\ y_s \end{pmatrix}$$

which is equivalent to Equations (2.5).

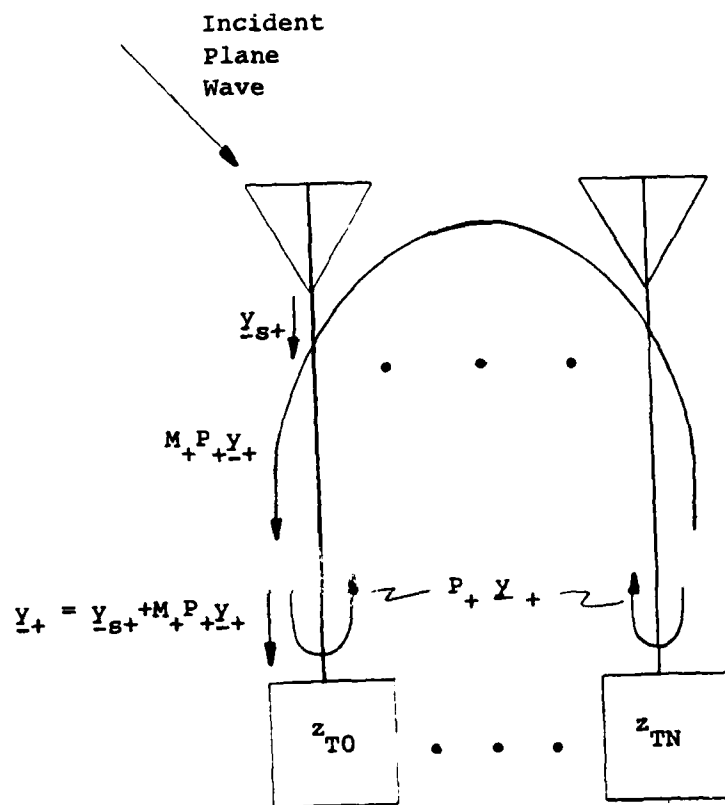


Figure 4 Illustration of Fundamental Equation of the Transmission Line Model

Let us now examine what happens during reception. The vector of voltages,  $y_+$ , incident on the terminations will be the sum of two terms,  $y_{s+}$  and  $M_+P_+y_+$ , as given in Equation (2.1). (See Figure 4.)

$$y_+ = y_{s+} + M_+P_+y_+ \quad (2.1)$$

The term  $y_{s+}$  is due to the incident plane wave. The term  $M_+P_+y_+$  is due to the incident voltages of  $y_+$  being reflected off the terminations as  $P_+y_+$  and then coupled via the mutual coupling matrix  $M_+$  into downward traveling voltages of  $M_+P_+y_+$ .

Equation (2.1) demonstrates that the system is one of multivariate linear feedback in terms of the incident voltages  $y_+$ . The input is  $y_{s+}$ . The "loop gain" is  $M_+P_+$ . Since active terminations are being allowed, the reflectivity of the matrix  $P_+$  may exhibit gain. Thus it is reasonable to ask when does the matrix product  $M_+P_+$  represent positive feedback which renders the system unstable. This issue of stability is addressed in Section 4.2.

Given that the system is stable, one may solve Equation (2.1) for the voltages incident on the terminals,  $y_+$ .

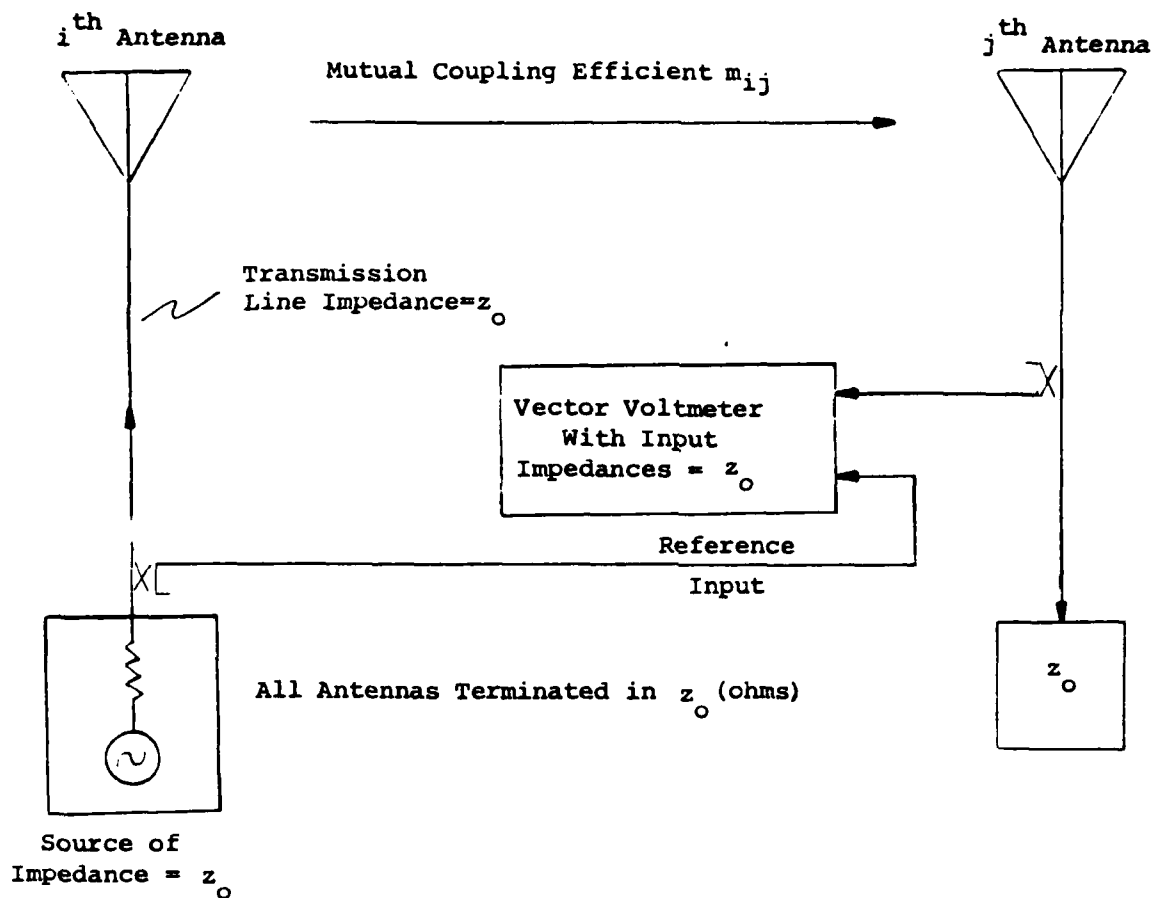
$$\begin{aligned} y_+ &= (I - M_+P_+)^{-1} y_{s+} \\ &= Q_+^{-1} y_{s+} \end{aligned} \quad (2.2)$$

where  $Q_+ = I - M_+P_+$

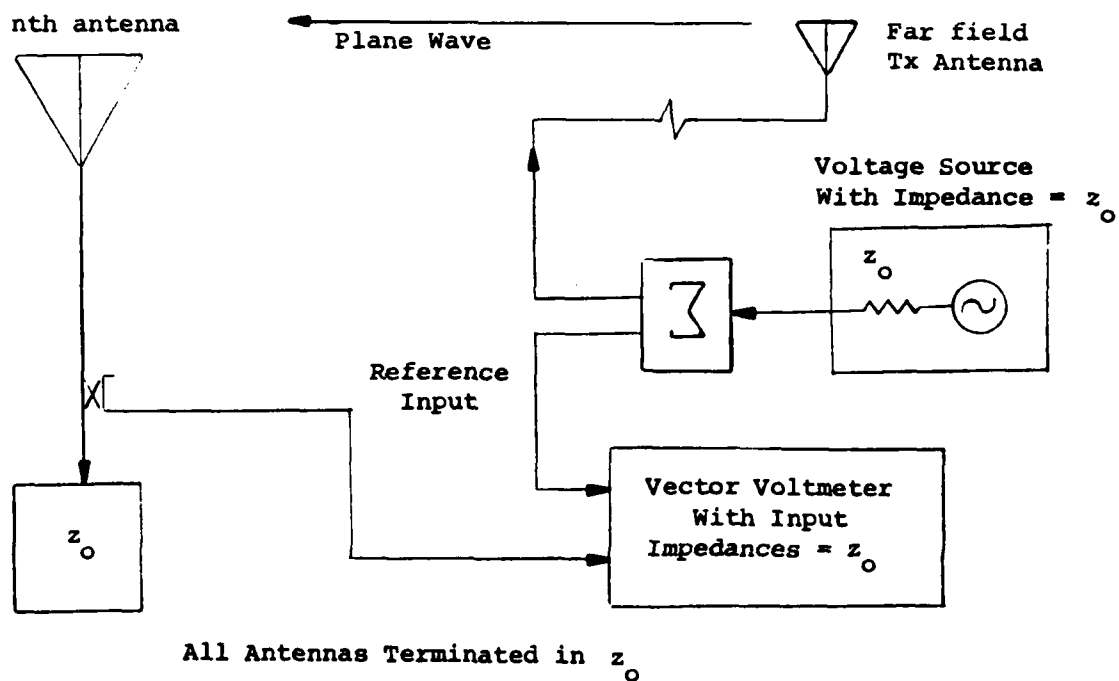
We can also separate Equation (2.1) into two equations, one for the main antenna and one for the parasitic auxiliaries.

$$y_0 = y_{s0} + \rho_{00} y_0 + \underline{m}_0^T P y \quad (2.3a)$$

$$y = y_s + \rho_{00} y_0 + M P y \quad (2.3b)$$



### 3.a Measurement of $m_{ij}$



### 3.b Measurement of $y_{sn}$

Figure 3 Measurement of Transmission Line Model Parameters

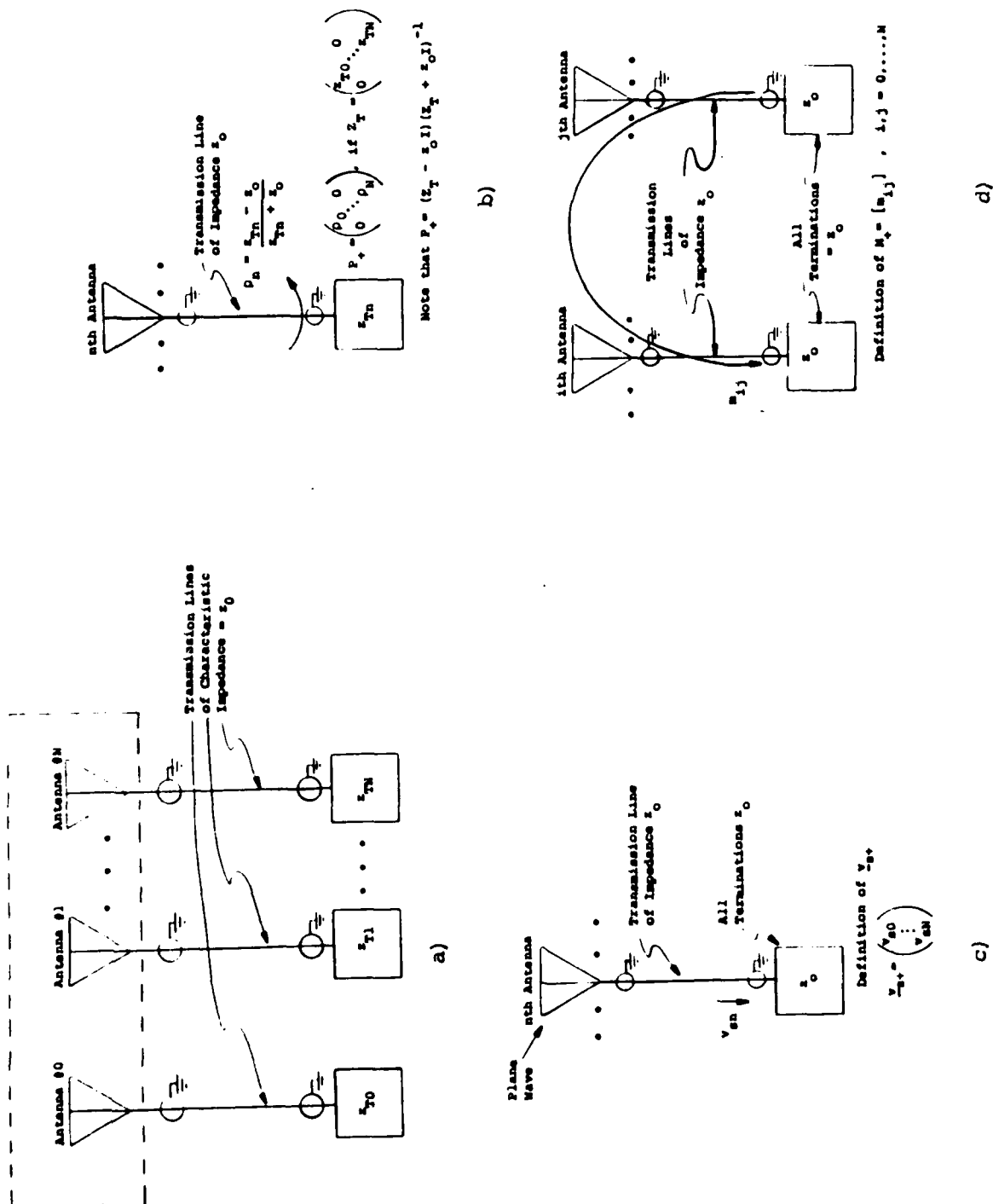


Figure 2 Definition of Transmission Line Model Parameters

The systematic approach considered the voltages in the array after all the "ping-ponging" has finished. The equations that described this state were written down and solved for the various traveling voltage waves. In matrix form, these equations are represented by Equation (2.1) below. In the initial analysis the systematic approach yielded little insight as to what values of the reflectivities,  $\rho_n$ , and mutual coupling coefficients,  $m_{ij}$ , allow stable operation. The only restriction that came out of the analysis was

$$\det |Q_+| = \det |I - M_+ P_+| \neq 0 .$$

This constraint was not restrictive enough. It did not prohibit all situations that were inoperable. In particular it did not prohibit the equivalent of positive feedback.

In the analysis that follows the systematic approach is refined. With this new model several issues are explored. These issues include stability, null forming, adaptive control, and the relationship to Harrington's impedance model.

The refined transmission line model and its parameters are illustrated in Figure 2(a-d). Note it has been assumed  $M_+$  is symmetric, or in general  $m_{ij} = m_{ji}$ . This is true, given that all the transmission lines connecting the antennas with the terminations have the same characteristic impedance. This is shown in Appendix C.2, when  $m_{ij}$  are calculated directly from their definition via the antenna mutual impedance matrix,  $Z_A$ . Hereafter, it is assumed that all these characteristic impedances are the same.

The parameters of the transmission line model have been defined in a manner that allows them to be measured relatively easily from a physical array. Configurations for measuring the entries of  $M_+$  and  $Y_{st}$  are given in Figures 3a and 3b respectively. Note adjustments in the calculations will have to be made due to the phase and amplitude effects of the directional couplers and the extra cable lengths.

In Sections 3.3 and 3.4, formulae for the computation of  $M_+$  and  $Y_{st}$  in terms of the open circuit mutual impedance matrix of the array,  $Z_A$ , are derived. However, calculation or measurement of  $Z_A$  is quite complicated. Indeed, for measuring  $Z_A$ , it is probably easier to measure  $M_+$  and then calculate  $Z_A$  from it.

## 2.0 CHARACTERIZATION OF PARASITIC ANTENNA ARRAYS

The two models of a parasitic array are described in this chapter. Each model will be described in terms of a receiving array. Then in Chapter 3, the relationships between the models will be established using both receiving and transmitting arrays. The models have about equal complexity when analyzing a receiving array. The impedance model is easier to analyze for a transmitting array. The transmission line model is easier to analyze for control of the terminations (particularly active terminations) as an adaptive nulling array. The transmission line model assumes transmission lines between the array and the terminations, although these lines may be of zero length. The impedance model may be used with transmission lines between the terminations and the array, although the calculations are more complex (as one sees in Chapter 3).

The main difference between a transmitting and a receiving array is in a transmitting array the termination is the source and the array is the load, while in a receiving array the array is the source and the termination is the load.

### 2.1 Transmission Line Model

The transmission line model of the array analyzes the voltage traveling-waves within the cables, antennas and terminations, the inter-coupling of these waves through the antennas, and the reflections of the waves off the terminations.

The parasitic array with complex terminations has been previously analyzed by ZAI with transmission line techniques, [1,2]. In this previous analysis two analytic approaches were used: the infinite series (ping-pong) approach and the systematic approach. These results are summarized below.

The infinite series approach considered all the possible reflections off the terminations and antennas and all the mutual coupling between antennas. The result was expressed as an infinite geometric series and summed. However, only the two antenna array could be analyzed. For larger arrays the mathematics become too unwieldy. In addition, the constraints on the reflectivities,  $\rho_n$ , and the mutual coupling factors,  $m_{ij}$ , necessary for convergence of the infinite series are too restrictive. They disallow regions where safe operation is possible. In particular, negative feedback of greater than unity gain. The general question of stability is very involved and is taken up later in Section 4.2.



v = vector of the  $N + 1$  terminal voltages of the antenna array.  
i = vector of the  $N + 1$  port currents of the antenna array.  
S =  $(N + 1) \times (N + 1)$  matrix of scattering parameters of the  
 $N + 1$  port antenna network.

$y_{sn}$  =  $y_n$  due to a plane wave incident on the array with all terminations =  $z_0$ , the characteristic impedance of the transmission lines.  $n = 0, 1, \dots, N$ .  $y_{sn}$  is dependent on the wave vector,  $\underline{k}$ , of the incident plane wave.

$$\underline{y}_s = \begin{pmatrix} y_{s1} \\ \vdots \\ y_{sN} \end{pmatrix}, \quad \underline{y}_{s+} = \begin{pmatrix} y_{s0} \\ \dots \\ y_s \end{pmatrix}$$

$m_{ij}$  = mutual coupling coefficients:

the ratio of the downward (toward the termination) voltage traveling wave incident on the  $j$ th termination to the upward (toward the antenna) voltage traveling wave transmitted into the cable from the  $i$ th termination. All other upward traveling waves being zero. All terminations =  $z_0$ .  $i, j = 0, 1, \dots, N$ . Note,  $M$  and  $M_+$  are symmetric matrices.

$$\underline{m}_0 = \begin{pmatrix} m_{01} \\ \vdots \\ m_{0N} \end{pmatrix}, \quad M = \begin{bmatrix} m_{ij} \end{bmatrix}, \quad i, j = 1, \dots, N.$$

$$M_+ = \begin{pmatrix} m_{00} & \vdots & \underline{m}_0^T \\ \dots & \dots & \dots \\ \underline{m}_0 & \vdots & M \end{pmatrix} = \begin{bmatrix} m_{ij} \end{bmatrix}, \quad i, j = 0, 1, \dots, N.$$

$$Q = I - MP, \quad Q_+ = I - M_+P_+ = \begin{pmatrix} 1 - m_{00}^0 & \vdots & -\underline{m}_0^T P \\ \dots & \dots & \dots \\ -\rho_0 \underline{m}_0 & \vdots & Q \end{pmatrix}$$

$z_0$  = characteristic impedance of transmission lines between antennas and terminations

$z_{Tn}$  = impedance terminating the cable from the  $n$ th antenna,  $n = 0, 1, \dots, N$ .

$$Z_T = \begin{pmatrix} z_{T0} & 0 \\ & \ddots \\ 0 & & z_{TN} \end{pmatrix}$$

$Z_A$  = open circuit mutual impedance matrix of the antenna array at the antenna ports (zero cable lengths).

(e.g.)

$$M_+ = \begin{pmatrix} m_{00} & \vdots & m_0^T \\ \vdots & \ddots & \vdots \\ m_0 & \vdots & M \end{pmatrix} = \begin{bmatrix} m_{ij} \end{bmatrix} \quad i, j = 0, 1, \dots, N$$

$$\text{and } M = \begin{bmatrix} m_{ij} \end{bmatrix} \quad i, j = 1, \dots, N$$

- 6) The absence of the subscript "+" on the matrices M, P, or Q, or the vectors  $\underline{y}$  or  $\underline{y}_s$  will denote that they are  $N \times N$  or  $N \times 1$  matrices or vectors, respectively. They will be composed of entries only corresponding to the auxiliary antennas (e.g., M or  $\underline{y}$ ).
- 7) The impedance model works exclusively with the total array of main antenna plus auxiliary. This shall be understood with all its associated variables ( $Z_T$ ,  $Z_A$ ,  $\underline{y}$ , S, etc.) without the subscript "+".
- 8) Subscripts "R" and "I" will denote, respectively, the real and imaginary components of the designated value.
- 9) The superscripts "T" and "\*" will denote, respectively, transpose and complex conjugation.
- 10) In the derivations that are devoted to the single element cases, all variables become scalars and will be denoted by the appropriate lower case, non-underlined letters. Also, all indices will be dropped.

$\underline{k}$  = the wave vector of a plane wave =  $\frac{2\pi}{\lambda} \underline{u}$ , where  $\lambda$  is the wavelength and  $\underline{u}$  is the unit direction vector of the plane wave.

$\rho_n$  = reflection coefficient of the nth termination.  
 $n = 0, 1, \dots, N.$

$$P = \begin{pmatrix} \rho_1 & & 0 \\ & \ddots & \\ 0 & & \rho_N \end{pmatrix}, \quad P_+ = \begin{pmatrix} \rho_0 & \vdots & 0 \\ \vdots & \ddots & \vdots \\ 0 & \vdots & \rho \end{pmatrix}$$

$y_n$  = the complex envelope of the voltage traveling wave incident on the nth termination.  $n = 0, 1, \dots, N.$

$$\underline{y} = \begin{pmatrix} y_1 \\ \vdots \\ y_N \end{pmatrix}, \quad \underline{y}_+ = \begin{pmatrix} y_0 \\ \vdots \\ y \end{pmatrix}$$

and its termination  $z_{Tn}$  has the value  $z_0$ , then:

$$\rho_n = (z_{Tn} - z_0) / (z_{Tn} + z_0) \quad (1.1)$$

The work described here introduces the following changes to the previous work of Harrington [6, 7, 8, 9]:

- a) Terminating impedances can have complex, not just imaginary (reactive) values.
- b) Terminating impedances can be active (have gain) so that the restriction  $|\rho_n| \leq 1$  is removed.
- c) The impedances are controlled to form nulls toward sources of interference.
- d) A closed loop adaptive algorithm controls the  $z_{Tn}$  for pattern control in order to avoid requiring a knowledge of the array geometry and to avoid computing the mutual impedance matrix for open loop pattern control.

### 1.3 Scope

The SIC program has been undertaken jointly by ZAI and Naval Research Laboratory (NRL). ZAI has completed a theoretical analysis of an SIC and built four electronically variable, active complex terminations for experimental use. NRL has built an experimental parasitic array. Tests have been run with this array using passive reactive terminations and also using the active complex terminations.

### 1.4 Glossary of Notation

The following conventions will be observed:

- 1) Upper case letters will represent matrices (e.g., M or P).
- 2) Lower case letters with an underline will represent vectors (e.g.,  $\underline{y}$  or  $\underline{y}_s$ ).
- 3) Lower case letters without an underline will represent scalars (e.g.,  $y_0$  or  $\rho_n$ ).
- 4) "0" as a subscript will reference the main antenna (e.g.,  $y_0$  or  $m_0$ ).
- 5) "+" as a subscript added to the matrices M, P, or Q, or the vectors  $\underline{y}$  or  $\underline{y}_s$  will denote that they have been augmented to include the corresponding entries of the main antenna in addition to those of the parasitic auxiliary antennas. Such a matrix or vector will now be  $(N + 1) \times (N + 1)$  or  $(N + 1) \times 1$  respectively (where N is the number of auxiliary antennas). To be consistent with Convention 4, as well as not to disturb the numbering of the auxiliary antennas, the main antenna is assigned an index of "0".

mentally, there is little information available on how the array parameters, mutual impedances, or mutual coupling factors of compact arrays vary over frequency. Harrington provides computer programs that can be used to compute these parameters, [12]. The problem is generally intractable for anything but numerical methods.

An issue that arises when considering a parasitic array for nulling is whether to use active or passive terminations. It is a question of stability versus degrees of freedom in the control space.

If passive terminations are used, then the array will always be stable. The mutual coupling between the antennas, however, is necessarily lossy. That is, 100% of the power is not coupled to other antennas. It is this loss of power, through re-radiation, that often prevents cancellation of an interference with only one auxiliary antenna or  $N$  interferences with  $N$  auxiliaries. It is usually necessary to use two or more passively terminated auxiliary antennas to cancel a single interference. Thus for the same amount of nulling capabilities a passively terminated parasitic array will require more elements than an actively terminated array.

An actively terminated parasitic array will give equal or better performance with fewer antennas. If, however, too much gain is used then the inherent feedback nature of the parasitic array could cause an unstable oscillation to start. The issue of stability is taken up in detail in Section 4.2. The stability analysis determines the optimal mutual coupling matrix,  $M_+$ . In order to increase the usable gain before instability, one should: 1) minimize the antenna mismatch or return loss or equivalently the self coupling  $m_{nn}$  of each antenna, 2) minimize the mutual coupling between auxiliary antennas, and 3) maximize coupling between the main and the auxiliary antennas. The optimal mutual coupling matrix,  $M_+$ , is of the form

$$M_+ = \begin{pmatrix} 0 & \vdots & \underline{m}_0^T \\ \dots & \ddots & \dots \\ \underline{m}_0 & \vdots & 0 \end{pmatrix} \quad (2.9)$$

The construction of such an ideal mutual coupling matrix can be approached by two methods, antenna element and array design and by connecting various impedances between the antennas of the array.

Another aspect of parasitic arrays is the inherent non-linear nature of any control algorithm of the variable terminations. To better understand this, consider the conventional beamforming array and the parasitic array illustrated in Figure 1. Both arrays behave linearly in that for a given set of complex weights or terminating impedances if the incident plane wave is scaled by a factor  $c$ , then the output of the array will be scaled by  $c$ . The conventional array is also linear in a control sense, in that if one of the complex weights are changed by an amount  $\Delta w$ , then the array output will change by an amount proportional to  $\Delta w$ , given all other weights and the inputs to the array remain constant. It is in this sense that the parasitic array is nonlinear. If one of the reflectivities,  $\rho_n$ , were to change by an amount  $\Delta \rho$ , the array output in general will not change by an amount proportional to  $\Delta \rho$ . From Equation (2.2), the change in the output ( $y_0$  or  $y_+$ ) is determined by the matrix inverse  $(I - M_+ P_+)^{-1}$ . Another way of looking at this is by the gradient of the array output with respect to the control variable, either the weights or the reflectivities; or equivalently be considering the appropriate individual partial derivatives. In the conventional array, the derivatives of the array output with respect to the weights,  $\partial y_0 / \partial w_n$ , are constant and depend only on the incident signals and array geometry. For the parasitic array, the derivatives of the output with respect to the reflectivities are functions of all the reflectivities themselves as well as the incident signals and array geometry. The nonlinear control of a parasitic array is discussed in greater detail in Chapter 5. Note a mutual coupling matrix as in Equation (2.9) above along with  $\rho_0 = 0$  would allow linear control of the array. In this case  $(I - M_+ P_+)^{-1} = I + M_+ P_+$ .

Lastly, in this chapter, some properties of a transmitting array are discussed. The array far field pattern and the radiated power will be calculated. A method of calculating the far field pattern based on the array impedance parameters is described by Dinger [4], for a parasitic array with reactive terminations. The results are easily extended for general terminating impedances. Consider the impedance model of an array illustrated in Figure 5. Let the voltage sources,  $v_{ocn}$ , and the load matrix,  $Z_T$ , be the  $N + 1$ -port Thevenin equivalent of the source network of the array during transmission. Note that the polarity of the voltage sources is the opposite of the usual convention. To calculate the far field, one must first find the port currents,  $i_n$ , of the array.

$$\underline{i} = -(Z_T + Z_A)^{-1} \underline{v}_{oc} , \quad (2.6)$$

Under the assumption that the current on each antenna is determined only by its port current, then one can use superposition to add up the contribution of each antenna in the far field.

Let us assume that all the antennas are identical monopoles and orientated in the z-direction. Then the far field pattern as a function of the azimuthal angle,  $\phi$ , is given below, [7].

$$E_z(\phi) = -\frac{j\eta e^{-jkr}}{2\pi r} \sum_{n=0}^N i_n e^{jk(x_n \cos \phi + y_n \sin \phi)} \quad (2.10)$$

where  $r$  is the distance from the array,  $\eta$  is the intrinsic impedance of free space, and  $x_n$  and  $y_n$  are the coordinates of the  $n$ th antenna relative to the array phase center. Note it is assumed  $|x_n|, |y_n| \ll r$ .

A comment on the assumption necessary for superposition. It is not being assumed there is no mutual coupling. The calculation of the port current takes that into account. Superposition holds for the currents on the antennas. But the calculations of Equation (2.6) give us only the port currents. Thus to use superposition we must assume that the currents on an antenna are due to its port current alone and that this antenna current distribution will be the same as that on an isolated antenna. To illustrate further, consider an array of a particular configuration with a set of source voltages. Assume that this establishes, inclusive of all mutual coupling effects, a current  $i_n$  at the port of the  $n$ th antenna. Now let us move the other antennas around and change the source voltages but always under the condition that the port current of the  $n$ th antenna is maintained at  $i_n$ . The assumption then asserts that currents on the  $n$ th antenna, which give rise to its radiated field, will not significantly change. This assumption is good for antennas that are small compared to a wavelength ( $< \lambda/4$ ) even in a compact array. The port current alone then will determine all antenna currents. If this assumption cannot be made then the far field pattern can be calculated using Harrington's computer programs [12].

If one wishes to use transmission line parameters, Equation (2.10) above is still used but the antenna port currents are calculated differently. In Appendix C.2, an expression for the antenna port cur-

rents in terms of the transmission line parameters is derived. In the notation of Appendix C.2,  $\underline{i}(\underline{l})$  is the vector of the antenna port currents.

$$\underline{i}(\underline{l}) = \frac{1}{2} Z_0^{-1} (D - D^{-1} M_+) (Q_+^{-1})^T (I - P_+) \underline{v}_{oc}, \quad (C32)$$

where  $Z_0$  is the diagonal matrix of the transmission line characteristic impedances,  $D$  is the diagonal matrix of delays through these transmission lines (see Equation 3.17) and  $\underline{v}_{oc}$  is the vector of voltage sources in the terminations.

Lastly, we calculate the power radiated by a transmitting array. With an impedance model the average power is given by Equation (2.11).

$$\begin{aligned} P &= 1/2 \operatorname{Re} [\underline{i}^{*T} \underline{v}_A] \\ &= 1/2 \operatorname{Re} [\underline{i}^{*T} Z_A \underline{i}] \\ &= 1/2 \underline{i}^{*T} \operatorname{Re} [Z_A] \underline{i} \end{aligned} \quad (2.11)$$

where  $\underline{i} = -(Z_A + Z_T)^{-1} \underline{v}_{oc}$ . The last step is true because  $Z_A$  is symmetric.

For the transmission line model the power radiated (assuming lossless transmission line) is

$$P = 1/8 \operatorname{Re} [\underline{v}_{oc}^{*T} (I - S_T^{*T} S_T) \underline{v}_{oc}] \quad (2.12)$$

where  $S_T$  is given in Equation (3.13) or (3.16).



### 3.0 RELATIONSHIPS BETWEEN TRANSMISSION LINE AND IMPEDANCE MODELS OF A PARASITIC ARRAY

In Chapter 3, we shall examine the relationship between the transmission line model and the impedance model of a parasitic array. This relationship will be illustrated by analyzing various aspects of receiving and transmitting arrays with each model. In particular, it is shown how to calculate the parameters of the transmission line model from the impedance parameters. The means of relating the two models will be scattering parameters. The derivation of the matrix of scattering parameters,  $S$ , is given in Appendix B. The scattering matrix is a generalization of the reflection coefficient,  $\Gamma$ , of a single port system. For an  $N$ -port network, with no sources, the  $i,j$ th scattering parameter,  $s_{ij}$ , is defined as the ratio of the voltage traveling wave coming out, "reflected", from the  $i$ th port due to the wave incident on the  $j$ th port with no other incident waves.

The matrix of these parameters,  $S = [s_{ij}]$ , can be calculated from  $Z$  and  $Z_0$ . Here,  $Z$  is the open circuit mutual impedance matrix of the  $N$ -port network, and  $Z_0$  is the diagonal matrix of the characteristic impedances of the media connected to the network ports. We repeat here equation (B13).

$$S = (Z - Z_0)(Z + Z_0)^{-1} \quad (B13)$$

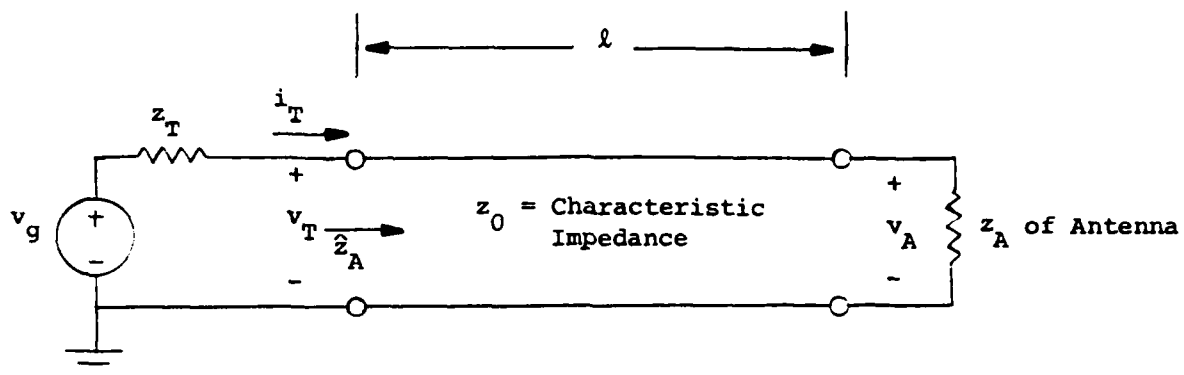
One comment before continuing, in the previous chapter it was assumed there were no transmission lines present with the impedance model. Hereafter, transmission line will be present and their affects explicitly calculated.

We begin with a treatment of the single element case.

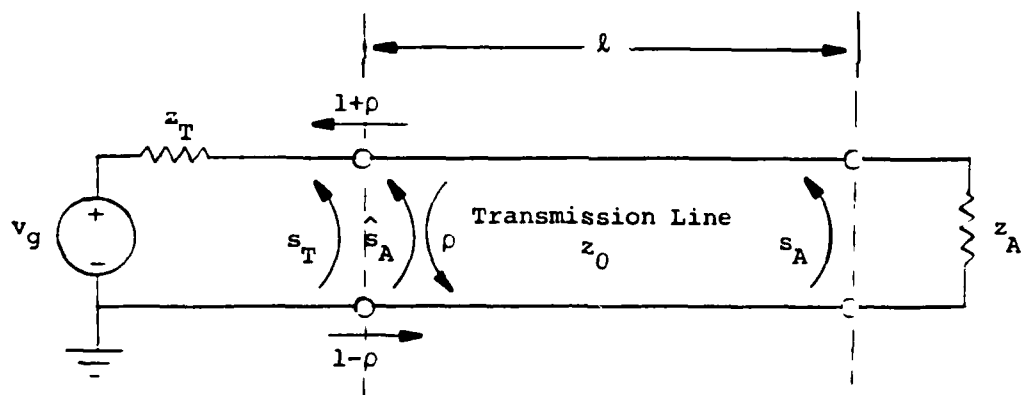
#### 3.1 Single Antenna Transmitting

The impedance model of a single antenna transmitting is given in Figure 6a. The difference between the transmitting and receiving versions of the impedance model is the placement of the voltage source (compare to Figure 5).

For a single antenna, the scattering matrix will be a scalar,  $s$ , which is simply the reflection coefficient,  $\Gamma$ , at the same point. We shall retain the notation,  $s$ , so that the generalization to an  $N$ -port network will be seen more readily.



6 a) Impedance Model (with transmission line)



6 b) Voltage Traveling Wave Relationships within the Transmission Lines

Figure 6 Impedance Model of Single Element Array Transmitting

In Figure 6b, the important relationships among the various voltage traveling waves are illustrated.  $s_A = (z_A - z_O)/(z_A + z_O)$  is the scattering parameter or reflection coefficient at the antenna port.  $\rho = (z_T - z_O)/(z_T + z_O)$  is the reflection coefficient of a voltage wave traveling toward the source, incident on the termination. The transmission coefficient of a voltage wave incident on a junction is the ratio of the voltage transmitted to the voltage incident. Ignoring any further reflections, continuity of the total voltage means the transmission coefficient is  $1 + \Gamma$ . Thus, for a voltage wave toward the source and incident on the terminations, the transmission coefficient is  $1 + \rho$ .

For a voltage wave from the source and incident on the termination-transmission line interface, the reflection coefficient is  $(z_O - z_T)/(z_O + z_T) = -\rho$ , ignoring subsequent reflections off the antenna. Thus, for a similar voltage wave the transmission coefficient is  $1 - \rho$ . The scattering parameter,  $s_T$ , for a voltage wave traveling toward the antenna and incident on the termination-transmission line interface can be calculated from the results of Appendix C.1.

$$s_T = (\hat{z}_A - z_T) / (\hat{z}_A + z_T) \quad \text{from Equation (C4)}$$

$$= \frac{\left[ (1 + \hat{s}_A) / (1 - \hat{s}_A) \right] z_O - z_T}{\left[ (1 + \hat{s}_A) / (1 - \hat{s}_A) \right] z_O + z_T} \quad \begin{array}{l} \text{from Rule 2 of} \\ \text{Appendix C.1} \end{array} \quad (3.1)$$

where  $\hat{z}_A$  and  $\hat{s}_A$  are respectively the open circuit impedance and scattering parameter (reflection coefficient) looking at the antenna within the antenna transmission line just before the termination. We can further manipulate Equation (3.1) to obtain:

$$\begin{aligned}
s_T &= \frac{(1 + \hat{s}_A) z_o - (1 - \hat{s}_A) z_T}{(1 + \hat{s}_A) z_o + (1 - \hat{s}_A) z_T} \\
&= \frac{(z_o - z_T) + \hat{s}_A (z_o + z_T)}{(z_o + z_T) + \hat{s}_A (z_o - z_T)} \\
&= \frac{\left[ (z_o - z_T) / (z_o + z_T) \right] + \hat{s}_A}{1 + \hat{s}_A \left[ (z_o - z_T) / (z_o + z_T) \right]} \\
&= \frac{\hat{s}_A - \rho}{1 - \hat{s}_A \rho} \tag{3.2}
\end{aligned}$$

If we compare the definition of  $s_T$  to the definition of the mutual coupling factor,  $m$ , and noting that when  $z_T = z_o$  the termination-transmission line interface becomes invisible, we see that  $m = s_T$  (with  $z_T = z_o$ ). Indeed this can serve as an alternate definition of  $m$ .

$$\begin{aligned}
m &= \hat{s}_A \\
&= s_T, \text{ when } z_T = z_o \text{ or equivalently } \rho = 0. \tag{3.3}
\end{aligned}$$

$$\begin{aligned}
&= e^{-j2\beta\ell} s_A = d^2 s_Z \\
&= d^2 (z_A - z_o) / (z_A + z_o) \tag{3.4}
\end{aligned}$$

where  $d = e^{-j\beta\ell}$ ,  $\beta$  is the propagation velocity of the transmission line, and  $\ell$  is the length of the line. Note that  $\hat{s}_A$  is independent of  $z_T$ . Thus, Equations (3.3) and (3.4) allow us to calculate the mutual coupling,  $m$ , from the impedance parameters  $z_A$  and  $z_o$ .

We shall now obtain Equation (3.2) via the transmission line model. Consider a voltage wave traveling toward the antenna and incident on the termination-transmission line interface. Let us call such a voltage wave  $v_{(+)}$  (see Figure 7). The voltage that gets transmitted into the transmission line, ignoring subsequent reflections, is then  $(1 - \rho) v_{(+)}$ . This voltage wave toward the antennas becomes a voltage wave toward the source incident on the termination of  $m(1 - \rho) v_{(+)}$ , again ignoring further reflections. The resultant (after all reflections) voltage wave incident on the termination from the antenna,  $y$ , can be computed from Equation (2.2) with  $y_s = m(1 - \rho) v_{(+)}$ .

$$\begin{aligned} y &= (1 - m\rho)^{-1} y_s \\ &= (1 - m\rho)^{-1} m(1 - \rho) v_{(+)} \end{aligned} \quad (3.5)$$

The total downward voltage incident on the termination transmits a voltage  $(1 + \rho)y$  into the termination, traveling toward the source. There is another component of this voltage,  $-\rho v_{(+)}$ , due to the initial reflection of the original incident voltage  $v_{(+)}$ . Thus, we can write:

$$\begin{aligned} s_T v_{(+)} &= (1 + \rho)y - \rho v_{(+)} \\ &= [(1 + \rho)(1 - m\rho)^{-1}(1 - \rho) - \rho] v_{(+)} \end{aligned}$$

and

$$s_T = (1 + \rho)(1 - m\rho)^{-1} m(1 - \rho) - \rho \quad (3.6)$$

$$\begin{aligned} &= \frac{(1 - \rho^2)m}{1 - m\rho} - \rho \\ &= \frac{m - \rho}{1 - m\rho} \end{aligned} \quad (3.7)$$

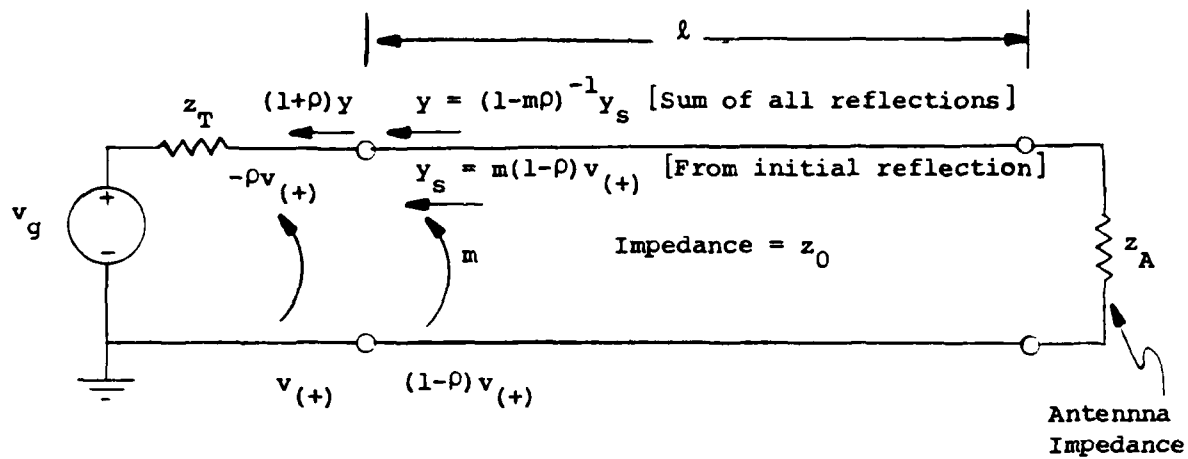


Figure 7 Transmission Line Model of Single Element Array Transmitting

But we know that  $m = \hat{s}_A$ , therefore Equation (3.7) is identical to Equation (3.2).

In this Section, we have demonstrated that  $m = \hat{s}_A = s_T(\rho)|_{\rho=0}$ , and have calculated  $s_T$  through both the impedance and transmission line models.

### 3.2 Single Antenna Receiving

The impedance model of a single antenna during reception is given in Figure 8a. Figure 8b illustrates the accompanying traveling wave parameters. Let us find the voltage across the termination,  $v_T$ . Let  $v_A$  be the voltage across the antenna port. Then we can find  $v_A$  from the current out of the port,  $i_A$ .

$$v_A = -\hat{z}_T i_A \quad (3.8)$$

But,  $i_A$  is given by

$$i_A = -(\hat{z}_T + z_A)^{-1} v_{oc} \quad (3.9)$$

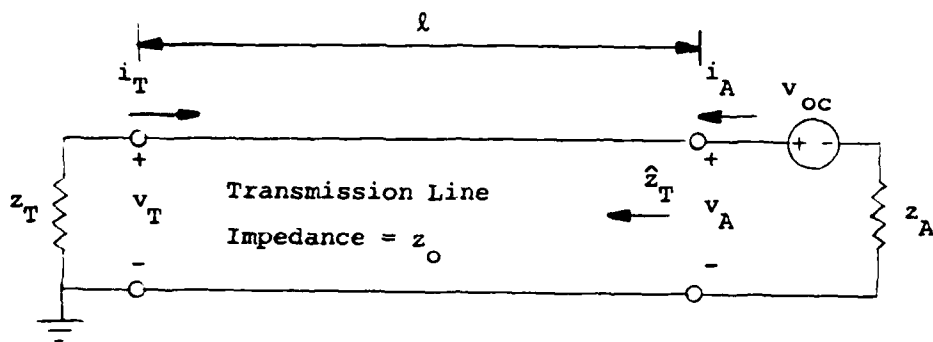
therefore, by combining Equations (3.8) and (3.9), we obtain

$$v_A = \hat{z}_T (\hat{z}_T + z_A)^{-1} v_{oc} \quad (3.10)$$

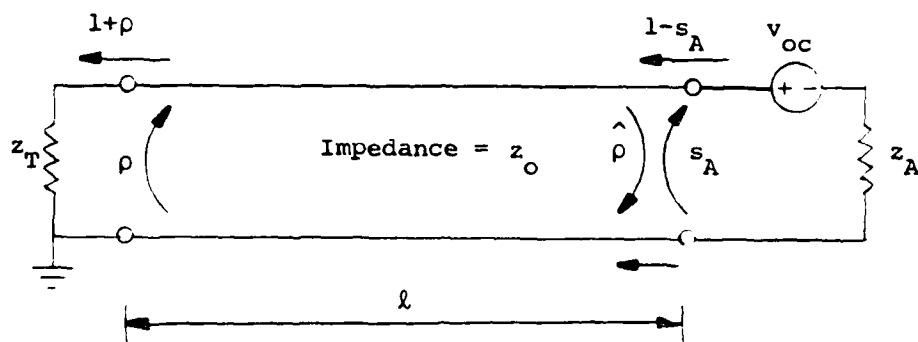
From Rule 2 of Appendix C.1, we know that

$$\hat{z}_T = (1 + \hat{\rho})(1 - \hat{\rho})^{-1} z_o$$

where  $\hat{\rho}$  is the reflection coefficient seen looking into the transmission line at the antenna. Substituting this into Equation (3.10), we obtain



8a) Impedance Model



8b) Voltage Traveling Wave Relationships within the Transmission Lines

Figure 8 Impedance Model of Single Element Array Receiving



$$\begin{aligned}
v_A &= (1 + \hat{\rho})(1 - \hat{\rho})^{-1} z_o [(1 + \hat{\rho})(1 - \hat{\rho})^{-1} z_o + z_A]^{-1} v_{oc} \\
&= (1 + \hat{\rho}) z_o [(1 + \hat{\rho}) z_o + (1 - \hat{\rho}) z_A]^{-1} v_{oc} \\
&= (1 + \hat{\rho}) z_o [(z_A + z_o) - \hat{\rho}(z_A - z_o)]^{-1} v_{oc} \\
&= (1 + \hat{\rho}) z_o (z_A + z_o)^{-1} [1 - \hat{\rho}(z_A - z_o)(z_A + z_o)^{-1}]^{-1} v_{oc}
\end{aligned}$$

But  $s_A = (z_A - z_o)(z_A + z_o)^{-1}$  and  $z_o(z_A + z_o)^{-1} = 1/2(1 - s_A)$ , therefore,

$$v_A = 1/2(1 + \hat{\rho})(1 - s_A)(1 - \hat{\rho}s_A)^{-1} v_{oc} \quad (3.11)$$

To relate  $v_A$  to  $v_T$ , we must consider the traveling waves within the transmission line. Let  $\hat{y}$  be the voltage traveling toward the termination, measured at the antenna end of the transmission line. Since there is no source in the termination, the total voltage at the antenna end of the transmission line is  $\hat{y}$  plus the corresponding reflected voltage  $\hat{\rho}\hat{y}$ . Therefore,

$$v_A = (1 + \hat{\rho})\hat{y} \quad \text{and}$$

$$\hat{y} = (1 + \hat{\rho})^{-1} v_A.$$

If  $y$  is the voltage traveling toward the termination, incident on the termination, then  $y = d\hat{y}$ , where  $d = e^{-j\beta\ell}$ , is the delay associated with the transmission line of length  $\ell$ . Finally, the total voltage at the termination,  $v_T$ , is the sum of incident and reflected voltages at the termination.

$$\begin{aligned}
v_T &= (1 + \rho)y \\
&= (1 + \rho)d\hat{y} \\
&= (1 + \rho)d(1 + \hat{\rho})^{-1}v_A \\
&= 1/2(1 + \rho)d(1 - s_A)(1 - \hat{\rho}s_A)^{-1}v_{oc} \\
&= 1/2(1 + \rho)(1 - \hat{s}_A\rho)^{-1}d(1 - s_A)v_{oc} \tag{3.12}
\end{aligned}$$

$$\text{where } \hat{\rho} = d^2\rho \text{ and } \hat{s}_A = d^2s_A.$$

If we compare  $v_T$  to the definition of  $y_s$ , we see that  $y_s = v_T$  with  $z_T = z_0$  or equivalently  $\rho = 0$ . Similarly, as in the case of  $m$ , this could serve as an alternate definition of  $y_s$ .

$$\begin{aligned}
y_s &= v_T \Big|_{\rho=0} \\
&= 1/2d(1 - s_A)v_{oc} \tag{3.13}
\end{aligned}$$

Let us examine Equation (3.13). From Equation (C6) of Appendix C.1 we know that the traveling voltage from the antenna, incident on the antenna-transmission line interface, is simply  $(1/2)v_{oc}$ . The reflection coefficient seen from the antenna is  $-s_A$  and the transmission coefficient is then  $1 - s_A$ . Thus, the traveling voltage wave that gets transmitted through this interface is  $(1/2)(1 - s_A)v_{oc}$ .  $y_s$  is simply this voltage multiplied by  $d$  to account for the delay in the length of the transmission line.

Equation (3.12) can also be quickly derived through the transmission line model. Let the argument in the preceding paragraph establish Equation (3.13). Then the total voltage in the transmission line incident on the termination,  $y$ , is given by Equation (2.2) as applied to a single antenna case.

$$y = 1/2(1 - m\rho)^{-1}d(1 - s_A)v_{oc}$$

The vector  $\underline{u}$  is physically dimensionless. While its physical meaning is not obvious,  $\underline{u}$  does contain all the information of the incident signals necessary to form the nulls. From Equation (4.7) we can write

$$P(\underline{Mu} - \underline{m}_0) = \underline{u} \quad (4.8)$$

Since  $P$  is a diagonal matrix, Equation (4.8) represents  $N$  equations of the form

$$\rho_n = \frac{[\underline{u}]_n}{[\underline{Mu}]_n - m_{0n}} \quad (4.9)$$

where  $[\cdot]_n$  represents the  $n$ th entry of the vector argument.

There are possible sets of initial signal vectors,  $\underline{y}_{sn}$ , which will result in a  $\underline{u}$  that causes the denominator of Equation (4.9) to be zero. This means the array, for that combination of the  $N$  incoming signals, loses a degree of freedom in the control space and will only be able to null  $N-1$  signals. This, however, is not a particularly scandalous result. Similar behavior is observed in a conventional adaptive array with an unweighted main antenna. Consider the 3 element array in Figure 13. Since the arrival directions of the signals are symmetric about an axis through the two auxiliary antennas, the relative phase between the two signals will be the same at both antennas. If the two antennas have identical azimuthal gain patterns, then the signal at one antenna will be linearly dependent on the other, i.e., the signals will be equal except for a complex scalar. In this case only one of the signals can be nulled.

The concept of degrees of freedom is a useful concept in adaptive arrays. In a conventional array with an unweighted main antenna, the number of degrees of freedom is generally the number of weighted auxiliaries. Similarly in a parasitic array, with a constant termination on the main antenna, the number of degrees of freedom is generally equal to the number of active complex terminations. The number of signals that can be canceled is equal to the number of degrees of freedom.

A degree of freedom can be lost in several ways. In the example above in Figure 13, a degree of freedom was lost because the signals were linearly dependent at the weighted antennas but the signal at the main antenna was independent of the weighted antenna signal. Also

Now the equations of (4.1) can be rewritten as

$$\begin{aligned}\underline{Y}_0^T &= \underline{Y}_{s0}^T + \underline{m}_{00} \rho_0 \underline{Y}_0^T + \underline{m}_0^T P Y \\ Y &= Y_s + \underline{m}_0 \rho_0 \underline{Y}_0^T + M P Y\end{aligned}\quad (4.2)$$

If the reflectivities needed for a null are used then  $\underline{Y}_0 = 0$ , and Equations (4.2) become

$$0 = \underline{Y}_{s0}^T + \underline{m}_0^T P Y \quad (4.3a)$$

$$Y = Y_s + M P Y \quad (4.3b)$$

Let us solve Equation (4.3b) for Y (compare to Equation 2.5b).

$$Y = (I - M P)^{-1} Y_s \quad (4.4)$$

Substitute Equation (4.4) into Equation (4.3a).

$$0 = \underline{Y}_{s0}^T + \underline{m}_0^T P (I - M P)^{-1} Y_s \quad (4.5)$$

If  $Y_s$  is not invertible, that means the set of vectors of initial auxiliary voltage waves is linearly dependent. The system is not fully constrained. Two signals may be arriving from the same direction. In the process of nulling N-1 signals the Nth will be nulled for "free".

Assuming that all the signal vectors are independent let us post multiply both sides of Equation (4.5) by  $Y_s^{-1}$ .

$$0 = \underline{Y}_{s0}^T Y_s^{-1} + \underline{m}_0^T P (I - M P)^{-1} \quad (4.6)$$

Now let us post multiply both sides of Equation (4.6) by  $(I - M P)$ .

$$\begin{aligned}0 &= \underline{Y}_{s0}^T Y_s^{-1} (I - M P) + \underline{m}_0^T P \\ &= \underline{Y}_{s0}^T Y_s^{-1} + (\underline{m}_0^T - \underline{Y}_{s0}^T Y_s^{-1} M) P \\ &= \underline{u}^T + (\underline{m}_0^T - \underline{u}^T M) P\end{aligned}\quad (4.7)$$

$$\text{where } \underline{u}^T = \underline{Y}_{s0}^T Y_s^{-1} \quad \text{or} \quad \underline{u} = (Y_s^{-1})^T \underline{Y}_{s0}$$

#### 4.0 NULL FORMING CAPABILITY OF AN ACTIVELY TERMINATED PARASITIC ARRAY

##### 4.1 Forming N Nulls on N Simultaneous Signals

In this section on forming multiple nulls, it has been assumed that all the signals are at the same frequency. This was required so that the array coupling matrix,  $M_+$ , would be the same for all the signals desired to be canceled. In Chapter 5 when adaptive control is discussed it will also be assumed that these signals are uncorrelated. This constraint is applied to keep the analysis tractable. Cancellation of signals of different frequencies is possible and is discussed briefly later, but a detailed analysis was not possible under this contract.

Given a parasitic array of a main antenna and N auxiliaries, let us find the reflectivities,  $\rho_n$ , necessary to null N signals. Let each incident signal be expressed by the voltage waves that the signal produces in each transmission line incident on the termination, in the absence of the other signals and with all terminations =  $z_0$  (the transmission line characteristic impedance). Let the vector of the voltage waves at the N auxiliary antennas from the nth signal be  $y_{sn}$  and the main antenna voltage  $y_{s0n}$ . Similarly, let  $y_n$  be the vector of final voltage waves incident on the auxiliary termination and  $y_{0n}$  the final voltage wave incident at the main antenna termination for the current set of reflectivities due to the nth signal. These quantities can be related by the following equations (see Equation 2.3).

$$\begin{aligned} y_{01} &= y_{s01} + m_{00}\rho_0 y_{01} + m_0^T P y_1 \\ y_1 &= y_{s1} + m_0 \rho_0 y_{01} + M P y_1 \\ &\vdots \\ y_{0N} &= y_{s0N} + m_{00}\rho_0 y_{0N} + m_0^T P y_N \\ y_N &= y_{sN} + m_0 \rho_0 y_{0N} + M P y_N \end{aligned} \quad (4.1)$$

The i,j indices of each  $y_{ij}$  denote the antenna and signal source respectively. To express these more compactly, let us define the following:

$$y_0 = \begin{pmatrix} y_{01} \\ \vdots \\ y_{0N} \end{pmatrix}, \quad y_{s0} = \begin{pmatrix} y_{s01} \\ \vdots \\ y_{s0N} \end{pmatrix}, \quad y = [y_1 | \dots | y_N]$$

$$\text{and } y_s = [y_{s1} | \dots | y_{sN}]$$

the antenna sources  $\underline{v}_{oc}$ , incident on the transmission line antenna port interfaces, will be  $\frac{1}{2} \underline{v}_{oc}$ . The voltages transmitted into the transmission lines will be  $\frac{1}{2} (I - S_A) \underline{v}_{oc}$ .  $\underline{v}_{s+}$  is simply the vector of transmitted waves as they appear at the other end of the transmission lines, i.e., phase-delayed by D.

Now knowing  $S_A$  (the scattering matrix of the antenna)  $= (Z_A - z_o I)(Z_A + z_o I)^{-1}$  and using identities A.3 and A.6 reduces Equation (3.26) further.

$$\underline{v}_A = \frac{1}{2}(I + \hat{P}_+)(I - S_A \hat{P}_+)^{-1}(I - S_A)\underline{v}_{oc} \quad (3.27)$$

The voltages of interest however are  $\underline{v}_T$ .

$$\begin{aligned} \underline{v}_T &= (I + P_+)\underline{y} \\ &= (I + P_+)D\hat{\underline{y}} \end{aligned} \quad (3.28)$$

$\hat{\underline{y}}$  is the vector of voltage traveling waves entering the transmission lines at the antenna ends and flowing toward the terminations; therefore,

$\underline{v}_A = (I + \hat{P}_+)\hat{\underline{y}}$ , and  $\hat{\underline{y}} = (I + \hat{P}_+)^{-1}\underline{v}_A$ . We now substitute this expression for  $\hat{\underline{y}}$  into Equation (3.28).

$$\begin{aligned} \underline{v}_T &= (I + P_+) D (I - \hat{P}_+)^{-1} \underline{v}_A \\ &= \frac{1}{2}(I + P_+) D (I - S_A \hat{P}_+)^{-1} (I - S_A) \underline{v}_{oc} \\ &= \frac{1}{2}(I + P_+) D (I - S_A D P_+ D)^{-1} (I - S_A) \underline{v}_{oc} \\ &= \frac{1}{2}(I + P_+) (I - D S_A D P_+)^{-1} D (I - S_A) \underline{v}_{oc} \\ &= \frac{1}{2}(I + P_+) (I - S_A P_+)^{-1} D (I - S_A) \underline{v}_{oc} \\ &= \frac{1}{2}(I + P_+) Q^{-1} D (I - S_A) \underline{v}_{oc} \end{aligned} \quad (3.29)$$

Equation (3.29) shows the relationship of the voltage across the terminations  $\underline{v}_T$  to the open circuit voltages using transmission line parameters. By comparing Equations (3.28) and (3.29), one can find an expression for  $\underline{y}_{s+} = Q_+ \underline{y}$  in terms of  $\underline{v}_{oc}$ .

$$\underline{y}_{s+} = \frac{1}{2} D (I - S_A) \underline{v}_{oc} \quad (3.30)$$

Let us analyze this equation a little. In a manner similar to the derivation of Equation (C18) it can be shown that the voltage waves from

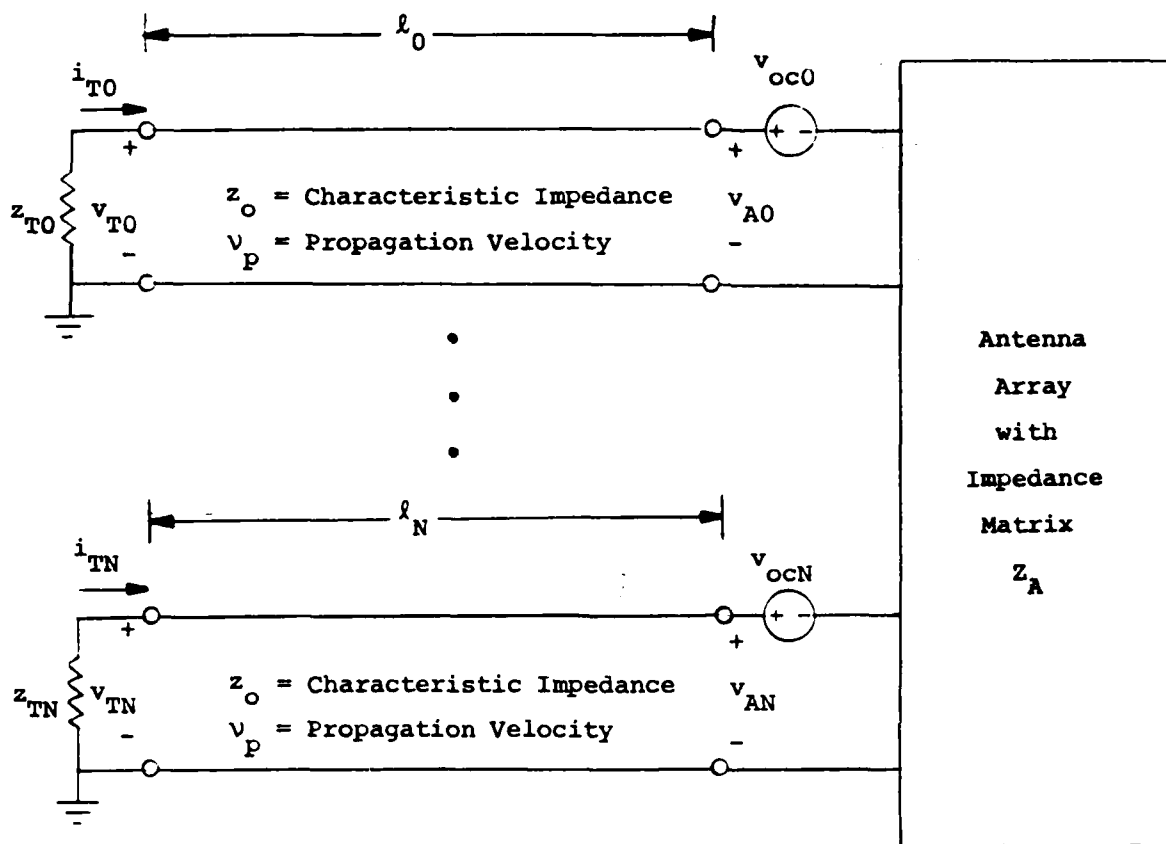


Figure 12 Impedance Model of Multiple Element Array Receiving



The impedance model of a multiple antenna array receiving is given in Figure 12. As in Section 3.3 the indices for  $N + 1$  antenna elements shall be  $0, \dots, N$ , where 0 is the main antenna. Figure 12 illustrates the various transmission line parameters for a receiving array. The usual quantities of interest for a receiving array are the voltages across the terminations  $\underline{v}_T$ .

Within the transmission line model,  $\underline{v}_T$  is the vector of voltages transmitted to the termination; therefore,

$$\underline{v}_T = (I + P_+) \underline{y}_+ . \quad (3.22)$$

Equation (2.2) tells us  $\underline{y}_+ = Q_+^{-1} \underline{y}_{S+}$ . This can be substituted into Equation (3.22) to obtain  $\underline{v}_T$  in terms of the transmission line parameters.

$$\underline{v}_T = (I + P_+) Q_+^{-1} \underline{y}_{S+} . \quad (3.23)$$

For the impedance model the calculation is more involved, unless the transmission lines are of zero length, in which case Equation (2.8) may be employed. With transmission lines one must use the equations of Appendix C.2. First one must find  $\underline{v}_A$ , the vector of port voltage of the array.

$$\underline{v}_A = \hat{Z}_T (\hat{Z}_T + Z_A)^{-1} \underline{v}_{oc} \quad (3.24)$$

where  $Z_T$  is the diagonal matrix of the terminating impedances as seen from the antenna end of the transmission lines. From Rule 2 of Appendix C.2, we find

$$\hat{Z}_T = (I + \hat{P}_+) (I - \hat{P}_+)^{-1} z_o \quad (3.25)$$

where  $\hat{P}_+$  is the diagonal matrix of reflection coefficients of the terminations translated down the transmission lines to the antennas and  $z_o$  (a scalar) is the characteristic impedance of the transmission lines. Substituting Equation (3.25) into (3.24) and manipulating the equations somewhat yields

$$\underline{v}_A = (I + \hat{P}_+) [I + (z_o I + Z_A)^{-1} (z_o - Z_A) \hat{P}_+] z_o (z_o I + Z_A)^{-1} \underline{v}_{oc} \quad (3.26)$$

At this point, let me restate the conventions on the use of "+" as a subscript, as put forward in the Glossary of Section 1.4. With the variables:  $y_+$ ,  $y_{s+}$ ,  $M_+$ ,  $P_+$ , or  $Q_+$ , the subscript signifies that the variable describes the entire array of main and auxiliary antennas. When "+" is used with parentheses with the variables:  $v_{(+)}$  or  $\underline{v}_{(+)}$ , it signifies that the variable represents a traveling wave or waves, and in particular voltage waves traveling toward the antennas (see Appendix C).

The individual total voltage wave,  $y_n$ , incident on each termination interface transmits a voltage wave of  $(1 + \rho_n)y_n$  through the interface and into the termination. This is expressed for all the voltage waves in vector form by  $(I + P_+)y_+$ .

The total voltage wave within the nth termination traveling away from the termination-transmission line interface is the sum of  $(1 + \rho_n)y_n$  and an initial reflection from  $v_{n(+)}$  incident upon the termination-transmission line interface. This initial reflection is  $-\rho_n v_{n(+)}$ . In vector form, this sum is  $(I + P_+)y_+ - P_+ \underline{v}_{(+)}$ . However, we also know that this total voltage wave is simply (by definition)  $S_T \underline{v}_{(+)}$ .

$$\begin{aligned} S_T \underline{v}_{(+)} &= (I + P_+)y_+ - P_+ \underline{v}_{(+)} \\ &= \left[ (I + P_+)(I - M_+ P_+)^{-1} M_+ (I - P_+) - P_+ \right] \underline{v}_{(+)} \end{aligned} \quad (3.20)$$

Thus we have found an expression for  $S_T$ .

$$\begin{aligned} S_T &= (I + P_+)(I - M_+ P_+)^{-1} M_+ (I - P_+) - P_+ \\ &= (I + P_+) Q_+^{-1} M_+ (I - P_+) - P_+ \end{aligned} \quad (3.21)$$

It can be shown that this form for  $S_T$  is equivalent to Equation (3.16), noting that  $M_+ = \hat{S}_A$ . This is done in Appendix D.

### 3.4 Multiple Element Array Receiving

The material presented in Section 3.2 is generalized in this section for the multiple antenna array. As in Section 3.3 voltage and currents will now become vectors of voltages and currents. The reflection and transmission coefficients will become matrices.

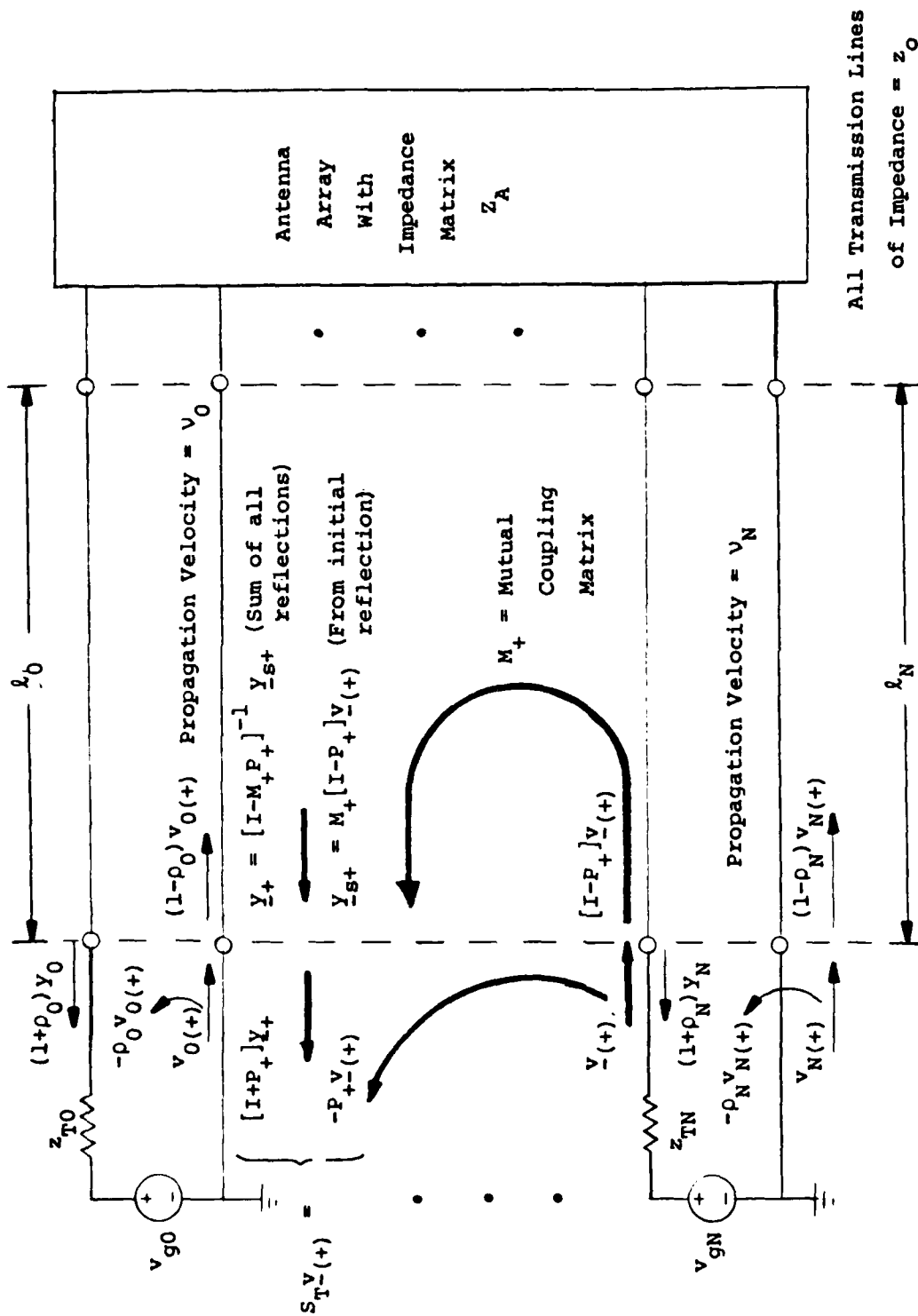


Figure 11 Transmission Line Model of Multiple Element Array Transmitting

$$\text{where } D = \begin{pmatrix} e^{-j\beta_0 \ell_0} & & 0 \\ & \ddots & \\ 0 & & e^{-j\beta_N \ell_N} \end{pmatrix} \quad \text{and } \beta_n = \frac{\omega}{v_n}$$

Note that  $\hat{S}_A$  is independent of the terminating impedances,  $z_{Tn}$ 's. Thus  $M_+ = \hat{S}_A$  and be used to calculate the mutual coupling matrix from the antenna impedance matrix,  $Z_A$ , the characteristic impedance  $z_0$ , and the transmission line length  $\ell_n$ 's.

In addition, one can solve Equation (3.17) for  $Z_A$  in terms of  $\hat{S}_A = M_+$ . If desired one can calculate  $Z_A$  from  $M_+$ .

$$Z_A = z_0 [I - D^{-1} M_+ D^{-1}]^{-1} [I + D^{-1} M_+ D^{-1}] \quad (3.18)$$

We shall now obtain Equation (3.16) from the transmission line model. Consider a voltage wave,  $v_{n(+)}1$  from each source, traveling toward the antenna and incident on the termination-transmission line interfaces. Let all these voltage waves be combined into the vector  $\underline{v}_{(+)}$ . At the  $n$ th interface, the transmitted wave (ignoring further reflections) is then  $(1 - \rho_n) v_{n(+)}$ . Considering all  $N + 1$  interfaces, in vector notation this becomes  $(I - P_+) \underline{v}_{(+)}$  where  $P_+$  is the diagonal matrix of the  $N + 1$  reflection coefficients (see glossary in Section 1.4). These voltage waves are illustrated in Figure 11. These voltage waves toward the antennas are coupled (or scattered or reflected) through the antennas to produce reverse traveling waves toward the terminations. The reverse voltage waves incident upon the terminations from a single round trip, in vector notation are  $M_+ (I - P_+) \underline{v}_{(+)}$ . Let us consider these initial reverse traveling waves as equivalent initial waves produced by an imaginary incident plane wave. Let the vector of these voltage waves be  $\underline{y}_{s+}$ . From Equation (2.2), the final (after all reflections) voltage waves traveling toward the terminations and incident on the termination-transmission line interface will be  $\underline{y}_+$ , where

$$\underline{y}_+ = (I - M_+ P_+)^{-1} \underline{y}_{s+} \quad (2.2)$$

$$= (I - M_+ P_+)^{-1} M_+ (I - P_+) \underline{v}_{(+)} \quad (3.19)$$

$\hat{Z}_A$ , the impedance matrix seen at the termination end of the cables, can be calculated from  $\hat{S}_A$  and Rule 3 of Appendix C.2, where  $\hat{S}_A$  is the scattering matrix seen from the termination ends just inside the cables.

$$\hat{Z}_A = [I - \hat{S}_A]^{-1} [I + \hat{S}_A] z_o \quad (3.14)$$

Thus Equation (3.13) can be rewritten as

$$S_T = \left[ [I - \hat{S}_A]^{-1} [I + \hat{S}_A] z_o - Z_T \right] \left[ [I - \hat{S}_A]^{-1} [I + \hat{S}_A] z_o + Z_T \right]^{-1} \quad (3.15)$$

Equation (3.15) is the generalized form of Equation (3.1). Let us manipulate further this form for  $S_T$ . From Identity A.3 of Appendix A, we see that  $[I - \hat{S}_A]^{-1} [I + \hat{S}_A] = [I + \hat{S}_A][I - \hat{S}_A]^{-1}$ .

$$\begin{aligned} S_T &= \left[ [I + \hat{S}_A][I - \hat{S}_A]^{-1} z_o - Z_T \right] \left[ [I + \hat{S}_A][I - \hat{S}_A]^{-1} z_o + Z_T \right]^{-1} \\ &= \left[ [I + \hat{S}_A] z_o - Z_T [I - \hat{S}_A] \right] [I - \hat{S}_A]^{-1} [I - \hat{S}_A] \left[ [I + \hat{S}_A] z_o + Z_T [I - \hat{S}_A] \right]^{-1} \\ &= \left[ [Z_T + z_o I] \hat{S}_A - [Z_T - z_o I] \right] \left[ [Z_T + z_o I] - [Z_T - z_o I] \hat{S}_A \right]^{-1} \\ &= [Z_T + z_o I] \left[ \hat{S}_A - [Z_T + z_o I]^{-1} [Z_T - z_o I] \right]^{-1} \\ &\quad \cdot \left[ I - [Z_T + z_o I]^{-1} [Z_T - z_o I] \hat{S}_A \right]^{-1} [Z_T + z_o I]^{-1} \end{aligned}$$

By applying Identity A.3 again,  $[Z_T + z_o I]^{-1} [Z_T - z_o I] = [Z_T - z_o I][Z_T + z_o I]^{-1} = P_+$ , and

$$S_T = [Z_T + z_o I] [\hat{S}_A - P_+] [I - P_+ \hat{S}_A]^{-1} [Z_T + z_o I]^{-1} \quad (3.16)$$

Here Equation (3.16) is the generalized form of Equation (3.2). As in the single antenna case let us now set all the terminating impedances to  $z_o$ , i.e.,  $Z_T = z_o I$ , or equivalently  $P_+ = 0$ .

$$\begin{aligned} S_T \Big|_{P_+=0} &= 2z_o I [\hat{S}_A - 0] [I - 0 \cdot \hat{S}_A]^{-1} [2 z_o I]^{-1} \\ &= \hat{S}_A \end{aligned}$$

But  $S_T$  when  $Z_T = z_o I$  is the definition of  $M_+$ , the matrix of mutual coupling factors. Therefore it is always the case that  $M_+ = \hat{S}_A$ .

We can also calculate  $\hat{S}_A$  from Rule 3 of Appendix C.2.

$$\hat{S}_A = D [Z_A - z_o I] [Z_A + z_o I]^{-1} D \quad (3.17)$$

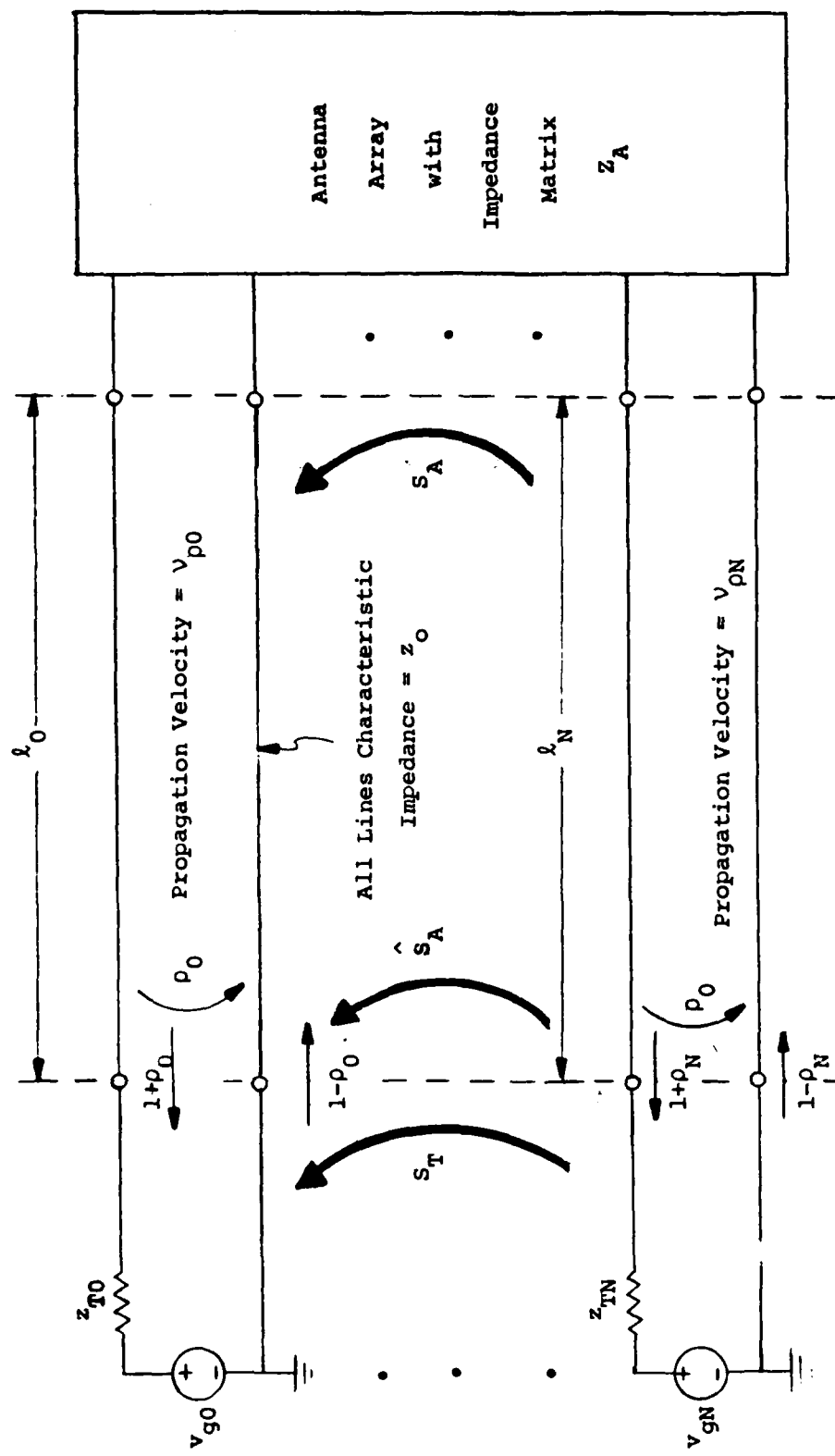


Figure 10 Voltage Traveling Wave Relationships for Multiple Transmission Lines

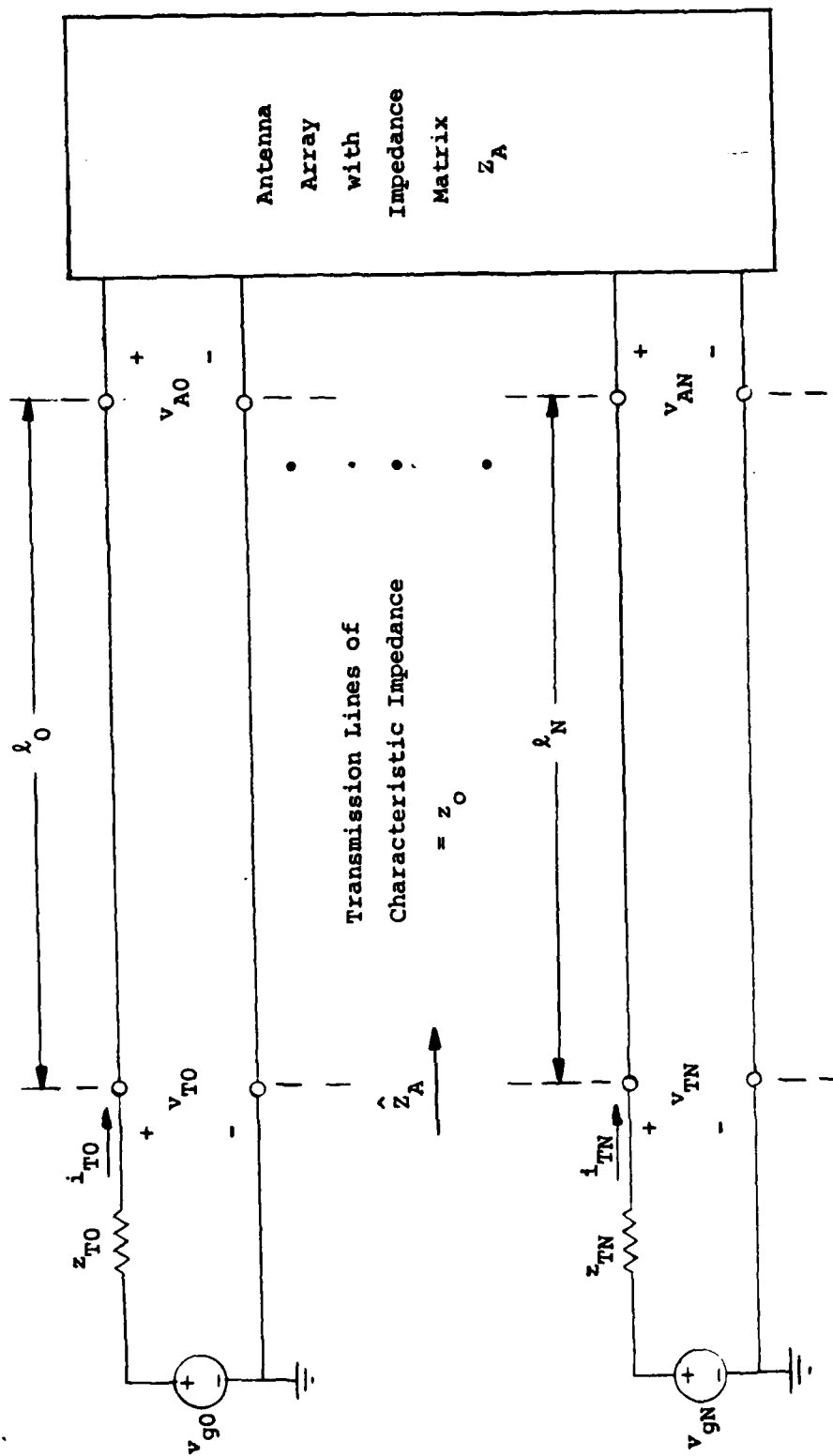


Figure 9 Impedance Model of Multiple Element Array Transmitting

The voltage across the termination,  $v_T$ , by continuity is the total voltage at the end of the transmission line. The total voltage is the sum of the incident and reflected traveling waves. Thus, we can write

$$\begin{aligned} v_T &= (1 + \rho)y \\ &= (1 + \rho)(1 - m\rho)^{-1}y_s \\ &= \frac{1}{2}(1 + \rho)(1 - m\rho)^{-1}d(1 - s_A)v_{oc} \end{aligned}$$

If we remember that  $m = \hat{s}_A$ , then we see that the above equation is indeed Equation (3.12).

In this section we have derived the relationships that exist between the transmission line model and the impedance model of a single antenna while transmitting. The voltage across the termination was derived through both models, and we obtained alternate definitions for  $y_s$ , the incident voltage on a matched termination due to a far field source, and for  $m$ , the mutual coupling coefficient.

### 3.3 Multiple Element Array Transmitting

The material presented in Section 3.1, is generalized in this section for the multiple antenna array. Voltages and currents will now become vectors of voltages and currents. The reflection and transmission coefficients will become matrices.

The impedance model of a multiple antenna array transmitting is given in Figure 9. To remain consistent with the rest of the text, we shall assume an array of  $N + 1$  elements and use the indices 0, 1, ..., N. Figure 10 illustrates the various transmission line parameters while the array is transmitting.

The transmitting array is characterized by  $S_T$ , the scattering matrix seen by the terminations looking into the transmission lines. An expression for the matrix  $S_T$  can be calculated from Equation (C11) of Appendix C.2.

$$S_T = [\hat{Z}_A - Z_T][\hat{Z}_A + Z_T]^{-1} \quad (3.13)$$



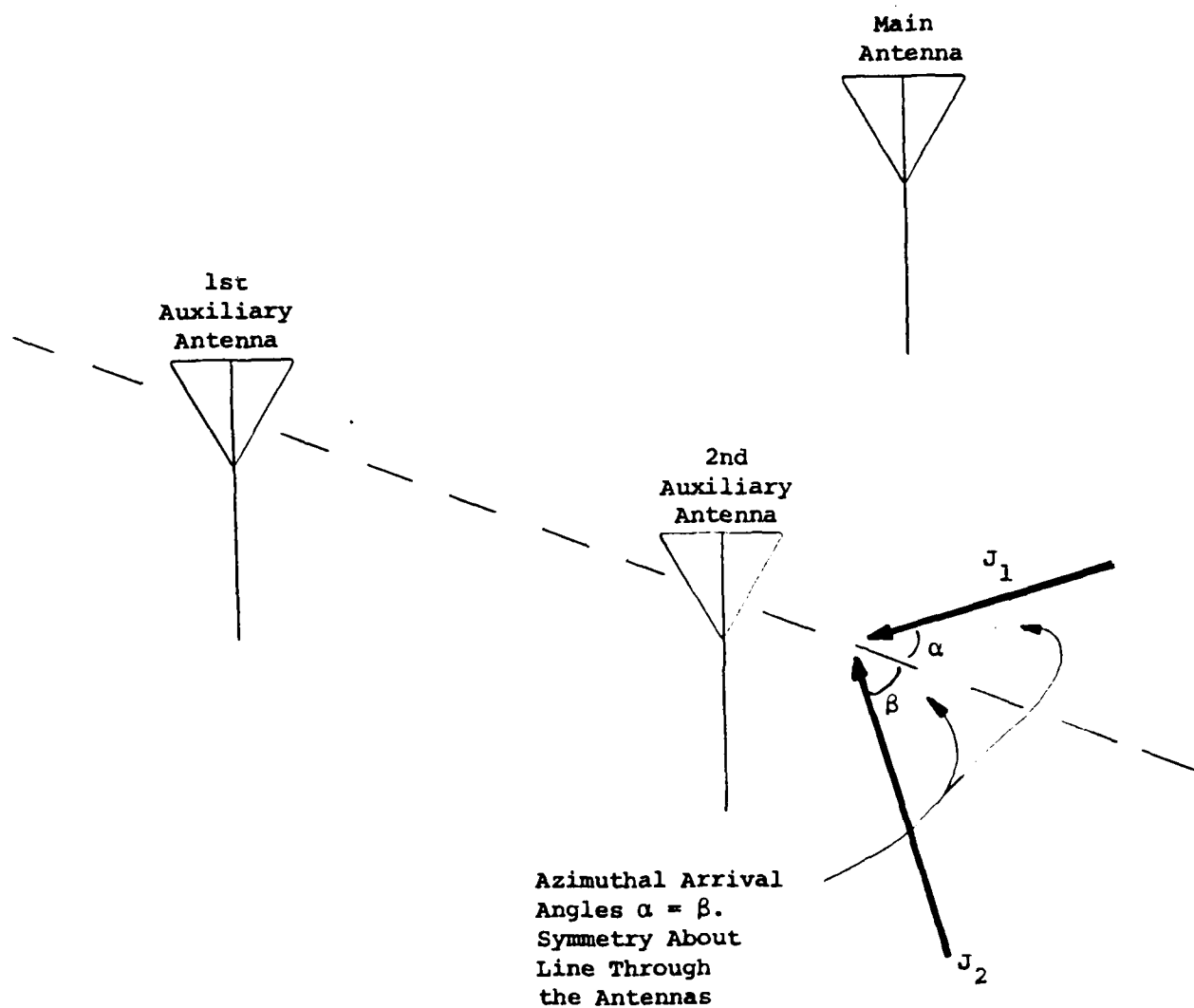


Figure 13 Scenario Which Removes a Degree of Freedom in Conventional Array

above, it was shown for a parasitic array certain combinations of incident signals could cause the loss of a degree of freedom. As will be discussed in the following section, the need to suppress an instability will also remove a degree of freedom.

The number of degrees of freedom is the dimensionality of the usable control space. Initially, the dimensionality is equal to the number of control variables, i.e., the number of complex weight or variable reflectivities. In the derivation above it was assumed the array was maximally constrained, that the  $N$  control variables were trying to null  $N$  signals. If there were fewer than  $N$  signals to null, then there would not be particular values for the reflectivities as given by Equation (4.9), but a range of suitable values.

The reflectivity values necessary to form nulls can be calculated from Equation (4.9). Before cancellation can be achieved, however, one must also determine that the array is stable for those reflectivity values. Stability is a separate issue and is addressed in the following section.

The issue of nulling signals at different frequencies will be briefly discussed. First note that at the different frequencies the mutual coupling coefficients will in general be different. Let us define  $\underline{m}_{0n}^T$  and  $M_n$  to represent the mutual coupling factors at the frequency of the  $n$ th signal. Rewriting Equation (4.1) and applying the constraint that the main antenna voltage is 0 at a null, we obtain the Equations (4.10).

$$\begin{aligned}
 0 &= y_{s01} + \underline{m}_{01}^T \underline{p} \underline{y}_1 \\
 \underline{y}_1 &= \underline{y}_{s1} + M_1 \underline{p} \underline{y}_1 \\
 &\quad \cdot \\
 &\quad \cdot \\
 0 &= y_{s0N} + \underline{m}_{0N}^T \underline{p} \underline{y}_N \\
 \underline{y}_N &= \underline{y}_{sN} + M_N \underline{p} \underline{y}_N
 \end{aligned} \tag{4.10}$$

Note these equations cannot be combined as was done before. However, the  $\underline{y}_n$  can be solved for and substituted.

$$\begin{aligned} 0 &= \underline{y}_{s01} + \underline{m}_{01}^T P (I - M_1 P)^{-1} \underline{y}_{s1} \\ &\vdots \\ 0 &= \underline{y}_{s0N} + \underline{m}_{0N}^T P (I - M_N P)^{-1} \underline{y}_{sN} \end{aligned} \quad (4.11)$$

This is a set of  $N$  nonlinear equations in  $N$  unknowns,  $\rho_1, \dots, \rho_N$ . The solutions of these equations are not easily obtained.

#### 4.2 Stability of a Parasitic Array With Active Complex Terminations

There are two types of stability that can be analyzed in reference to a parasitic adaptive array, RF stability and control stability. The issue of RF stability is independent of whatever control algorithm is being used. RF stability determines whether the system is stable for a given set of reflectivities. This section deals with RF stability. Control stability is the issue of stability and convergence of the algorithm controlling the reflectivities. Control stability is discussed in Chapter 5.

It was pointed out in Section 2.3, that given a set of reflectivity values, a parasitic array is linear in terms of plane wave inputs relative to an output to the receiver. The domain of RF stability is simply those sets of reflectivity values for which this linear system is stable. The determination of that domain is extremely complex and shall be accomplished in two steps. First a necessary condition for stability is derived and discussed. This condition is shown to be sufficient in certain cases. Several examples are analyzed to give insights into the behavior of an actively terminated parasitic array. Then a general sufficient condition is derived.

The necessary condition is derived for a specific frequency of operation. In general the mutual coupling factors,  $m_{ij}$ , will be functions of frequency. The reflectivities will also not be constant over frequency due to characteristics of the electronics. The necessary condition requires that at the frequency of operation, the array does not exhibit positive feedback.

Let us first study a single antenna. Figure 14a illustrates the signals in a single antenna. Figure 14b illustrates these signals in a system block diagram. From the equation for simple feedback the output is computed to be  $y = (1 - mp)^{-1} y_s$ , given the system is stable. It is a well known result that a necessary condition for stability is  $\text{Re}[mp] < 1$ . Stating this condition another way,  $\text{Re}[mp] > 1$  is a sufficient condition for instability.

Looking at the complete array we obtain Equation (2.1).

$$\underline{y}_+ = \underline{y}_{s+} + \underline{M}_+ \underline{P}_+ \underline{y}_+ \quad (2.1)$$

As long as  $\underline{M}_+ \underline{P}_+$  does not represent positive feedback in some manner, the array will be stable. To study the multidimensional feedback represented by  $\underline{M}_+ \underline{P}_+$  it will be convenient to introduce the concept of eigenvalues and eigenvectors.

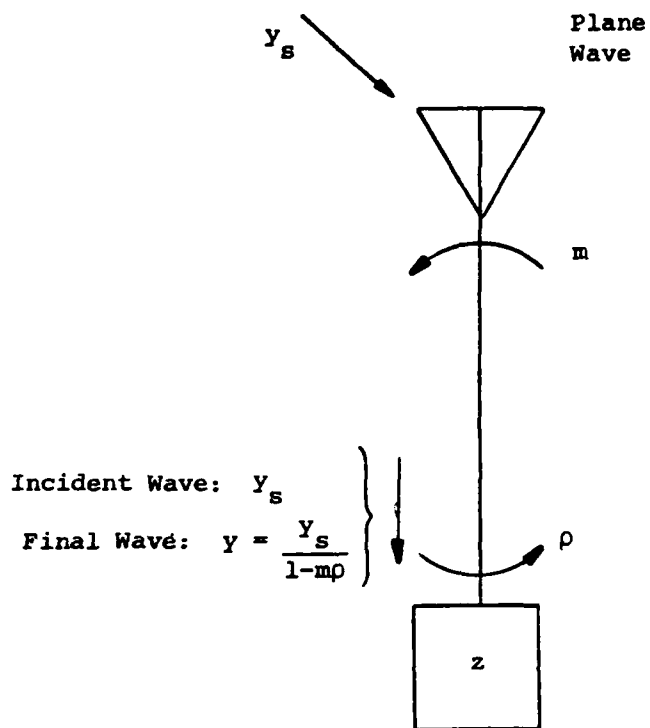
For a matrix, A, there are certain vectors called eigenvectors, that when operated on by the matrix A return a scaled version of themselves. The scale factor,  $\lambda$ , for an eigenvector,  $\underline{x}$ , is called an eigenvalue. Equation (4.12) illustrates this relationship for an eigenvalue,  $\lambda$ , and an eigenvector,  $\underline{x}$ .

$$\underline{A}\underline{x} = \lambda\underline{x} \quad (4.12)$$

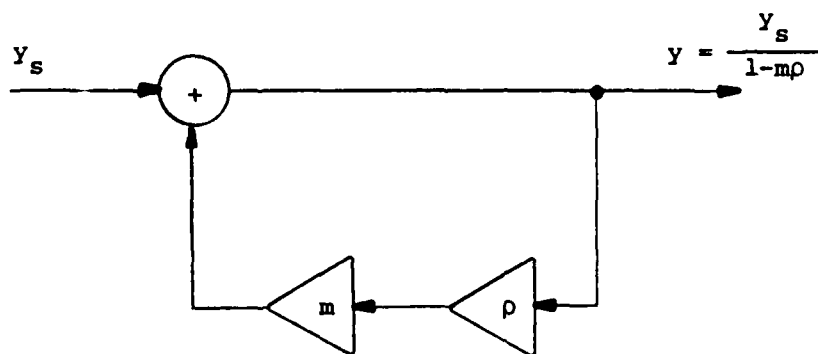
For an NxN matrix there are N eigenvalues not necessarily distinct. These eigenvalues are found as the roots of the polynomial  $\text{Det}(\lambda I - A)$ . For each eigenvalue there is an eigenvector,  $\underline{x}$ , determined to within a scalar factor. If the eigenvalues are distinct then the set of eigenvectors is linearly independent and in fact mutually orthogonal. The matrix of these eigenvectors,  $T = [\underline{x}_0 | \dots | \underline{x}_N]$ , will diagonalize A.

$$TAT^{-1} = \begin{pmatrix} \lambda_1 & & & 0 \\ & \ddots & & \\ & & \ddots & \\ 0 & & & \lambda_N \end{pmatrix}$$

If the eigenvalues are not distinct, then the set of eigenvectors may or may not be linearly independent. If they are not, a set of generalized eigenvectors can be found which is linearly independent, [16, Chapter 2]. The matrix of these generalized eigenvectors, in a manner identical to that above, will transform A into what is called Jordan form. Jordan form



14a) Signals on a Single Element Array



14b) Block Diagram Representation of a Single Element Array

Figure 14 Single Element Array Model for Stability Analysis

has the eigenvalues on the main diagonal, 1's in particular spots on the diagonal directly above it and 0's every where else. In the discussion that follows, for computational ease, it will be assumed that  $M_+ P_+$  has distinct eigenvalues. The results derived, however, can be shown valid for general matrices by considering generalized eigenvectors and their accompanying Jordan forms [16].

Let  $\lambda_0, \dots, \lambda_N$  be the  $N$  distinct eigenvalues of  $M_+ P_+$  and  $\underline{x}_0, \dots, \underline{x}_N$  the corresponding eigenvectors. Finally, let  $T = [\underline{x}_0 | \dots | \underline{x}_N]$ . Since the eigenvectors are linearly independent, the vector  $\underline{y}_+$  of Equation (2.1) can be expressed as a weighted sum of them.

$$\begin{aligned} \underline{y}_+ &= \sum_{i=0}^N a_i \underline{x}_i \\ &= T \underline{a} \text{ where } \underline{a} = \begin{pmatrix} a_0 \\ \vdots \\ a_N \end{pmatrix} \end{aligned} \quad (4.13)$$

From Equation (4.13), the weighting value for  $\underline{x}_i$  is seen to be the  $i$ th component of the vector  $T^{-1} \underline{y}_+$ . Similarly,  $\underline{y}_{s+}$  can also be written as a weighted sum of the eigenvectors.

$$\begin{aligned} \underline{y}_{s+} &= \sum_{i=0}^N b_i \underline{x}_i = T \underline{b} \\ \text{where } \underline{b} &= \begin{pmatrix} b_0 \\ \vdots \\ b_N \end{pmatrix} \text{ and } \underline{b} = T^{-1} \underline{y}_{s+} \end{aligned} \quad (4.14)$$

With Equations (4.13) and (4.14) one can rewrite Equation (2.1) as below.

$$\begin{aligned} \sum_{i=0}^N a_i \underline{x}_i &= \sum_{i=0}^N b_i \underline{x}_i + M_+ P_+ \sum_{i=0}^N a_i \underline{x}_i \\ &= \sum_{i=0}^N (b_i + \lambda_i a_i) \underline{x}_i \end{aligned} \quad (4.15)$$

We see that Equation (4.15) really represents  $N + 1$  independent equations of the form,

$$a_i = b_i + \lambda_i a_i, \quad \text{for } i = 0, \dots, N \quad (4.16)$$

Here the  $N + 1$  dependent variables  $y_0, \dots, y_N$  have been transformed into the independent variables  $a_0, \dots, a_N$ . Thus the feedback nature of the array can be expressed by  $N + 1$ , independent subsystems of the form illustrated in Figure 14b, where the loop gain is  $\lambda_i$  for the  $i$ th subsystem. We can apply the previously derived stability condition to each of these subsystems and thereby generalize the result for an  $N + 1$  element array. Given the array parameters,  $m_{ij}$  and  $\rho_n$ , as measured for a particular frequency, one can find  $\lambda_0, \dots, \lambda_N$ , the  $N + 1$  eigenvalues of  $M_+ P_+$ . Then a necessary condition for stability is  $\text{Re}[\lambda_i] < 1$  for all  $i = 0, \dots, N$ . As previously stated, this result can be shown valid for general  $M_+ P_+$ .

With a parasitic array, a useful and practical constraint is often that the reflectivity of the main antenna be zero. This means the receiver is well matched to the transmission line. Under this condition one eigenvalue of  $M_+ P_+$  is necessarily 0, and the rest are the eigenvalues of  $MP$ . Thus if  $\rho_0 = 0$ , one need only consider the array of auxiliary elements in a stability analysis.

It is shown in Appendix E if the reflectivities contain a single stage, narrow bandpass filter, such that the mutual coupling coefficients appear constant over the passband, then this stability condition is both necessary and sufficient. Such a filter was designed into the active terminations built by ZAI.

Under the assumption that a single stage narrowband filter is in use, one can perform some insightful stability analysis. In Appendix F a stability analysis is made with regard to a two element array.

Consider an example of a two element array of auxiliary antennas. It is assumed that the first antenna is well matched to its transmission line so that its self coupling, or return loss, is zero. It is also assumed that the reflectivity and self coupling of the second antenna is such that by itself it would be unstable, i.e.,  $\text{Re}[m_{22}\rho_2] \geq 1$ . It is shown in Appendix F under certain conditions,  $\text{Re}[m_{22}\rho_2] < 2$ , that an appropriate choice of  $\rho_1$  will stabilize the array.

The most general stability criterion is obtained from [16, p. 376]. Assume that the mutual coupling matrix  $M_+(s)$  is known as a function of complex frequency,  $s$ . In particular, that each entry of  $M_+(s)$  is a rational polynomial in  $s$ . Similarly, assume that the diagonal entries of  $P_+(s)$  are

rational polynomials in  $s$ . Let the polynomial  $\Delta(s)$  be the least common denominator of all the minors of all orders<sup>1</sup> of  $M_+(s)P_+(s)$ . Then the array is stable if and only if  $\det[I - M_+(\infty)P_+(\infty)] \neq 0$  and the polynomial  $\Delta(s)\det[I - M_+(s)P_+(s)]$  has no right half plane zeros.

In Appendix E, it is shown from this general criterion, that if  $f(s)$  is a single stage narrowband filter, then the necessary stability condition,  $\text{Re}[\lambda_n] < 1$ , is both necessary and sufficient.

<sup>1</sup> A minor of the  $k$ th order is formed by taking the determinant of all the elements common between  $k$  distinct rows and  $k$  distinct columns. A minor of order 1 is an element. Minors of order  $n-1$  are the minors people are most acquainted with. These are formed by "blocking out"

a row and a column and then taking the determinant. There are  $\binom{n}{k} \binom{n}{k}$  number of minors of the  $k$ th order, where  $\binom{n}{k} = \frac{n!}{k!(n-k)!}$ .

Note,  $\Delta(s)$  is not necessarily the denominator of the determinant. Consider the multivariate feedback represented by

$$G(s) = \begin{bmatrix} \frac{1}{(s+1)(s-1)} & \frac{-s}{(1+s)} \\ \frac{1}{(s-1)} & -1 \end{bmatrix} \quad . \quad \text{Then } \det G(s) = \frac{1}{s+1}, \text{ but}$$

$$\Delta(s) = (s+1)(s-1) \quad .$$



## 5.0 ADAPTIVE CONTROL OF PARASITIC ARRAY NULLS

For a parasitic array to be useful in practice, adaptive control of the terminations or reflectivities must be employed. There are several adaptive control algorithms and several ways of implementing each algorithm. We shall discuss the gradient algorithm and various search and dither algorithms and also possible methods of implementing each.

The gradient algorithm would be the fastest and probably achieve deeper nulls. The gradient tells not only when to change, but also in which direction. It will, however, use more hardware and cabling and may require a training pilot signal.

There are several possible dither algorithms, some of them closely related to the gradient algorithm and some more akin to a search algorithm. Performance and hardware needs will vary greatly depending on the algorithm and its implementation. The best compromise of performance over hardware might be some kind of dither algorithm.

Search algorithms generally will be slower. They may achieve as deep of nulls. Search algorithms, however, will require the least amount of hardware and cabling. The only connections to the terminations needed are DC control and power.

### 5.1 Least Mean Square Control of Active, Complex Terminations

In the search for an adaptive control algorithm of a compact array, one might first ask why not take the outputs of the antennas and put them into a conventional adaptive array combiner as in Figure 1. One could use such a system, but there are a few drawbacks.

First, the practical variable RF weight has a high reflection coefficient for much of its operating range. Such weights, unbuffered with the strong mutual coupling of a compact array would have an unpredictable and possibly uncontrollable effect on the array. To buffer the antennas from the weights, one would have to take a high degree of insertion loss or include active elements like an amplifier.

Second and more importantly, the mutual coupling can cause blind spots in the array pattern [19]. The effect of these blind spots might be the array loses some degrees of freedom for jammers arriving from particular directions, or there might be some direction which is always nulled and the desired signal cannot be received from that direction. Note the effects of these blind spots would be independent of the weight values, assuming the weights have been buffered.

In a parasitic array, terminated in variable impedances, blind spots due to the mutual coupling are not as great a problem. One has control over them through the variable terminations. It is possible, as was described in Section 4.1, that certain combinations of jammers can cause the loss of a degree of freedom of operation, but for an array of several elements this is highly unlikely.

## 5.2 Gradient Control

Adaptive control of a conventional array is a linear problem. The change in the output of the array is proportional to the change in any of the complex weights. Adaptive control of a parasitic array, however, is a nonlinear problem. How the array output changes with a change in a reflectivity will depend not only on the current value of that reflectivity, but also on the values of all the other reflectivities.

A generalization of the LMS algorithm for nonlinear problems is the gradient control algorithm. The gradient control law for complex variables is derived in Appendix G.2. The control law is stated in Equation (G17). This control law is applied to adaptive control of parasitic termination in Appendix G.3. The result is given in Equation (G33).

$$\rho_n = -2k y_0 (\alpha_n y_n)^* \quad (5.1)$$

$$\text{where } \alpha_n = \frac{\underline{e}_n^T Q^{-1} \underline{m}_0}{1 - \rho_0 (\underline{m}_{00} + \underline{m}_0^T P Q^{-1} \underline{m}_0)}$$

$$\text{or } = \frac{\underline{m}_0^T (I + P Q^{-1} M) \underline{e}_n}{1 - \rho_0 (\underline{m}_{00} + \underline{m}_0^T P Q^{-1} \underline{m}_0)}$$

$$\text{and } \underline{e}_n = \begin{pmatrix} 0 \\ \vdots \\ 0 \\ 1 \\ \vdots \\ 0 \end{pmatrix} \leftarrow \begin{matrix} \text{nth} \\ \text{place} \end{matrix}$$

The two expressions for  $\alpha_n$  can be shown to be equivalent. The first is more convenient for calculations. A physical understanding can be gleaned more easily from the second form. Consider the factor  $\alpha_n y_n = \partial y_0 / \partial \rho_n$ . It is the proportionality constant between a small change in  $\rho_n$  and the resultant change in  $y_0$ . Let us assume a small change  $\Delta \rho_n$ , in  $\rho_n$  and see how it changes  $y_0$ . For the moment, also assume that  $\rho_0 = 0$  so there are no

reflections off the main receiver. The change  $\Delta\rho_n$  in  $\rho_n$  changes the upward traveling wave (toward the antenna) reflected off the  $n$ th termination by  $y_n\Delta\rho_n$ . This signal is coupled to the main antenna by the factor  $m_{0n}$ . Thus  $y_0$  changes by the amount  $m_{0n}y_n\Delta\rho_n$ . Let us write this as  $\underline{m}_0^T \underline{e}_n y_n \Delta\rho_n$ . But this is not the end of the story. The signal  $y_n\Delta\rho_n$  also couples to the other antennas, changes their voltages, and this change couples to the main antenna. One can consider the initial change of  $y_n\Delta\rho_n$  in the upward traveling wave at the  $n$ th antenna as an initial change in the vector of upward traveling voltages of  $\underline{e}_n y_n \Delta\rho_n$ . This signal couples to the other auxiliary antenna by the coupling matrix  $M$ . The initial vector of downward voltages due to a change  $\Delta\rho_n$  in  $\rho_n$  is then  $\underline{M} \underline{e}_n y_n \Delta\rho_n$ . This is like a change in  $\underline{y}_s$ . The final change in the downward voltages,  $\underline{y}$ , is then  $Q^{-1} \underline{M} \underline{e}_n y_n \Delta\rho_n$ . This signal gets reflected by  $P$  and coupled to the main antenna by  $\underline{m}_0$ . Thus the change in  $y_0$  due to the change in the auxiliary voltages caused by the change in  $\rho_n$  is  $\underline{m}_0^T P Q^{-1} \underline{M} \underline{e}_n y_n \Delta\rho_n$ . If we sum these two terms and divide by  $\Delta\rho_n$ , we obtain the numerator of the second expression for  $\alpha_n$ .

If  $\rho_0 \neq 0$ , this creates a feedback loop to the main antenna through the self coupling  $m_{00}$ , and the coupling to the auxiliaries  $\underline{m}_0$ . The loop gain of this feedback is the sum of two terms. The first term, from the self coupling, is  $\rho_0 m_{00}$ . The second term takes the gain of the reflectivities  $\rho_0$  and couples it to the auxiliaries by  $\underline{m}_0$ . As above, this signal can be considered an initial signal and is turned into a final signal by  $Q^{-1}$ . This final signal gets reflected by  $P$  and coupled back to the main antenna again by  $\underline{m}_0$ , completing the loop. Thus the gain of the second loop is  $\underline{m}_0^T P Q^{-1} \underline{m}_0 \rho_0$ . The total loop gain is  $\rho_0 (m_{00} + \underline{m}_0^T P Q^{-1} \underline{m}_0)$ . We see that the denominator of  $\alpha_n$  represents positive feedback with this loop gain.

One might ask if the feedback loop is stable. It can be shown with the formula for the determinant of a partitioned matrix (Identity A.10) that this denominator is an eigenvalue of  $Q_+$  or equivalently the loop gain is an eigenvalue of  $M_+ P_+$ . The stability conditions for this loop are therefore a special case of the stability conditions described in Section 4.2.

Gradient control can be implemented with basically the same equipment as LMS control, except a method of obtaining or calculating the factor  $\alpha_n$  is needed. A basic implementation is illustrated in Figure 15. Note the

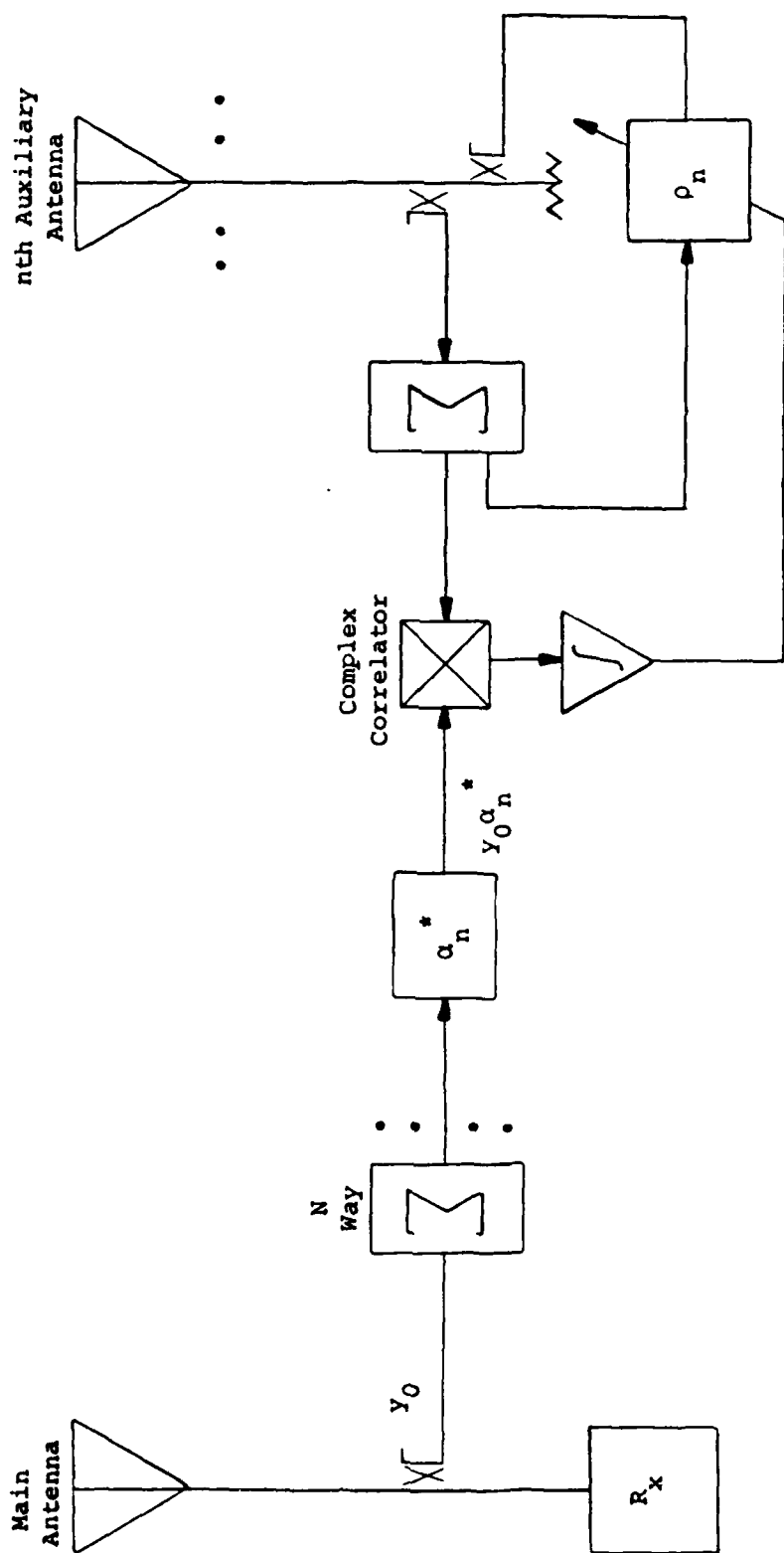


Figure 15 Basic Gradient Control Implementation

main antenna signal  $y_0$  must be sent to the control circuitry of each auxiliary. Also note that an extra complex weight will probably be needed to implement the multiplicative factor  $\alpha_n$ , or  $\alpha_n^*$ , depending on where it is placed.

In implementing gradient control in this manner, it is only necessary to determine the phase of  $\alpha_n$ . The amplitude of  $\alpha_n$  appears simply as a modification to the control loop gain  $k$ . Furthermore, small errors in the estimation of the phase of  $\alpha_n$  are not significant. Theoretically, the control loop will still work with up to  $89^\circ$  of phase error. Phase errors manifest themselves by reducing the loop gain by a factor of the cosine of the error. In practice, if one is not too concerned with settling time, phase errors of up to  $40^\circ$  can be tolerated. All this shows that whatever process is used to estimate the factor  $\alpha_n$ , it need not be extremely accurate.

Three methods of obtaining the factor  $\alpha_n$  are presented. The first method uses a pilot signal, close in frequency, sent out of the main antenna. In appendix H, it is shown that such a pilot signal (with the condition  $\rho_0 = 0$ ) will be received at the  $n$ th auxiliary antenna multiplied by the factor  $\alpha_n$ . This is measured and then used to complete the gradient algorithm. The second method is to determine all the mutual coupling factors of the array over all frequencies as well as how the filter characteristics of the reflectivities vary over frequency. This information would be stored and used to digitally calculate the necessary values of the  $\alpha_n$ . These values would then be implemented with a digitally controlled weight. The third method uses a dither to approximate  $\alpha_n$  which is then used in a gradient control system. This method also requires  $\rho_0 = 0$ . The description of this algorithm is included in this section because it implements gradient control as expressed in Equation (5.1).

Figure 16 illustrates an analog implementation of the pilot algorithm with the factor  $\alpha_n$  determined and applied by an adaptive weight. There are several points to make about this design. First, we give a description of the general operation. The reflectivity at the auxiliary antenna is implemented in polar form, as is currently being done on the NRL test array. The phase control is obtained by reflecting the signal off a variable reactance. The amplitude control is obtained with a bi-



of the reactances while observing the receiver output responding to one or more signals incident on the array. That is, the pattern was formed adaptively. Some preliminary attempts were made to use the array in a deterministic manner by using the theory developed by Harrington [6] to calculate the set of reactance values that comes closest to synthesizing a given pattern. Using a commercial RF bridge to measure the reactance value, the reactive terminations were then adjusted to have the corresponding calculated reactance. However, the approximations in the theory and the inability to measure the reactance values sufficiently accurately usually resulted in a measured pattern that differed substantially from the desired pattern. Therefore, we ended all efforts to use the array in a deterministic manner.

## 6.2 Experimental Measurements

The manual adaptation investigations were performed using two techniques to adjust the reactance values. In the first technique a single CW source was installed approximately 70 m from the array. The center element was connected to a HF receiver, tuned to the source, whose output was observed on an oscilloscope. We then adjusted the six terminating reactances sequentially and iteratively to produce a minimum in the receiver output. The azimuthal antenna pattern was then measured. In Figure 22 we show a typical pattern formed in this manner. There are two noteworthy features. First, a sharp null has indeed been formed in the direction of the source, as desired, that has a depth approximately 30 dB below the pattern main lobe, and that has a width of about 10 degrees. The remainder of the pattern is relatively featureless; except for the small dip near 240 degrees, the pattern away from the null varies no more than 3 dB.

The second noteworthy feature is that the gain of the array in azimuthal directions away from the null is, on the average, only 4.7 dB less than the gain for a monopole resonant at 20 MHz. In the sector from 30 degrees to 180 degrees, the difference decreases to 2.4 dB. Hence, the sensitivity of the array is nearly that of a monopole and does not suffer the large degradation that one might expect from such a small array. Patterns similar to Figure 10 (that is, an essentially omnidirectional pattern with a notch in the direction of an incident signal) could be formed for an incident signal of any bearing.

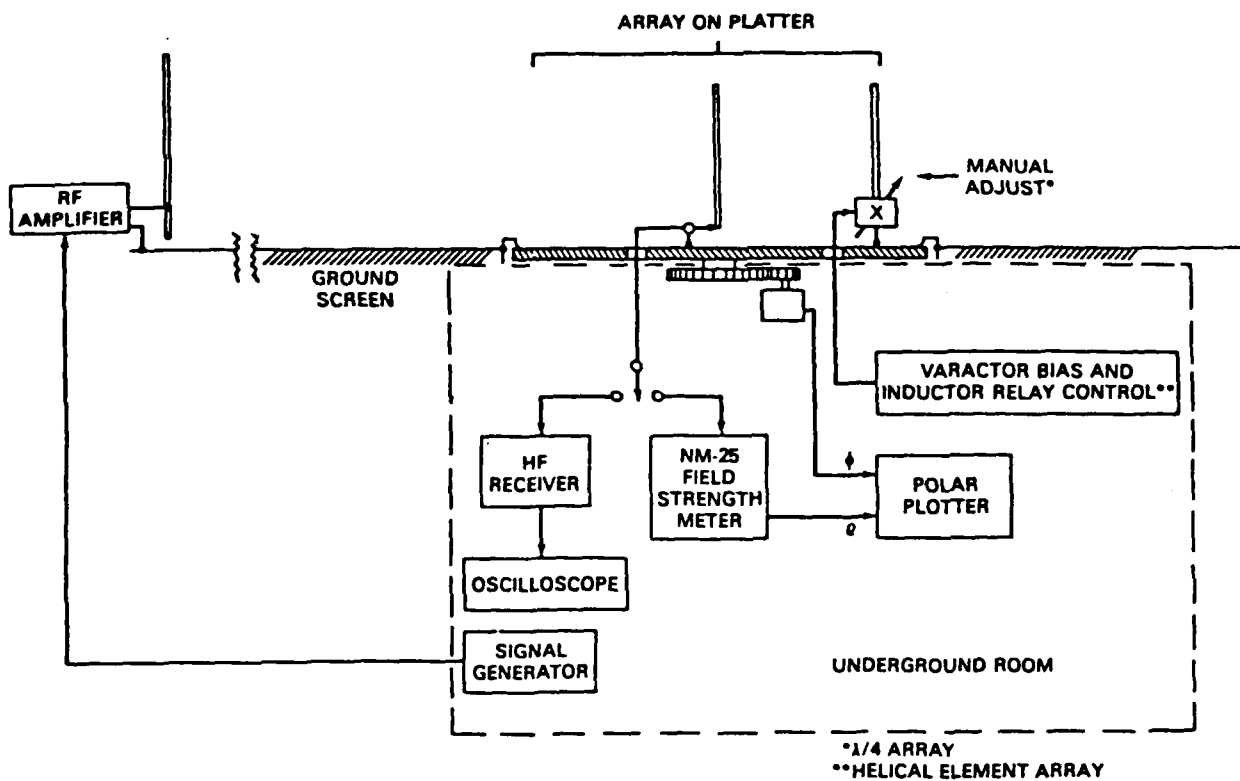


Figure 21 Antenna Array Test Setup



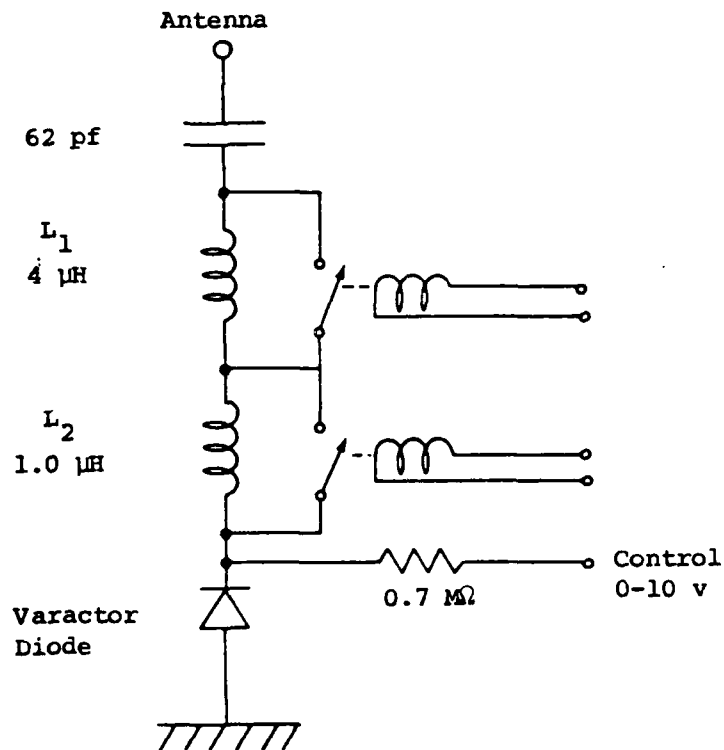


Figure 20 Variable Reactance Termination Mounted at Base of Parasitic Elements



Figure 19 Experimental Antenna Array

## 6.0 EXPERIMENTAL RESULTS WITH A PASSIVE REACTIVELY TERMINATED PARASITIC ARRAY

NRL has built an electrically small parasitic array for experimental testing. At first the elements of the array were terminated with only variable reactances. Test results with these terminations are detailed in [2-5] and are summarized here. Tests with active complex terminations are discussed in Chapter 8.

### 6.1 Experimental Parasitic Array

A seven element array was fabricated and tested by NRL to evaluate the pattern control achievable with reactively terminated parasitic arrays. Figure 19 is a photograph of the array. This array has one central element connected to a receiver and six parasitic elements. All elements are uniformly-wound helices with a 5 cm diameter and an overall height of one meter. The antennas are constructed to have a resonant frequency of about 20 MHz, and the spacing between the central element and the surrounding parasitic elements is 40 cm ( $0.027 \lambda$  at 20 MHz). The top plate visible in Figure 19 is non-metallic and is solely for rigid support of the elements.

The electronically-controllable variable reactances are mounted in the boxes at the base of each parasitic element. A schematic diagram of the reactance is given in Figure 20. Continuous control of the reactance termination is achieved by adjusting the bias voltage on a varactor diode; the continuous control range mid-point is determined by the combination of the series inductors switched into the reactance circuit. At the 20 MHz resonant frequency of the elements, the terminating reactance can be varied over a range from -450 ohms (capacitive) to +450 ohms (inductive).

The terminations shown in Figure 20 provide control only of the phase of the incident waves reflected from a parasitic element. Amplitude control, using variable attenuators alone or in conjunction with amplifiers, had not yet been implemented in the array. There is a similarity between the parasitic array described here and various "phase-only" adaptive arrays described in the literature [22].

Measurements of the array antenna pattern were made at NRL's Brandywine Antenna Range (see Figure 21). The antenna range includes a large ground plane and a rotating platter for measuring the azimuthal radiation pattern. All of the measurements reported here were made by manual adjustment

accelerated random search (GARS) algorithm is discussed in the references [22]. A guided random search always has the possibility of choosing a new point far away from the current operating region. At first glance this aspect may seem a hinderance to convergence, but because of this property a guided random search can only get temporarily hung up at a local extrema.

it may then go into a tracking mode.

We shall discuss two types of random search algorithms, the random search and the guided random search. These algorithms are somewhat akin to the exhaustive and guided univariate search algorithms discussed above. We say somewhat because the guided random search is not univariate.

The random search assigns a probability distribution to the whole control space. It may be uniform or it may be shaped by certain apriori information of the control system and/or the optimal point. The algorithm then selects an operating point at random based on this distribution and evaluates its PA. If the PA satisfies the threshold, then it stops. Otherwise it obtains another randomly generated operating point. Random search algorithms can be run with or without replacement. In an algorithm with replacement the probability distribution is unchanged from one trial to the next. In an algorithm without replacement, if an operating point selected in a trial does not pass the threshold test, then that point is removed from the control space and the distribution is renormalized. If it is a continuous distribution, then a region around the point is removed. Generally, one would want to use an algorithm without replacement unless the system is not time-invariant over the time it takes to converge. The random search without replacement is very much like the exhaustive search, except the random search stops when it finds a satisfactory operating point. It is conceivable, however, that the random search would search through all the points before finding the right one.

Just as the univariate and guided univariate searches were attempts to expedite the exhaustive search, the guided random search is an attempt to expedite the random search. In the guided random search the probability distribution described above is used for the first trial. To choose a point for a second trial a random direction from the first point is selected. Then a random distance out in this direction is selected from a distribution whose mean might be the interval used in the guided univariate search above. After the second point, one now squints the direction probabilities distribution either in the direction of the second point or in the opposite direction, depending on whether the PA was better or worse. One can also accelerate a guided random search just as the guided univariate search was accelerated. A guided

completed with it, etc. This algorithm has advantages over the exhaustive search. First, as the algorithm proceeds the output becomes more and more minimized. We reap the benefits of previous computations as we go along. Second, the algorithm converges faster, particularly if the array is underconstrained. In practice, usually after several iterations negligible further increase in performance is observed. This is the method NRL is currently using in their computer run adaptive algorithm.

A third search algorithm is the guided univariate. This algorithm is the same as the univariate except an attempt is made to minimize the number of operating points analyzed within each iteration. When the algorithm begins a new iteration of a control variable, a point, a certain interval away from current operating value is chosen. If the output at this point is less than at the initial point, the algorithm continues in this direction until the output stops decreasing. The algorithm then zeros in on the local optimal value of this variable. If the output of the first guess was higher than at the initial point, the algorithm continues in the opposite direction until the output stops decreasing and then zeros in on the local optimum. A way to reduce the number of operating points evaluated is to make the step sizes between the evaluated points variable. If a big change in the output was noticed between the last two evaluations, then make a big step in the control variable. If only a small change was noticed, then make a small step. This is called accelerating the algorithm. The guided univariate search is a more complex algorithm than the univariate search, but it will converge faster because fewer operating points are evaluated.

One problem that both the univariate search and the guided univariate search have is that they can get hung up on a local minimum of the output, or a local maximum of S/I. Random search algorithms may temporarily get hung up on a local output minimum, but will eventually find the global optimal operating point or at least a satisfactory operating point.

In all random search algorithms, one computes a performance assessment (PA) statistic for each new operating point. In our case this might be the array output power (to be minimized) or the S/I (to be maximized). Whenever the algorithm finds a point for which the PA is less than (if minimizing) or greater than (if maximizing) a particular threshold, then the algorithm stops searching. If need be,

#### 5.4 Search Algorithms

Search algorithms attempt to search the control space for the optimal operating point. Given the value of the function to be minimized at the current operating point and the past history of the function at previous operating points, a search algorithm makes a guess as to where the optimal operating point might be. All search algorithms are sequential, i.e., they choose an operating point, evaluate it and then choose another, etc. Unless the evaluation and selection of operating points is done manually, search algorithms must be implemented digitally.

An advantage of search algorithms is they require the minimal amount of hardware of all the algorithms, neglecting the computer. Other than the computer, they require only D.C. control lines to the terminations and a signal to interference ratio (S/I) detector. There is no need for correlators, adaptive control loops, pilots, or extra complex weights. Furthermore, search algorithms, because of their digital implementation, are more flexible. If one desires to modify the algorithm, he need only change the computer program. The main disadvantage of search algorithms is that they tend to be slow.

There are many types of search algorithms. We shall describe several here. The simplest in theory is the exhaustive search algorithm. In this algorithm every operating point is analyzed. The one which gives optimal performance is noted and then applied. In most systems the number of possible operating points is too great for this algorithm to be practical. This is the case here. Consider an array two complex terminations controlled by two 8 bit signals each. Thus the number of operating points to evaluate is  $2^8$  raised to the fourth power. This is  $2^{32}$  or approximately  $4 \times 10^9$ . If we could evaluate an operating point every micro-second, it would take over an hour to evaluate them all. The one advantage of the exhaustive search is that it will always select the optimal operating point.

A second type of search algorithm is the univariate search algorithm. In the univariate search one of the control variables is selected. An exhaustive search is conducted upon this variable along with all the other variables held constant. The value of this variable which gave the minimum output (or maximum S/I) over its range is then applied to it. A second variable is then selected and a similar procedure is

### 5.3 Dither Algorithms

Most dither algorithms attempt to measure the partial derivative of the function to be minimized with respect to some other variable of the system. The measurement procedure of the partial derivative is taken straight from the definition of the partial derivative: the ratio of a small change in output to the small change in the input that caused it. A particular variable of the system is "dithered" about its present value with a small amplitude A.C. signal, e.g. a sine wave, square wave, or PN coded signal. The output signal, or the signal to be minimized, is correlated with the A.C. signal. The correlator output is the partial derivative. The distinction being made here between dither algorithms and gradient algorithms is that a gradient algorithm uses a coherent (i.e. inphase and quadrature) correlator, while a dither algorithm simply detects the change in the array output power.

The dither algorithm can be implemented in an analog or digital manner. In an analog implementation the introduction of the A.C. dither signal and correlation with the output would be accomplished with analog components. The subsequent adjustment of the undithered value of the control variable could also be accomplished with analog circuitry driven by the correlator outputs. In a digital implementation the dither of the control variable and measurement of the change in the output could all be accomplished and controlled digitally. For example if the control variable is a digitally controlled weight, the dither could be implemented by alternating between to adjacent settings.

Consider the case where the various control variables are dithered individually and then all variables are changed simultaneously to new values. The amount that each variable is changed is proportional to the amount the output changed during the dither for that variable, i.e. the correlator output. Such an algorithm implements sequential gradient control.

The advantage of dither algorithms over gradient algorithms is the reduction in the amount and complexity of the analog hardware. In fact, besides the variable weights, a dither algorithm could be implemented with a computer, a power detector, an A/D convertor, and  $2 \times N$  D/A convertors. The cost for this reduction in hardware is an increase in the adaptation time for the array and under some conditions less null depth. In a changing RF environment the array may never completely adapt.



Main Antenna

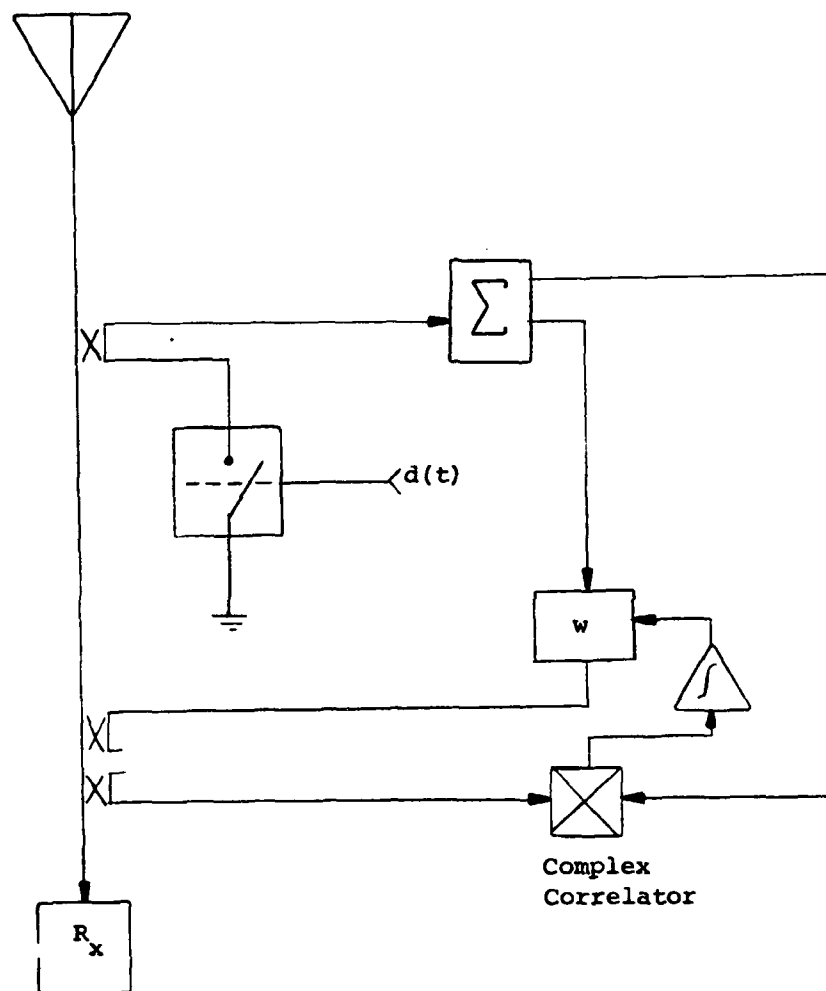


Figure 18 Main Antenna Dither Signal Canceler

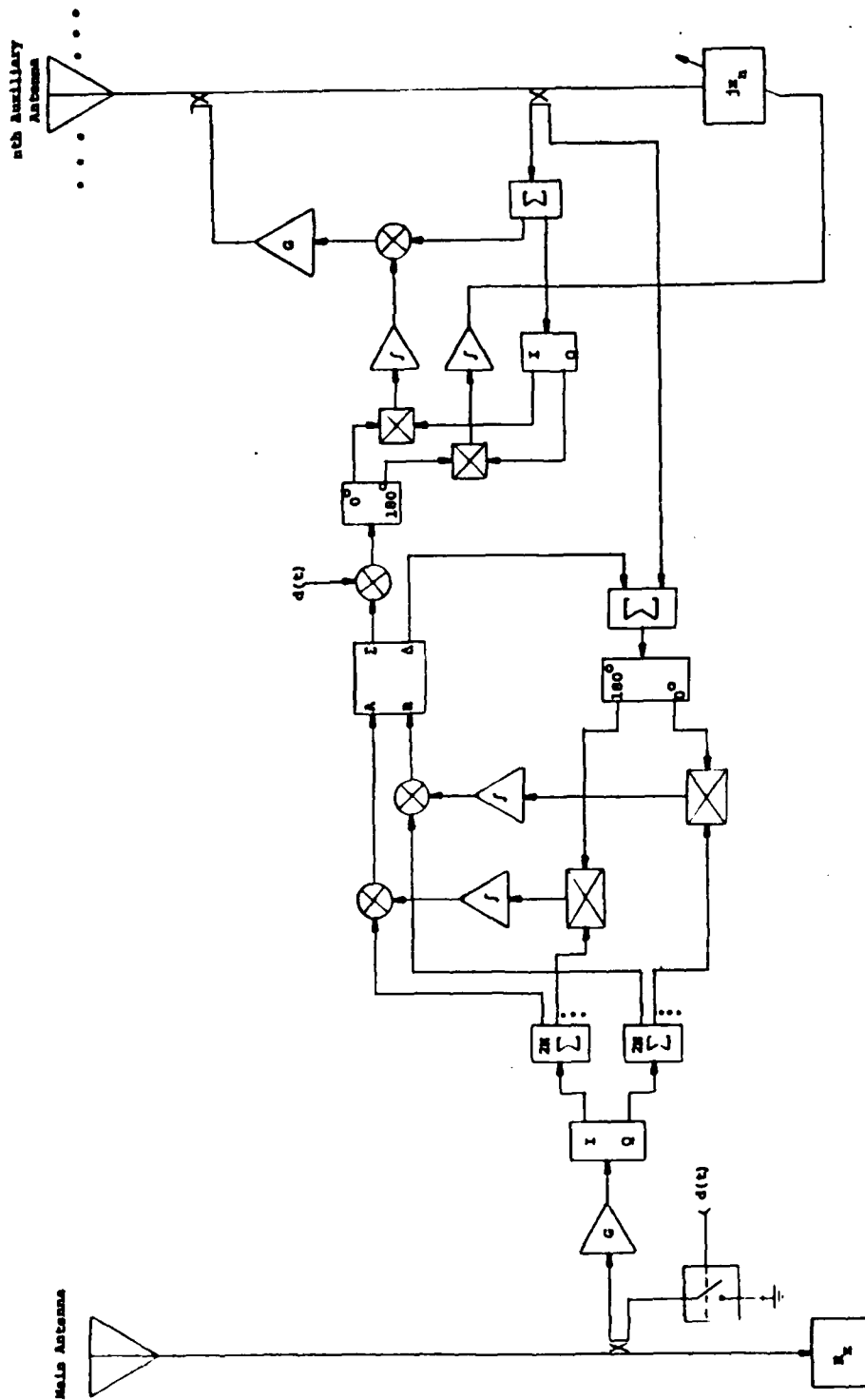


Figure 17 Design for SIC with Dither Driven Gradient Algorithm

measurement errors get compounded into significant final errors by the many mathematical operations of the computation. Here again the limitation is more severe in a larger array where there will be more operations in the calculation.

A third implementation of the gradient algorithm is a cross between a gradient algorithm and a dither algorithm. The algorithm is based on the following derivative

$$\left. \frac{\partial y_n}{\partial \rho_0} \right|_{\rho_0 = 0} = \underline{e}_n^T \underline{Q}^{-1} \underline{m}_0 y_0 = \alpha_n(\rho_0=0) \cdot y_0 \quad (5.2)$$

for  $n = 1, \dots, N$ .

These derivatives are derived in a manner similar to that used to derive  $\partial y_0 / \partial \rho_n$ . The derivatives are approximated by dithering  $\rho_0$  about  $\rho_0 = 0$  and monitoring the changes in  $y_n$ . A design for an implementation of this method is given in Figure 17. The reflectivity  $\rho_0$  is dithered by alternately terminating the appropriate port on the directional coupler with a short and open circuit. The remaining circuitry is similar to that used in the pilot implementation to estimate  $\alpha_n$ . The dither basically replaces the pilot signal. The advantage of this method is that one dither signal allows the calculation of all the gradient law constants,  $\alpha_n$ . There is no need for multiple, mutually orthogonal dither signals.

One possible disadvantage to this method is that dithered components of the desired signal may enter the receiver. For some combinations of desired signal modulation and dither signal this may corrupt reception. If the frequency of the fundamental component of the dither signal is greater than the information bandwidth of the signal than this distortion will be minimal. If the amount of distortion is too great an extra adaptive loop at the main antenna can be used as in Figure 18. This loop will cancel the dither component that might enter the receiver. The adaption of this loop can proceed concurrently with that of the array, but will fully adapt only after the array has acquired. The adaption of the array, however, can proceed completely independently of this main antenna loop (assuming  $\rho_0 = 0$ ).

The gradient can also be obtained by measuring the individual partial derivatives directly. Most dither algorithms take something of this approach. These algorithms are discussed in the next section.

polar attenuator in the return path of this reflected signal. The factor  $\alpha_n$  necessary for the gradient algorithm is implemented by multiplying the main antenna signal,  $y_0$ , by  $\alpha_n^*$  before the correlators that drive the complex reflectivity. This is exactly what is illustrated in Figure 15, except now the reflectivity is implemented in polar form. Note for a polar weight the reference signal for the correlator must come from a point after the variable phase control.

In the design of Figure 16 a second adaptive complex weight is used to both determine  $\alpha_n$  (actually  $\alpha_n^*$ ) and multiply  $y_0$  by it. This is done simultaneously because the input to the weight is a sum of the two signals,  $y_0$  and  $y_p$ . The weight and its control are structured so that the weight value needed for  $y_p$  to cancel the signal  $\alpha_n y_p$  from the  $n^{\text{th}}$  auxiliary is the weight value desired applied to  $y_0$  before the correlators of the complex reflectivity. This weight value is  $\alpha_n^*$ . Note the combiner after the weights,  $w_I$  and  $w_Q$ , invert the signal from  $w_Q$  before adding. This means the signal out of the combiner is  $w^* (y_0 + y_p)$  where  $w = w_I + jw_Q$ . In order for the signal  $\alpha_n y_p$  to be cancelled in the combiner,  $w^*$  must equal  $\alpha_n$ . The adaptive control therefore drives  $w = \alpha_n^*$ . Two types of tunable filters are used in the design. These filters are needed to keep undesired signals out of the correlators. TF1 rejects  $y_p$ , and TF2 rejects  $y_n$  or  $y_0$ . Note quadrature hybrids are generally considerably more expensive than power splitters and an effort has been made to use as few as possible.

The second method of implementing gradient control uses a computer. It is assumed that all the coupling parameters of the array have been measured over all the desired frequencies. From these parameters and the known or measurable reflectivity one can digitally compute the vector  $Q^{-1} \underline{m}_0$ . This is the vector of the  $\alpha_n$  needed for gradient control (with  $\rho_0 = 0$ ). One can then use a programable complex weight to either multiply  $y_n$  by  $\alpha_n$  or to multiply  $y_0$  by each  $\alpha_n^*$  as in Figure 15. This method would work particularly well when the reflectivities are digitally controlled as well. The  $\alpha_n$  are functions of the reflectivity values and when these values change the  $\alpha_n$  must be recomputed. Thus this method is limited by the speed at which the  $\alpha_n$  can be computed. As the size of the array increases the computation time increases rapidly and this limitation becomes more significant. A second limitation is the accuracy of the calculation. Small

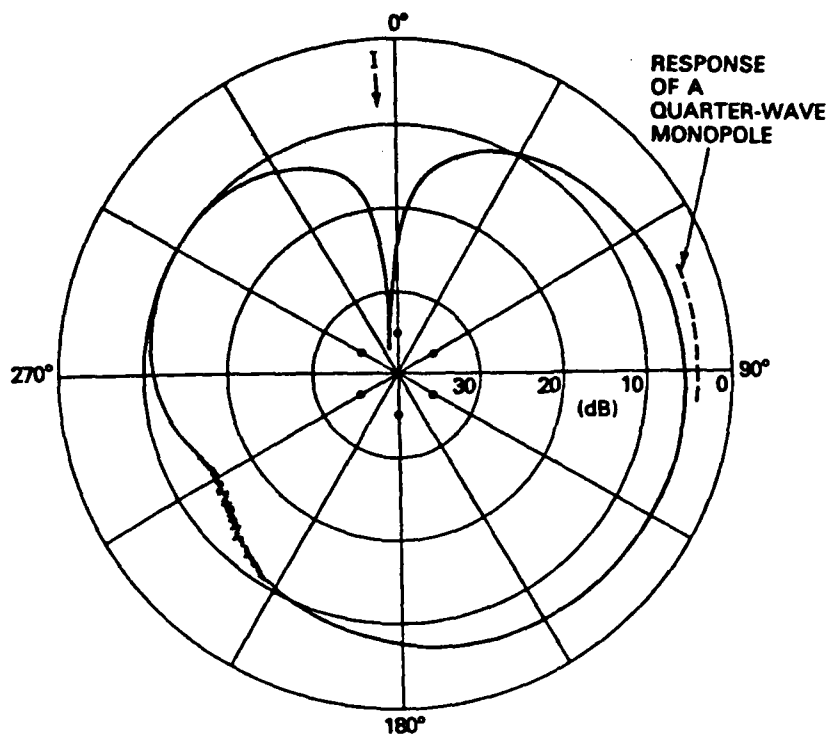


Figure 22 Antenna Pattern After Nulling an Interference Source

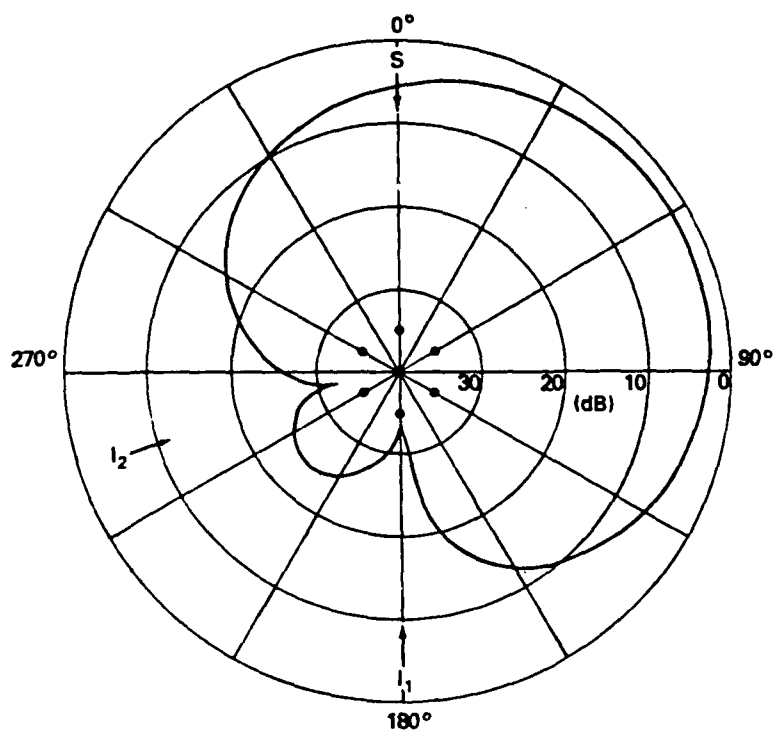


Figure 23 Antenna Pattern After Manual Adaptation to a Desired Signal S and Two Interferers  $I_1$  and  $I_2$

The second technique by which the reactance values were adjusted used a desired signal, in whose azimuthal direction a main lobe was required, and one or more interference signals, in whose direction a pattern null was required. The desired signal and the interference signals were slightly offset in frequency ( $\sim 1$  kHz), so that they all fell within the 16 kHz bandwidth of the receiver, but were separated sufficiently that a subsequent narrow band filter (10 Hz bandwidth) could be tuned only to the desired signal. By using a hard limiter between the receiver output and the narrow band filter, the output of the narrow band filter was a voltage proportional to the output signal-to-interference ratio (SIR), when  $SIR \ll 1$ . This voltage was monitored, and the reactances were manually varied to maximize it.

Two examples of patterns produced in this manner are shown in Figures 23 and 24. In Figure 23 a desired signal was incident on the array at 0 degrees and two strong interferers were incident at 180 degrees and 252 degrees. After the adjustment of the reactances,  $I_1$  and  $I_2$  were decreased 28 dB and 26 dB, respectively, relative to the desired signal. The pattern in Figure 24 was generated during a series of measurements to investigate the minimum angular separation necessary to resolve the desired signal from the interference. The interference was separated 20 degrees from the desired signal and was suppressed by 24 dB relative to the signal.

The array and the variables terminations were also interfaced with a PDP-11 computer to allow automatic control by the computer. The control algorithm was a univariate search (see Section 5.4). The automatically controlled array formed nulls like those with manual control. A tracking program was also written and implemented with the computer. This allowed the array to maintain cancellation of one or more jammers as the platform was slowly rotated, representing a changing signal environment. Results of the computer controlled array are described in [4,5].

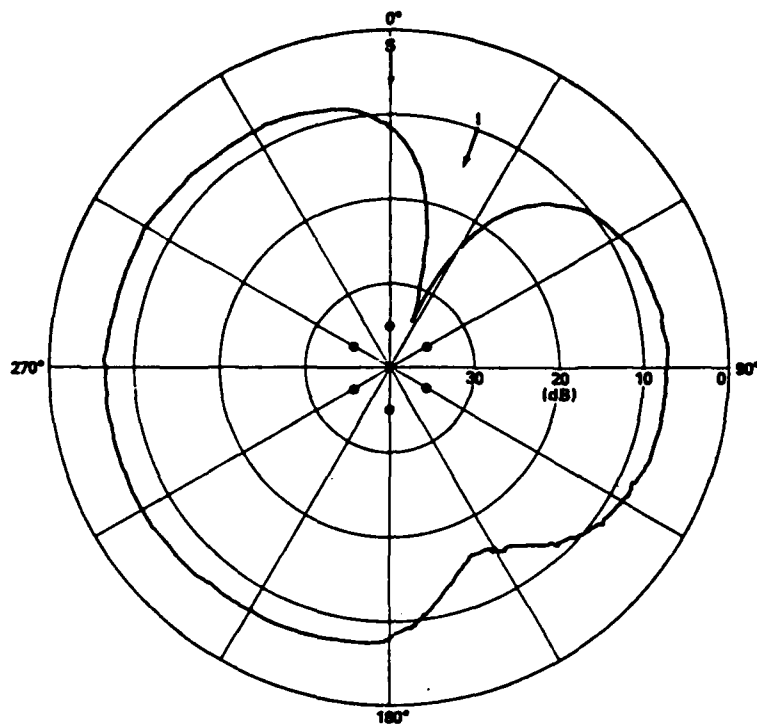


Figure 24 Antenna Pattern After Manual Adaptation to a Desired Signal S and an Interferer I

## 7.0 DEVELOPMENT BY ZA OF ACTIVE CONTROLLABLE COMPLEX TERMINATIONS

### 7.1 Design

In designing the active variable complex termination, two ground rules were established. These ground rules were established to make interfacing with the current array easier, make any necessary debugging and testing of the terminations or array easier, and to increase the flexibility in array configurations. These ground rules were: 1) that the terminations should use the existing variable reactances as variable phase shifters and 2) that the "loop" of the reflectivity be easily opened. A block diagram in Figure 25 illustrates the design used. The termination was assembled in three separate small aluminum boxes in order to meet the ground rules established.

A signal is captured by the antenna and is transferred to the load by the matching network. The matching network need not be ideal over all frequencies but it should be good enough to prevent the reverse signal of the mismatch from dominating the reflectivity. After the matching network is a two-way splitter-combiner. This device is being used as a three-port circulator (even though it has 3 dB loss each way). The forward flowing signal enters both the upper and lower paths (in Figure 25), but is blocked by the isolation amplifier in the lower path. In the upper path, the signal receives some amplification and then enters another two-way splitter-combiner again acting as a 3-port circulator. Coming out of the splitter-combiner the signal is reflected off the variable reactance to vary the phase for phase control. The reverse flowing signal reenters the splitter-combiner and enters both the upper and lower paths. In the upper path it is stopped by the isolation amplifier. In the lower path it passes through a bipolar amplitude modulator for amplitude control and then is amplified. The signal is then narrowband filtered and returned to the first splitter-combiner, which sends it out the antenna again through the matching network.

The termination comprises three boxes: the antenna interface box, the amplitude control box and the phase control box. A complete schematic of the antenna interface box and the amplitude control box is given in Figure 26. The antenna interface box is simply a four to one broadband transformer (16 to 1 impedance convertor) and a two-way splitter-combiner.







The transformer attempts to match the real part of the antenna impedance to 50Ω. The splitter-combiner is included in the antenna interface box so that the "loop" of reflectivity may be opened for analysis and testing. A 2 dB attenuator is included between the transformer and the splitter-combiner to improve the impedance match the splitter-combiner sees. The power loss is not a problem because of the gain within the termination.

Upon exiting the splitter-combiner the signal also exits the antenna interface box. Before entering the amplitude control box the signal is passed through a manually variable attenuator that varies from 0 to 25 dB and is mounted on the side of the amplitude control box. The attenuator is bidirectional so either port can be used for input. The attenuator will account for variations in the strength of the antenna mutual coupling in different array configurations. For a given array configuration the attenuator is set so the array is usually stable. (Remember in Section 4.2 it was shown that an unstable array can often be stabilized if an extra degree of freedom is available in the control space.) For a given configuration this attenuation need not be changed. In practice the correct value of attenuation would be built into the termination.

The signal now enters the amplitude control box. It first passes through a 32 MHz lowpass filter to reject out-of-band signals. Then the signal passes through an MWA-130 amplifier for both gain and reverse signal isolation. After the amplifier the signal is sent to the phase control box via a splitter-combiner and a 3 dB pad to improve the impedance match seen by the splitter-combiner.

The signal is reflected off the variable reactance and it reenters the amplitude control box, passing again through the 3 dB pad and into the splitter-combiner. The signal is then amplified by another MWA-130 amplifier. After the amplifier the signal passes through a 2 dB pad and then into a Mini-Circuits PAS-3 bipolar variable attenuator.

The D.C. control for the variable attenuator comes from the computer and should be sent to the amplitude control box through a twisted pair of wires (or like means) to reduce the effect of RF pickup. The control signal is received differentially inside the amplitude control box and then sent through a linearization circuit to account for the nonlinear diode effects of the PAS-3. This circuit improves the linearity between the RF amplitude out of the PAS-3 to the applied D.C. control voltage.

The output of the linearization circuit is sent to the PAS-3 through a relay. The relay is controlled externally to enable or disable the termination. If  $\pm 15\text{v}$  is connected to the relay control line, the relay will energize and allow the control of the variable attenuator to pass through. If the relay control line is open circuited or grounded then the output of the linearization circuit is open circuited and the control line to the attenuator is grounded. This causes the attenuator to apply maximum attenuation so virtually no signal passes through. This disables both amplitude and phase control because the phase control precedes the attenuator.

Following the attenuator is a final MWA-130 amplifier, which is followed by a tunable narrowband filter. The filter is composed of a series inductor and variable capacitor. With the current component values the center frequency of the narrowband filter can be varied from 12 to 23 MHz with a constant 3 dB bandwidth of about 900 KHz.

After the narrowband filter the signal is returned to the antenna through the first splitter-combiner and the matching network.

Let us now conduct a gain analysis of the reflectivity loop. The termination was designed so that, with minimum attenuation in both the manually variable attenuator and the electronically variable bipolar attenuator, the gain of the signal returned to the antenna would be 10 dB. Figure 27 details the gains and losses of the termination in this situation. Note to get the desired amount of gain two MWA-130 amplifiers were not sufficient so three were used. This necessitated the distribution of extra attenuation throughout the termination. This distributed attenuation was also desired to improve the impedance match between the various components.

Finally one must consider the problem of added noise. The added noise comes mainly from the MWA-130 amplifiers. These amplifiers have a noise figure of 7 dB. Consider first the configuration discussed above, i.e. that of minimum attenuation. The termination looks like a gain of 10 amplifier. Using the 7 dB noise figure for the amplifiers, one finds the termination (with 10 dB gain) has a 15 dB noise figure overall. This noise figure for the termination is not constant over all control settings. It is probably more instructive to look at the noise power independent of the signal. Note the output noise power will be independent of the manually variable attenuator. The output noise power will vary with

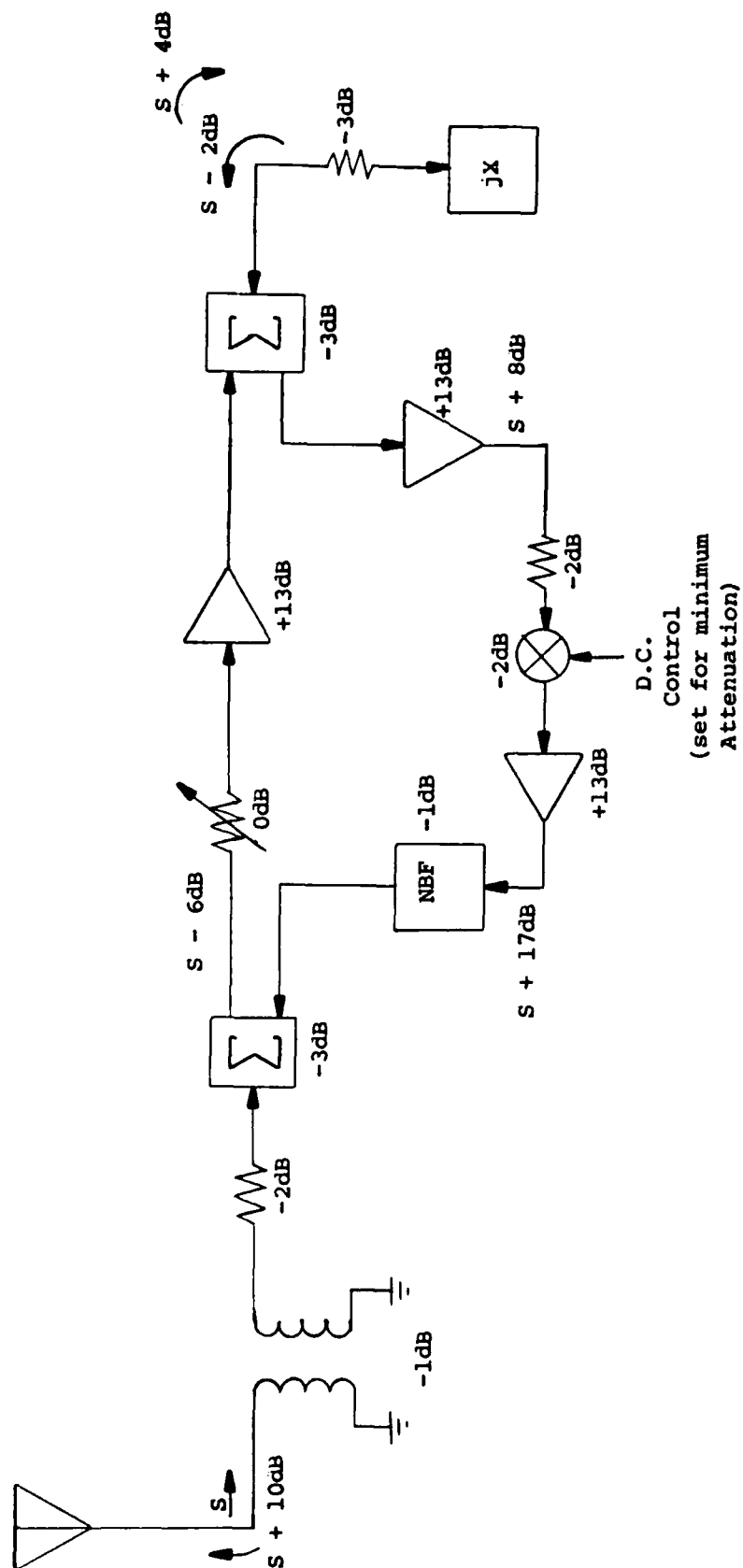


Figure 27 Signal Level Analysis for Active Termination

the electronic bipolar attenuator. The maximum output noise will be when the electronic attenuator has minimum attenuation, for which the output noise is 25 dB above thermal noise. The minimum output noise will be when the electronic attenuator has maximum attenuation. Then the output noise comes totally from the last amplifier and appears at the output 13 dB above thermal.

## 7.2 Laboratory Experimental Data

In the laboratory at Z-A three experiments were conducted on the amplitude control box of the active termination. These experiments determined dynamic range, verified simple phase control, and determined the bandwidth of the amplitude control.

The setup for the dynamic range experiment is given in Figure 28. The control voltage  $v_c$  was varied for minimum and maximum attenuation of the RF signal. Minimum attenuation occurs when  $v_c = 0v$  or  $+10v$  (in the picture  $v_c = +10v$ ). Maximum attenuation occurs when  $v_c = +5v$ . The pictures of Figure 29a and b show a dynamic range of 83 dB.

The phase control experiment is diagramed in Figure 30. In the experiment the reactance port was alternately open then short circuited. The photos in Figure 31a and b show the results. We see that the output does indeed shift by  $180^\circ$  as expected.

The experiment to determine the bandwidth of the amplitude control is diagramed in Figure 32. Four tests were run. Control signals of sine waves and square waves were used, each at 1 KHz and 40 KHz. The results of these tests are given in the photos of Figures 33 and 34. In Figure 33a a control signal of 1 KHz sine wave is used and in Figure 33b a control signal of 1 KHz square wave is used. In each of the photos the low frequency control signal is superimposed on the resultant RF output signal.

The feature to note in Figure 33a is that the zero crossings of the control signal and of the RF modulation occur together. Thus, at a control frequency of 1 KHz, group delay is not significant. In Figure 33b, the important feature is the nonlinear relationship shown between the control voltage and the resultant RF amplitude modulation, in particular the soft limiting nature of the relationship.

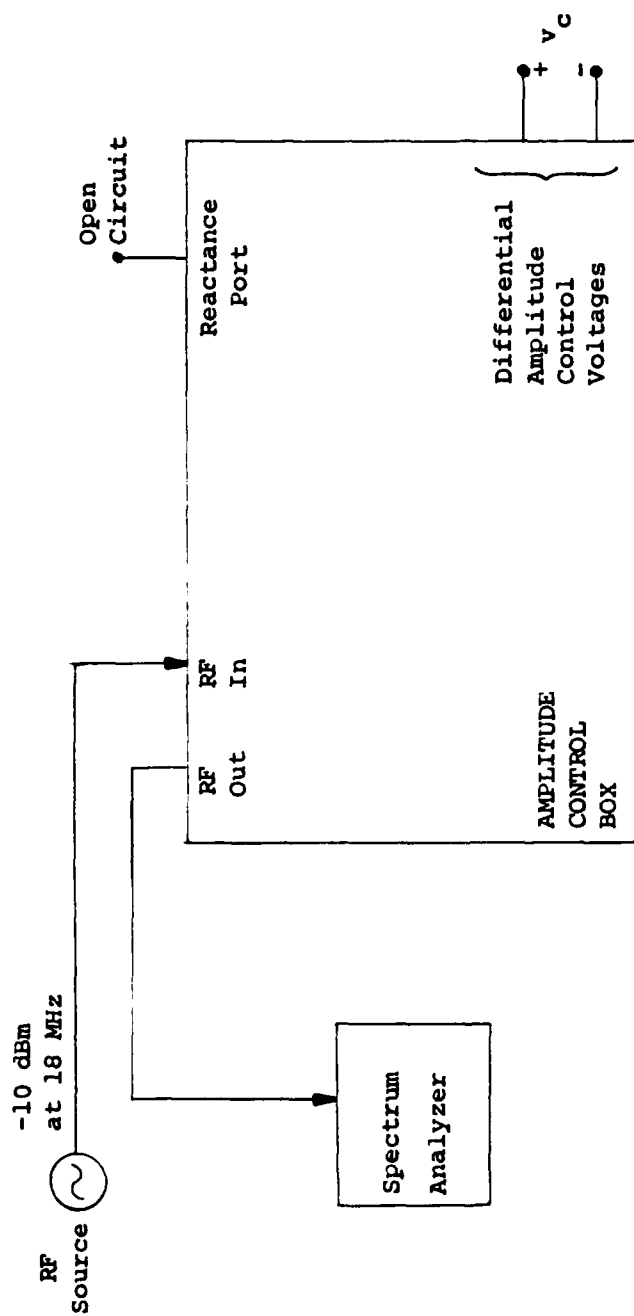
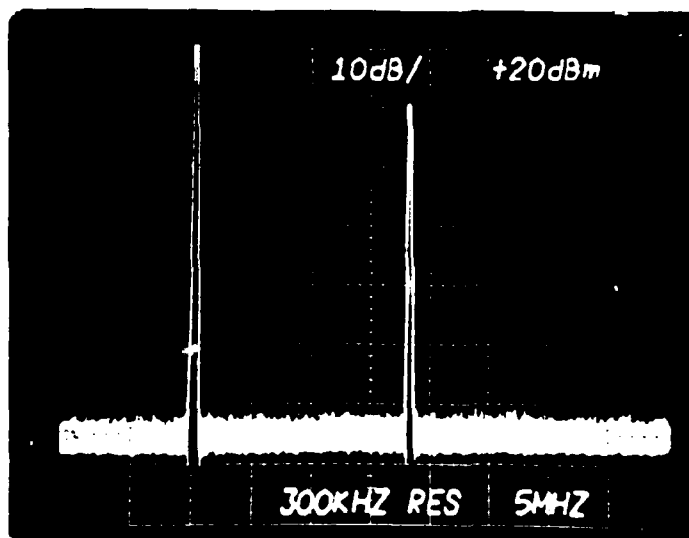
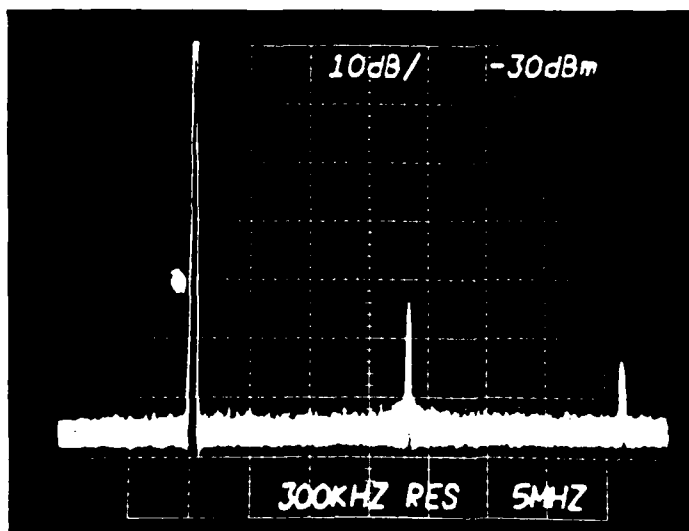


Figure 28 Dynamic Range Test Setup



a) Minimum Attenuation



b) Maximum Attenuation  
(note scale change)

Figure 29 Dynamic Range Test Results



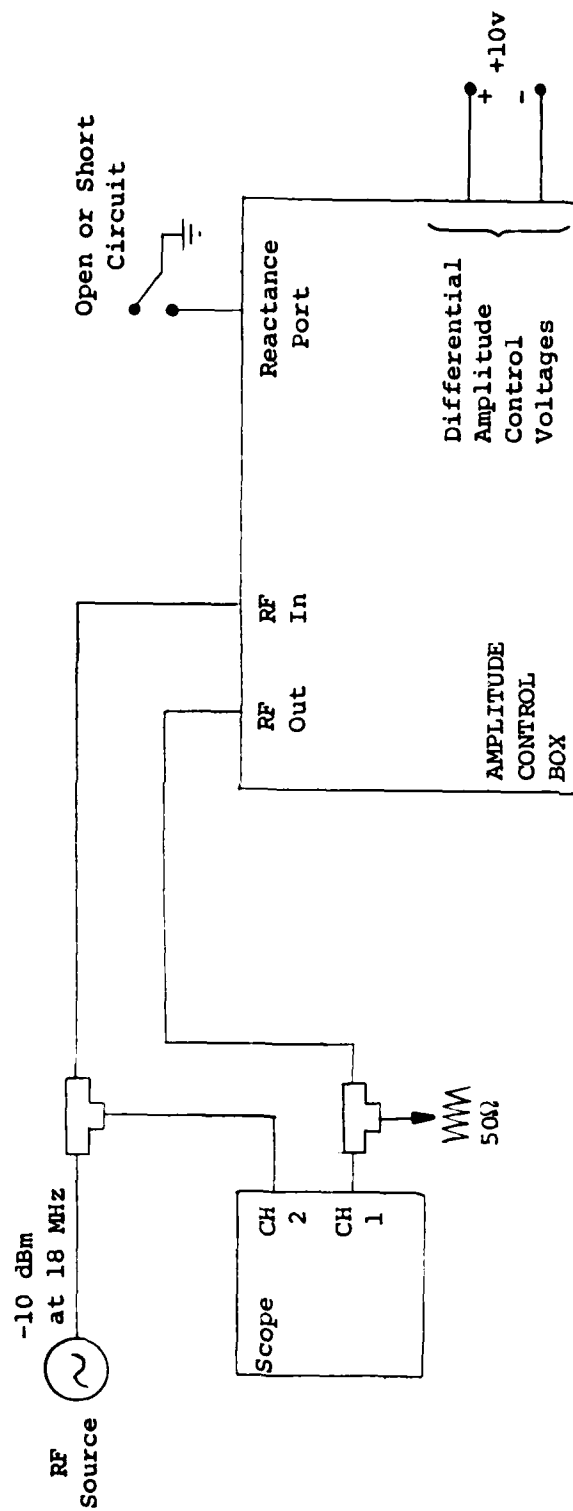
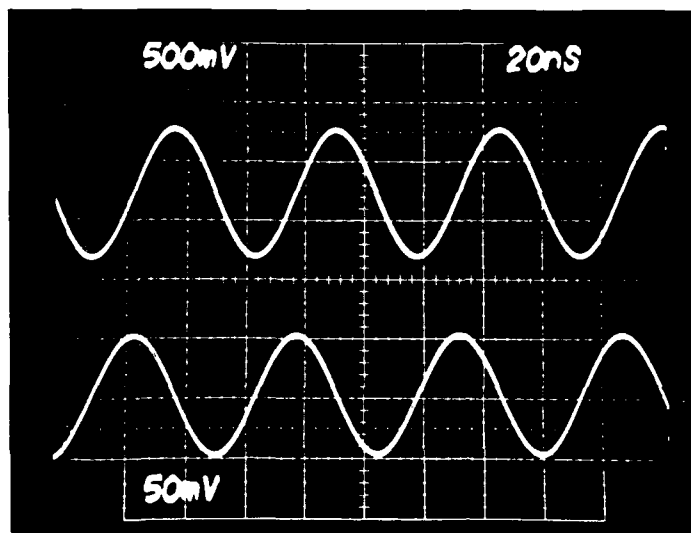
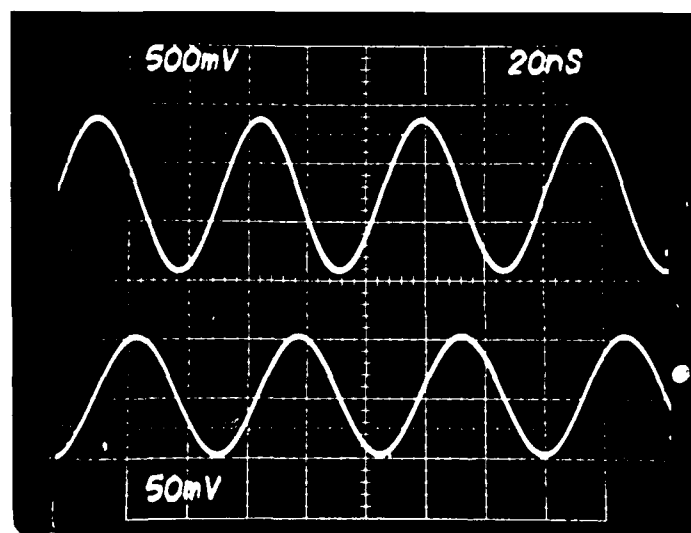


Figure 30 Phase Control Test Setup



a) Reactance Port Open Circuit



b) Reactance Port Short Circuit

Top Trace = Output

Bottom Trace = Input

Figure 31 Phase Control Test Results

ADAPTIVE NULLING AT HF USING A COMPACT ARRAY OF ACTIVE  
PARASITIC ANTENNAS(U) ZEGE-ABRAMS INC GLENSIDE PA  
T E JONES ET AL. MAR 85 R85-NRL-1 N00173-78-C-0265

PARASITIC ANTENNAS(U) ZEGGER-ABRAMS INC GLENSIDE PA  
T E JONES ET AL. MAR 85 R85-NRL-1 N00173-78-C-0265

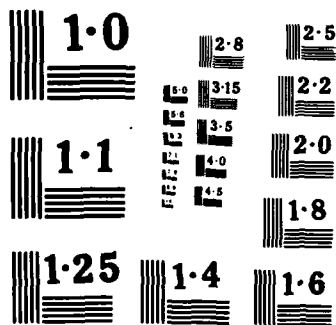
F/G 9/5

NL

END

9. 10. 11. 12. 13. 14. 15. 16. 17. 18. 19. 20. 21. 22. 23. 24. 25. 26. 27. 28. 29. 30. 31. 32. 33. 34. 35. 36. 37. 38. 39. 40. 41. 42. 43. 44. 45. 46. 47. 48. 49. 50. 51. 52. 53. 54. 55. 56. 57. 58. 59. 60. 61. 62. 63. 64. 65. 66. 67. 68. 69. 70. 71. 72. 73. 74. 75. 76. 77. 78. 79. 80. 81. 82. 83. 84. 85. 86. 87. 88. 89. 90. 91. 92. 93. 94. 95. 96. 97. 98. 99. 100. 101. 102. 103. 104. 105. 106. 107. 108. 109. 110. 111. 112. 113. 114. 115. 116. 117. 118. 119. 120. 121. 122. 123. 124. 125. 126. 127. 128. 129. 130. 131. 132. 133. 134. 135. 136. 137. 138. 139. 140. 141. 142. 143. 144. 145. 146. 147. 148. 149. 150. 151. 152. 153. 154. 155. 156. 157. 158. 159. 160. 161. 162. 163. 164. 165. 166. 167. 168. 169. 170. 171. 172. 173. 174. 175. 176. 177. 178. 179. 180. 181. 182. 183. 184. 185. 186. 187. 188. 189. 190. 191. 192. 193. 194. 195. 196. 197. 198. 199. 200. 201. 202. 203. 204. 205. 206. 207. 208. 209. 210. 211. 212. 213. 214. 215. 216. 217. 218. 219. 220. 221. 222. 223. 224. 225. 226. 227. 228. 229. 230. 231. 232. 233. 234. 235. 236. 237. 238. 239. 240. 241. 242. 243. 244. 245. 246. 247. 248. 249. 250. 251. 252. 253. 254. 255. 256. 257. 258. 259. 260. 261. 262. 263. 264. 265. 266. 267. 268. 269. 270. 271. 272. 273. 274. 275. 276. 277. 278. 279. 280. 281. 282. 283. 284. 285. 286. 287. 288. 289. 290. 291. 292. 293. 294. 295. 296. 297. 298. 299. 300. 301. 302. 303. 304. 305. 306. 307. 308. 309. 310. 311. 312. 313. 314. 315. 316. 317. 318. 319. 320. 321. 322. 323. 324. 325. 326. 327. 328. 329. 330. 331. 332. 333. 334. 335. 336. 337. 338. 339. 340. 341. 342. 343. 344. 345. 346. 347. 348. 349. 350. 351. 352. 353. 354. 355. 356. 357. 358. 359. 360. 361. 362. 363. 364. 365. 366. 367. 368. 369. 370. 371. 372. 373. 374. 375. 376. 377. 378. 379. 380. 381. 382. 383. 384. 385. 386. 387. 388. 389. 390. 391. 392. 393. 394. 395. 396. 397. 398. 399. 400. 401. 402. 403. 404. 405. 406. 407. 408. 409. 410. 411. 412. 413. 414. 415. 416. 417. 418. 419. 420. 421. 422. 423. 424. 425. 426. 427. 428. 429. 430. 431. 432. 433. 434. 435. 436. 437. 438. 439. 440. 441. 442. 443. 444. 445. 446. 447. 448. 449. 450. 451. 452. 453. 454. 455. 456. 457. 458. 459. 460. 461. 462. 463. 464. 465. 466. 467. 468. 469. 470. 471. 472. 473. 474. 475. 476. 477. 478. 479. 480. 481. 482. 483. 484. 485. 486. 487. 488. 489. 490. 491. 492. 493. 494. 495. 496. 497. 498. 499. 500. 501. 502. 503. 504. 505. 506. 507. 508. 509. 510. 511. 512. 513. 514. 515. 516. 517. 518. 519. 520. 521. 522. 523. 524. 525. 526. 527. 528. 529. 530. 531. 532. 533. 534. 535. 536. 537. 538. 539. 540. 541. 542. 543. 544. 545. 546. 547. 548. 549. 550. 551. 552. 553. 554. 555. 556. 557. 558. 559. 560. 561. 562. 563. 564. 565. 566. 567. 568. 569. 570. 571. 572. 573. 574. 575. 576. 577. 578. 579. 580. 581. 582. 583. 584. 585. 586. 587. 588. 589. 590. 591. 592. 593. 594. 595. 596. 597. 598. 599. 600. 601. 602. 603. 604. 605. 606. 607. 608. 609. 610. 611. 612. 613. 614. 615. 616. 617. 618. 619. 620. 621. 622. 623. 624. 625. 626. 627. 628. 629. 630. 631. 632. 633. 634. 635. 636. 637. 638. 639. 640. 641. 642. 643. 644. 645. 646. 647. 648. 649. 650. 651. 652. 653. 654. 655. 656. 657. 658. 659. 660. 661. 662. 663. 664. 665. 666. 667. 668. 669. 670. 671. 672. 673. 674. 675. 676. 677. 678. 679. 680. 681. 682. 683. 684. 685. 686. 687. 688. 689. 690. 691. 692. 693. 694. 695. 696. 697. 698. 699. 700. 701. 702. 703. 704. 705. 706. 707. 708. 709. 710. 711. 712. 713. 714. 715. 716. 717. 718. 719. 720. 721. 722. 723. 724. 725. 726. 727. 728. 729. 730. 731. 732. 733. 734. 735. 736. 737. 738. 739. 740. 741. 742. 743. 744. 745. 746. 747. 748. 749. 750. 751. 752. 753. 754. 755. 756. 757. 758. 759. 760. 761. 762. 763. 764. 765. 766. 767. 768. 769. 770. 771. 772. 773. 774. 775. 776. 777. 778. 779. 780. 781. 782. 783. 784. 785. 786. 787. 788. 789. 790. 791. 792. 793. 794. 795. 796. 797. 798. 799. 800. 801. 802. 803. 804. 805. 806. 807. 808. 809. 810. 811. 812. 813. 814. 815. 816. 817. 818. 819. 820. 821. 822. 823. 824. 825. 826. 827. 828. 829. 830. 831. 832. 833. 834. 835. 836. 837. 838. 839. 840. 841. 842. 843. 844. 845. 8

DRIC



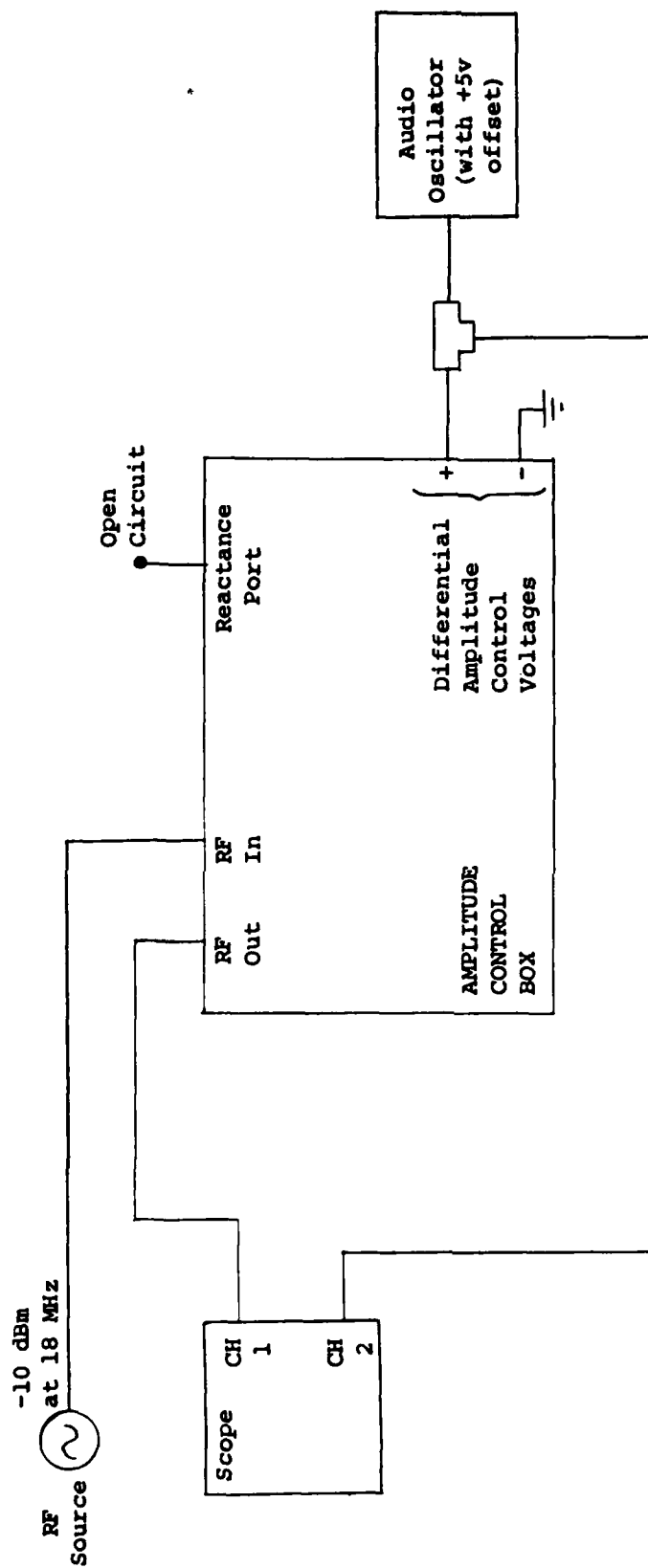
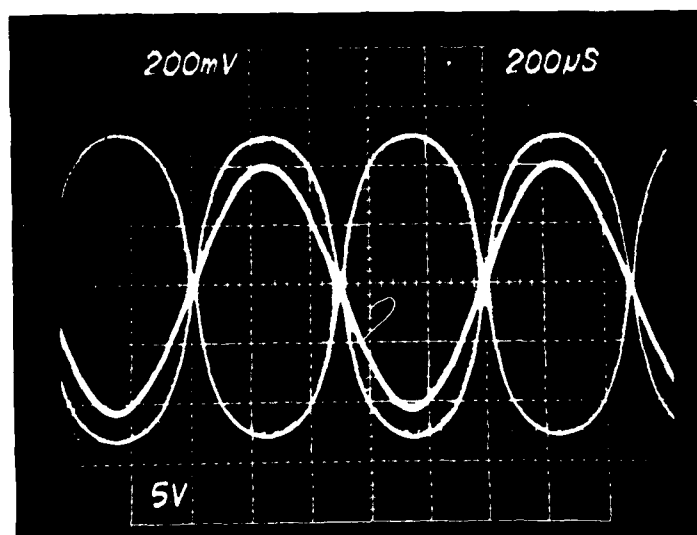
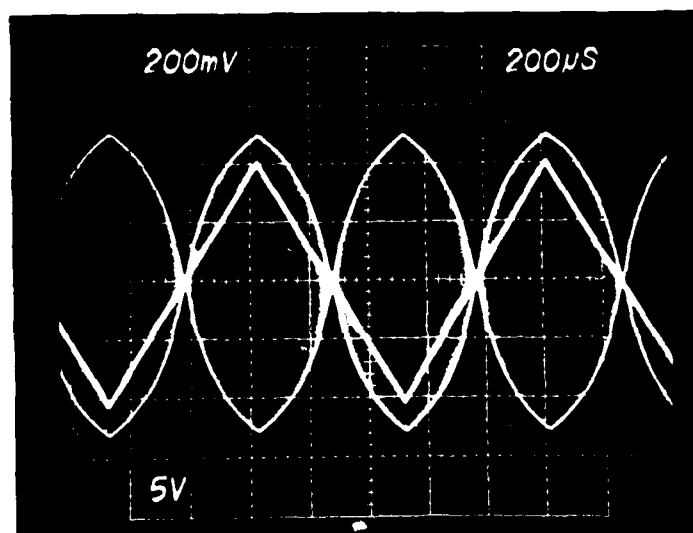


Figure 32 Amplitude Control Bandwidth Test Setup

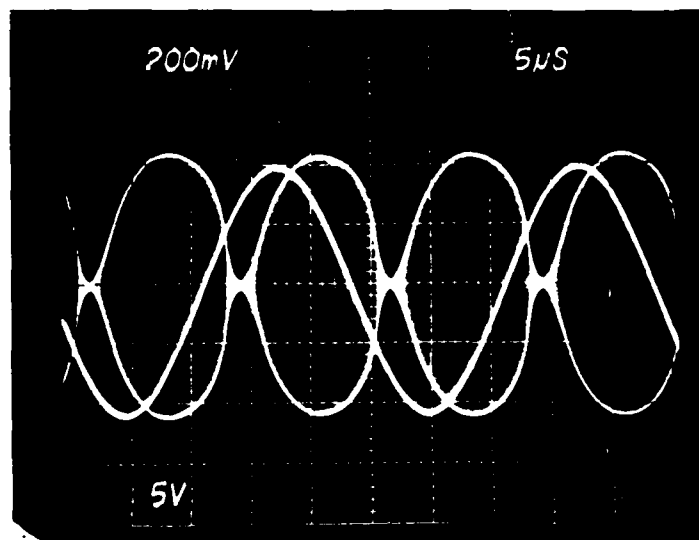


a) Sine Wave

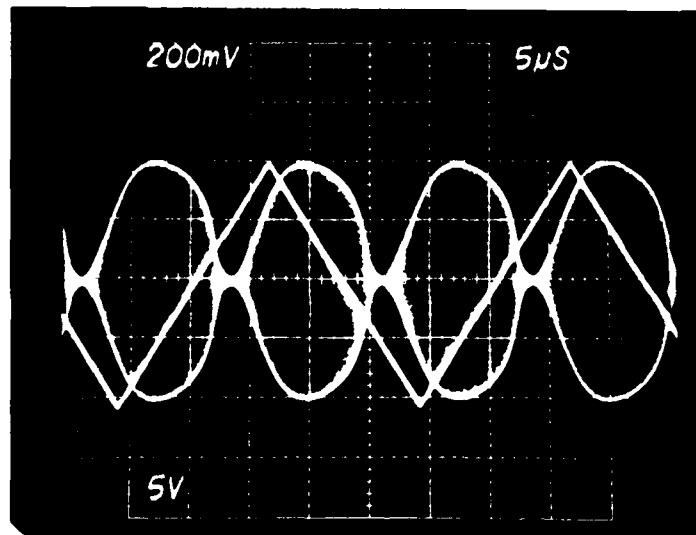


b) Square Wave

Figure 33 Amplitude Control Bandwidth Test Results  
with 1 KHz Control Signal



a) Sine Wave



b) Square Wave

Figure 34 Amplitude Control Bandwidth Test Results with 40 KHz Control Signal (note shift in time scale from Figure 33)

In Figure 34a one notices that the sine wave control signal and the resultant RF amplitude modulation are  $45^\circ$  apart. In particular, the modulation lags the control by  $45^\circ$ . Thus 40 KHz must be the 3 dB bandwidth of the amplitude control system.

### 7.3 Experimental Results of Parasitic Array with Active Complex Terminations

Zeger-Abrams built for NRL four active terminations as described in the previous two sections. The first termination was delivered to NRL in June 1982. At this time it was demonstrated that in a small, closely coupled, two element array, a single active termination on one of the elements can effectively form a null in a desired direction. Figure 35 shows the adapted pattern in one such case.

The remaining three active terminations were delivered to NRL later in 1982. Work at NRL has been ongoing to fully determine the capabilities of active terminations in arrays with more than 2 elements.



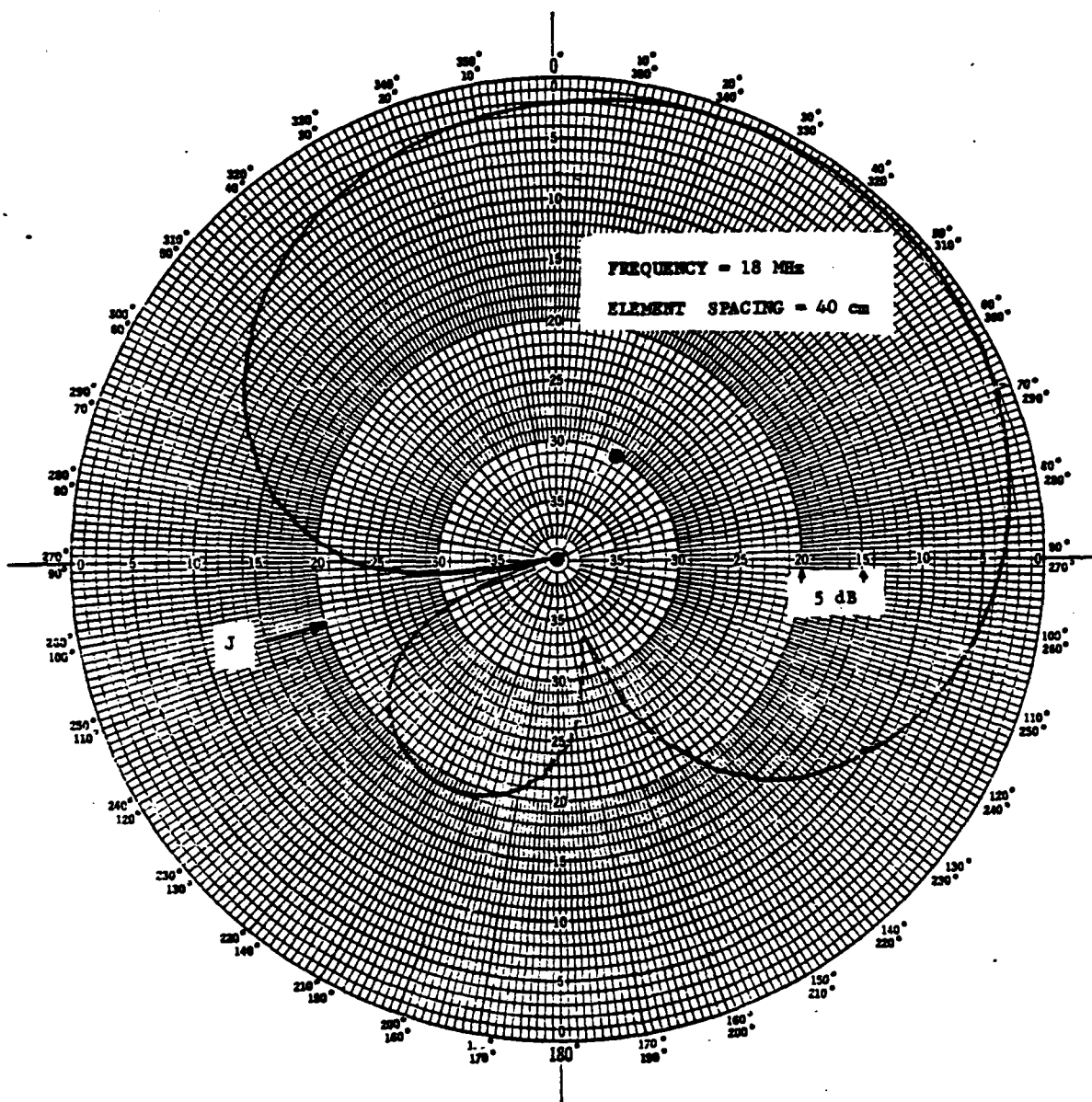


Figure 35 Adaptive Pattern for a Single-Jammer Threat; Small, Actively Terminated, Two Element Array

## 8.0 DEVELOPMENT OF A CONTROL ALGORITHM FOR ACTIVE TERMINATIONS

An algorithm is proposed here for control of an actively terminated parasitic array to find a stable null. This algorithm is a modification to the univariate search algorithm currently used by NRL. The algorithm presumes the use of oscillation, or instability, detectors as described in Section 8.1. These detectors are minor modifications to the active termination design given in Chapter 7 and would be incorporated into each active termination. The algorithm also presumes the use of a performance assessment indicator (PAI), possibly a signal to interference ratio detector. An improved version of the current detector used by NRL is given in the following chapter.

The algorithm searches for a stable null by restricting its search to that region of the control space for which the array is stable. The stability criterion of Chapter 4 ( $\text{Re} [\text{all eigenvalues of } M_{++}P_{++}] < 1$ ) is difficult to apply in practice, because  $M_{++}P_{++}$  is hard to measure and finding the eigenvalues is an involved computation. This is where the oscillation detector comes of use. It allows us to find the stable region of the control space without knowing  $M_{++}P_{++}$  or its eigenvalues.

### 8.1 Oscillation Detector (Unstable States)

The oscillation detector is based on the following principle: the final amplifier in at least one of the active terminations will saturate when the array goes unstable (starts to oscillate at some frequency). This fact, along with the knowledge that the signals encountered in normal operation (interference or desired) should not saturate this amplifier, allows us to detect when an array is unstable. We can detect an unstable array by noting when any of these final amplifiers saturate.

Figure 36 shows a modification to the design of the active termination of Figure 26. This modification detects when the peak amplitude of the MWA-130 output RF crosses a certain threshold. The op amp is configured as a comparator. The 1.4 M $\Omega$  feedback resistor provides positive feedback for hysteresis to prevent chatter. The op amp is one of two unused op amps currently within the termination. Laboratory experiments have determined that when the op amp threshold is set for 1.4v, the

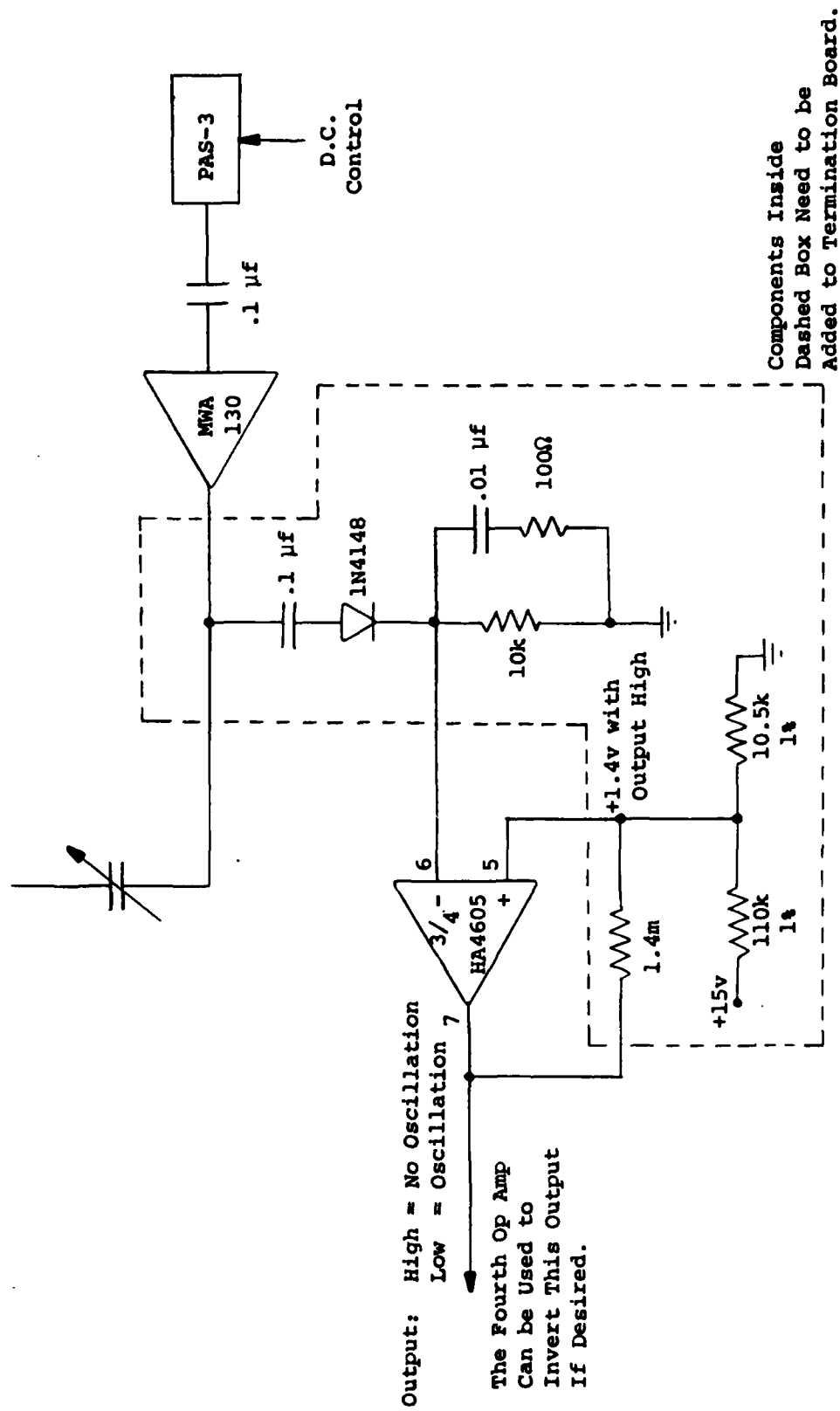


Figure 36 Oscillation Detector

output RF is +15 dBm. We selected to trip the threshold with +15 dBm output of the MWA amplifier, because this is higher than any expected operational signal (interference or desired) and yet slightly less than the saturation point of the amplifier (its 1 dB compression point is +18 dBm). With the threshold set in this manner, we can detect when the array is near oscillation but the MWA-130 is still linear. The output of the op amp is +15v if no oscillation is present and -15v if an oscillation is present. If an inverted output is desired, the final unused op amp can be employed to invert this signal. In practice, eight of these signals would probably be combined to represent one I/O byte to the computer.

Finally, if it is found that the detector will trigger on operational signals (in particular strong interferences) and not just on oscillations, one can obtain some extra operating signal range with some modifications. First, one may raise the threshold of the comparator slightly. Secondly, the 2 dB pad and the splitter-combiner within the antenna interface box can be replaced with a 10 dB directional coupler. In this case the ports on the antenna interface box will no longer be symmetric. The antenna is connected to the IN port of the directional coupler (through the matching transformer). The COUPLED port of the coupler is output to the termination. The OUT port of the coupler is the return signal from the termination. In this configuration, one gains about 4 dB more range for operating signals. The sacrifice is a corresponding increase in added noise.

## 8.2 Modified Univariate Search Algorithm

The simplest way to control the active terminations will be to modify the current algorithm, which is a univariate search. The simplest modification of all is to conduct the univariate search as before; however, consider only those operating points for which no termination is oscillating. More specifically, while ramping one of the control variables (either amplitude or phase) and just before evaluating the performance assessment indicator (PAI) for each new operating point, one checks to see if any of the terminations are oscillating. If an oscillation is present in any of the terminations, then this operating point is rejected (without bothering to check the PAI) just as if its PAI had been insufficient. Upon reaching a null, the same process of checking for oscillations is continued even in tracking mode.

The main advantage of this algorithm is its ease of implementation. The main disadvantage is inherent to the univariate search algorithm, namely, it is slow. However, the current algorithm use two different step sizes for when it varies the control signal. A large step size when cancellation is poor and a small step size for fine tuning a null. This arrangement greatly reduces the number of operating points evaluated while cancellation is still poor and greatly speeds up the algorithm. Thus it is felt that more speed is not essential to the current experiments with parasitic arrays.

A second possible problem with this algorithm, which also is a possible problem with any non-random algorithm, is that it may get hung up at a local minimum which is not an adequate null. This is only called a possible problem because it becomes unlikely with excess degrees of freedom in the array, i.e., when there are more actively terminated elements than there are interferences to be nulled. It should be noted that it may be desirable to have more than one excess degree of freedom. Excess degrees of freedoms may also be used to stabilize an otherwise unstable array. Finally, if the array still forms an inadequate null, even with the extra degrees of freedom, the current algorithm will recognize this and start over from a new location which hopefully will lead to a suitable null.

## 9.0 DEVELOPMENT OF AN IMPROVED PERFORMANCE ASSESSMENT INDICATOR (PAI)

Every control algorithm needs some method to evaluate the current utility of the system being controlled. The device which does the evaluating is the performance assessment indicator (PAI). For a conventional adaptive array with LMS control the PAI is simply the array error signal which one then tries to minimize. For an SIC the usual PAI is the signal to interference ratio at the array output (to be maximized).

In designing a PAI for the current experimental array, working at an IF frequency would greatly ease the complexity of the circuit. Since the current PAI for the array uses a Watkins-Johnson WJ8718 receiver, it was felt that the same receiver should be incorporated into the new design. Figure 37 shows a basic design of a PAI using the WJ8718 receiver. The main antenna is connected to receiver through an antenna matching network (possibly as simple as a transformer). The receiver is set up to convert the signal to a 455 KHz IF with 16 KHz bandwidth. At an IF, the operation of the signal-interference discriminator is greatly simplified.

One may ask: since the discriminator separates the desired signal from the interference, why have an adaptive array at all? The problem is that the discriminator is not a perfect separator. The discriminator simply uses some feature of the desired signal which distinguishes it from the interference and then produces two outputs such that one of the outputs looks more like the signal and less like the interference than the other. The amount of discrimination is far from enough to allow one to attach a receiver to the desired signal port but is enough to control an adaptive array.

The two signals out of the discriminator are each sent through detectors, either power or peak detectors. The outputs of these detectors are D.C. signals which are then each input to a log ratio amp. A log ratio amp outputs a voltage proportional to the logarithm of the ratio of the two inputs. In this case the output is an attempt at measuring SIR in dB.

The key element of this design is the discriminator. Three types of signal discriminators will be introduced. The recommended type will be described in detail. The three different signal-interference discriminants

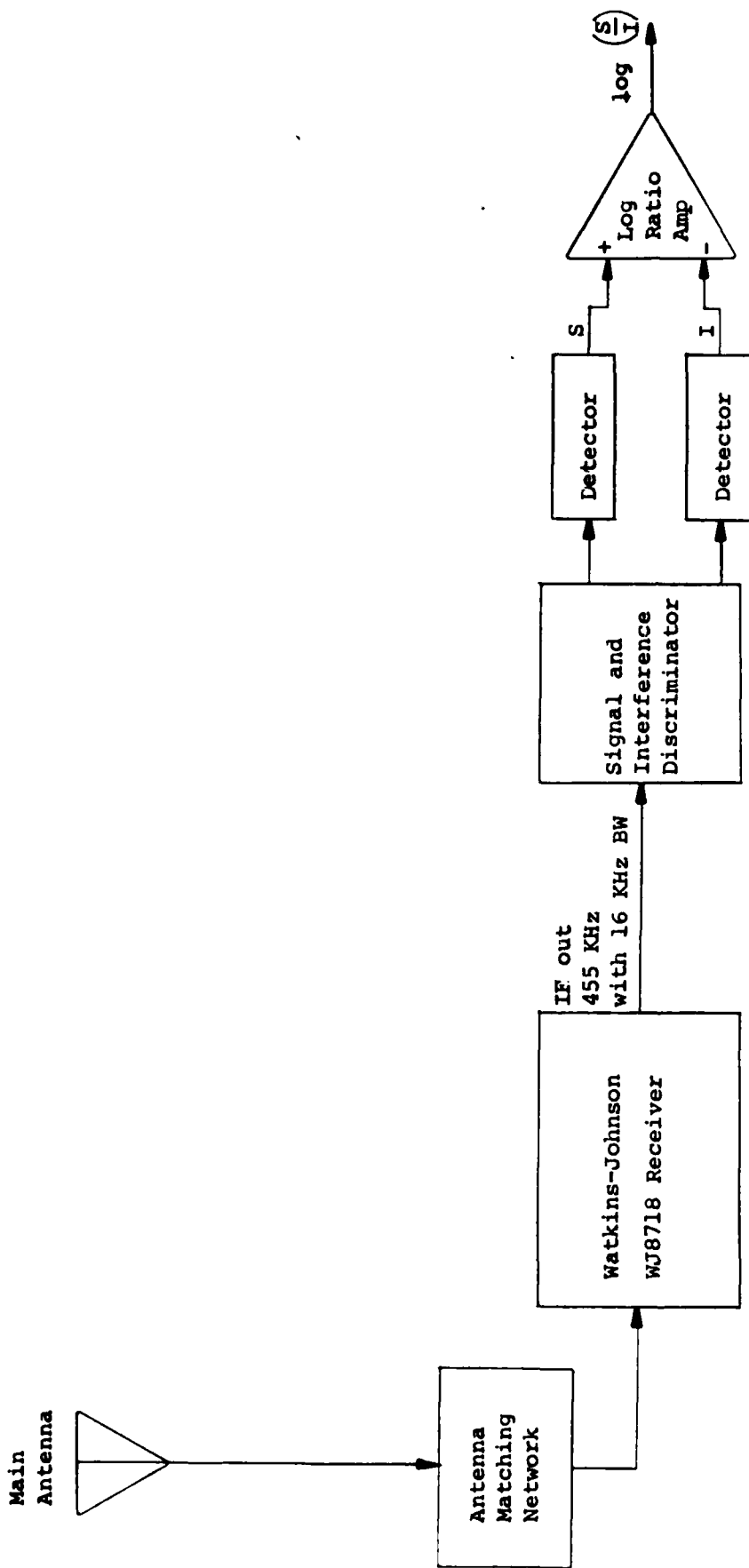


Figure 37 Basic PAI Design

are: 1) the signal and jammer are narrowband (or even CW) and slightly separated in frequency, 2) the signal is modulated with a psuedo-noise (PN) sequence and the jammer can be arbitrary, and 3) the signal is narrowband (doublesided bandwidth  $\leq 6$  KHz) and the jammer is wideband.

The jammer-signal environment required for the type 1) discriminator is really a fairly benign environment. It is not likely to be the jammer-signal environment encountered in practice. This discriminator would be used only with experimental arrays to demonstrate nulling capabilities. This discriminator would typically be composed of two narrowband filters; however with a single notch filter (at the desired signal frequency) one could use the same technique as described below for the type 3) discriminator.

Type 2) discriminator has the advantage of working against any jammer that is uncorrelated with the PN sequence. The total signal going into the discriminator is split into two paths. Both paths are multiplied by the PN sequence. One path (the signal path) then passes through a narrowband filter at the IF frequency. The other path (the interference path) is passed through a notch filter at the IF frequency.

The outputs of these filters are then sent to detectors as in Figure 37. The disadvantages with the PN discriminator are the increased hardware complexity and the need to synchronize to the PN sequence of the desired signal (which will have come from a distant transmitter in practice).

The type 3) discriminator is the type recommended. It requires little more hardware than the type 1) and may be employed against a far greater variety of jammers. In fact, it can be used anytime type 1) can be used, as long as the frequency separation is wider than 3 KHz. The type 3) discriminator assumes that the jammer has wider bandwidth than the signal, or at least has a good fraction of its power out of this band. The input signal ( $S + I$ ) is split and one part is sent through a notch filter at the IF frequency. The power remaining in this signal will be proportional to the interference power. We now have two signals: one is  $S + I$  and the other representative of  $I$ . We would like to have two signals such that one is representative of  $I$  and the other of  $S$  alone. If we use the signals  $I$  and  $S + I$  in the detectors of Figure 37, then the output of the log ratio amplifier will be  $\log[(S + I)/I]$ . This output cannot be used for a PAI because if  $I \gg S$  the output is  $\approx 0$ . The PAI will change little even for large changes in  $I$ .



A.14 If  $y$  is a scalar function of  $n$  variables,  $x_i$ , arranged into a column (row) vector  $\underline{x}$  ( $\underline{x}^T$ ), the expression

$$\partial y / \partial \underline{x} \quad (\partial y / \partial \underline{x}^T)$$

denotes a column (row) vector with elements  $\partial y / \partial x_i$ .

A.15 If  $\underline{y}$  is a column vector with  $m$  elements, each a function of  $n$  variables,  $x_i$ , arranged into a row vector  $\underline{x}^T$ , the expression  $\partial \underline{y} / \partial \underline{x}^T$  denotes a matrix with  $m$  rows and  $n$  columns, with elements  $\partial y_i / \partial x_j$ .

$$A.16 \quad \partial UV / \partial \underline{x} = (\partial U / \partial \underline{x})V + U(\partial V / \partial \underline{x})$$

A.17  $\partial Y / \partial y_{ij} = E_{ij} = \underline{e}_i \underline{e}_j^T$  where  $E_{ij}$  is a matrix of all zeroes, except for the  $i, j$ -th element which = 1; and  $\underline{e}_i$  is a vector of all zeroes except for the  $i$ -th element which = 1.

A.18  $\partial \underline{a}^T \underline{x} / \partial \underline{x} = \underline{a}$  and  $\partial \underline{a}^T \underline{x} / \partial \underline{x}^T = \underline{a}^T$  (if the elements of  $\underline{a}$  are not functions of any  $x_i$ ).

$$A.19 \quad \partial A \underline{x} / \partial \underline{x}^T = A$$

$$A.20 \quad \text{Chain Rule: } \partial \underline{y} / \partial \underline{x}^T = (\partial \underline{y} / \partial \underline{z}^T)(\partial \underline{z} / \partial \underline{x}^T)$$

$$A.21 \quad \partial Y^{-1} / \partial \underline{x} = -Y^{-1}(\partial Y / \partial \underline{x})Y^{-1}$$

$$A^{-1} = \begin{pmatrix} (B - CE^{-1}D)^{-1} & \vdots & -B^{-1}C(E - DB^{-1}C)^{-1} \\ \dots & \dots & \dots \\ -E^{-1}D(B - CE^{-1}D)^{-1} & \vdots & (E - DB^{-1}C)^{-1} \end{pmatrix}$$

This can be verified by multiplying  $A$  and  $A^{-1}$  and showing that the result reduces to the identity.

A.10 Determinant of a partitioned Matrix given:

$$A = \begin{pmatrix} B & \vdots & C \\ \dots & \dots & \dots \\ D & \vdots & E \end{pmatrix} \quad \text{and}$$

$$\text{then } |A| = |E| \cdot |B - CE^{-1}D| \quad \text{if } E^{-1} \text{ exists,}$$

$$\text{and } = |B| \cdot |E - DB^{-1}C| \quad \text{if } B^{-1} \text{ exists.}$$

#### MATRIX DIFFERENTIATION FORMULAE

A.11 If the elements of a matrix  $Y(m \times n)$  are functions of a scalar,  $x$ , the expression

$$\partial Y / \partial x$$

denotes a matrix of order  $(m \times n)$  with elements  $\partial y_{ij} / \partial x$ .

A.12 If the elements of a column (row) vector  $y$  ( $y^T$ ) are functions of a scalar,  $x$ , the expression

$$\partial y / \partial x \quad (\partial y^T / \partial x)$$

denotes a column (row) vector with elements  $\partial y_i / \partial x$ .

A.13 If  $y$  is a scalar function of  $m \times n$  variables,  $x_{ij}$ , arranged into a matrix,  $X$ , the expression

$$\partial y / \partial X$$

denotes a matrix with elements  $\partial y / \partial x_{ij}$ .

- A.4 If  $(A + B)^{-1}$  exists, then  $AB^T$  is symmetric (i.e.,  $AB^T = (AB^T)^T$ ) if and only if  $(A + B)^{-1}(A - B)$  is symmetric.

proof of "if":

$$\begin{aligned}(A + B)^{-1}(A - B) &= [(A + B)^{-1}(A - B)]^T = (A^T - B^T)(A^T + B^T)^{-1} \\(A - B)(A^T + B^T) &= (A + B)(A^T - B^T) \\AA^T - BA^T + AB^T - BB^T &= AA^T + BA^T - AB^T - BB^T \\AB^T &= BA^T = (AB^T)^T\end{aligned}$$

proof of "only if": Reverse the above argument.

- A.5 If  $(A + B)^{-1}$  exists, then  $A^TB$  is symmetric if and only if  $(A - B)(A + B)^{-1}$  is symmetric.

This can be proved with minor variations to the proof of (A.4).

- A.6 If  $(A + B)^{-1}$  exists, then:

$$\begin{aligned}(A - B)(A + B)^{-1} &= (A + B + 2B)(A + B)^{-1} = I - 2B(A + B)^{-1} \\2B(A + B)^{-1} &= I - (A - B)(A + B)^{-1}\end{aligned}$$

- A.7 If  $(A + B)^{-1}$  exists, then:

$$\begin{aligned}(A - B)(A + B)^{-1} &= [2A - (A + B)](A + B)^{-1} = 2A(A + B)^{-1} - I \\ \text{or} \quad 2A(A + B)^{-1} &= I + (A - B)(A + B)^{-1}\end{aligned}$$

The following two identities and the matrix differentiation formulae are taken from CRC, Standard Mathematical Tables.

- A.8 Given  $A = B + UV$ , where  $A$  and  $B$  are  $n \times n$ ,  $U$  is  $n \times p$ ,  $V$  is  $p \times n$ , and  $B^{-1}$  exist, then:

$$A^{-1} = B^{-1} - B^{-1}U(I + VB^{-1}U)^{-1}VB^{-1}$$

This can be verified by multiplying  $A$  and  $A^{-1}$  and showing that the result reduces to the identity.

- A.9 Formula for inverting a partitioned matrix. Given:

$$A = \begin{pmatrix} B & C \\ \cdot & \cdot \\ D & E \end{pmatrix}, \text{ where } A \text{ is } (p + q) \times (p + q), B \text{ is } p \times p,$$

$C$  is  $p \times q$ ,  $D$  is  $q \times p$ ,  $E$  is  $q \times q$ , and  $B^{-1}$  and  $E^{-1}$  exist, then:

## APPENDIX A

### MATRIX IDENTITIES AND DIFFERENTIATION FORMULAE

Identities (A.1) through (A.7) are specialized identities found to be useful in the text. They are given with proof. Identities (A.8) and (A.9) and the differentiation formulae are taken from CRC, Standard Mathematical Tables, 21st Edition [12], pp. 125-136.

#### MATRIX IDENTITIES

In Identities (A.1) through (A.8), A and B are square matrices.

A.1 If  $A^{-1}$  exists, then  $A^{-1}B = BA^{-1}$  if and only if  $AB = BA$ .

proof of "if":

$$\begin{aligned}AB &= BA \\ A^{-1}ABA^{-1} &= A^{-1}BAA^{-1} \\ BA^{-1} &= A^{-1}B\end{aligned}$$

proof of "only if":

$$\begin{aligned}A^{-1}B &= BA^{-1} \\ AA^{-1}BA &= ABA^{-1}A \\ BA &= AB\end{aligned}$$

A.2  $(A - B)(A + B) = (A + B)(A - B)$  if and only if  $AB = BA$ .

proof of "only if":

$$\begin{aligned}(A - B)(A + B) &= (A + B)(A - B) \\ A^2 - BA + AB - B^2 &= A^2 + BA - AB - B^2 \\ -BA + AB &= BA - AB \\ AB &= BA\end{aligned}$$

proof of "if": Reverse the above argument.

A.3 If  $(A + B)^{-1}$  exists, then  $(A + B)^{-1}(A - B) = (A - B)(A + B)^{-1}$  if and only if  $AB = BA$ .

proof: Apply (A.1) to (A.2).

- [17] Reference Data for Radio Engineers, Chapter 24, Howard W. Sams & Co., Inc., Indianapolis, Indiana, 1977.
- [18] Johmk, C.T.A., Engineering Electromagnetic Fields and Waves, John Wiley & Sons, N.Y., 1975.
- [19] Amitay, N., Galindo, V., and Wu, C.P., Theory and Analysis of Phased Array Antennas, John Wiley & Sons, N.Y., 1972.
- [20] Rastringen, L.A., "The Convergence of a Random Search Method in the External Control of a Many Parameter System", Translated from *Antomatika i Telemekkanika*, Vol. 24, No. 11, pp. 1467-73, Nov. 1963.
- [21] Widrow, B., and McCool, J.M., "A Comparison of Adaptive Algorithms Based on the Methods of Steepest Descent and Random Search", IEEE PCAP, Sept. 1976, pp. 615-637.
- [22] Barron, R.L., "Guided Accelerated Random Search as Applied to Adaptive Array AMTI Radar", Adaptive Array Workshop, NRL 7803, March 1974 (U).
- [23] Dinger, R.J., "Adaptive Microstrip Antenna Array Using Reactively Terminated Parasitic Elements", paper presented at Session AP-11 of IEEE AP Society Symposium, Albuquerque, NM, May 1982.

# References

- [1] Zeger, A.E., Wismer, L.D., and Tibet, D.A., "Adaptive Techniques Applied to Spatial Interference Cancellation", Zeger-Abrams Inc., Report R79-NRL-3 under Naval Research Laboratory (NRL) Contract N00173-78-C-0265, Dec. 1979.
- [2] Zeger, A.E., Wismer, L.D., and Dinger, R.J., "Adaptive Control of Parasitic Elements", presented at the USAF Academy in Colorado Springs, CO, Proc. of the 1980 Adaptive Antenna Symposium, Vol. I, pp. 87-105, July 1980 [Rome Air Development Center In-House Report RADC-TR-80-378].
- [3] Dinger, R.J. and Meyers, W.D., "A Compact Reactively Steered Antenna Array", paper presented at the IEEE Antenna and Propagation (AP) Society and URSI Symposium, Quebec, Canada, 1980.
- [4] Dinger, R.J. and Meyers, W.D., "A Compact HF Antenna Array Using Reactively-Terminated Parasitic Elements for Pattern Control", NRL Memorandum Report 4797, May 11, 1982.
- [5] Wagner, L.S., Meyers, W.D., Zeger, A.E., and Jones, T.E., "Compact Adaptive Array of Parasitic Elements at HF", presented at HF Communication Symposium, at RADC, Griffiss AFB, NY 13441, November 17-18, 1982.
- [6] Harrington, R.F., "Reactively Controlled Directive Arrays", IEEE Trans. on AP, Vol. AP-26, No. 3, pp. 390-95, May 1978.
- [7] Harrington, R.F., Wallenberg, R.F., and Harvey, A.R., "Design of Reactively Controlled Antenna Arrays", Rep. TR-75-10, Office of Naval Research (ONR), Contract N00014-67-A-0378-0006 to Dept. of Electrical and Computer Engineering at Syracuse Univ., Sept. 1975.
- [8] Harrington, R.F., and Mautz, J.R., "Reactively Loaded Directive Antennas", Rep. TR-74-6, ONR Contract N00014-67-A-0378-0006 to Dept. of Electrical and Computer Engineering at Syracuse Univ., Sept. 1974.
- [9] Harrington, R.F., and Mautz, J.R., "Synthesis of Loaded N-Port Scatterers", Rep. ARCRL-72-0665, Sci. Rept. No. 17 on Air Force Cambridge Research Laboratories (AFCRL) Contract No. F19628-68-C-0180, Oct. 1972.
- [10] Harrington, R.F., and Mautz, J.R., "Modal Analysis of Loaded N-Port Scatterers", Rep. AFCRL-72-0179, Sci. Rep. No. 16 on AFCRL Contract No. F19628-68-C-0180, March 1972.
- [11] Harrington, R.F., Field Computation by Moment Methods, Macmillan Co., New York, 1968.
- [12] Mautz, J.R., and Harrington, R.F., "Computer Programs for Characteristic Modes of Wire Objects", Rep. AFCRL-71-0174, AFCRL Contract No. F19628-68-C-0180 to Syracuse Univ., March 1971.
- [13] CRC Standard Mathematical Tables, Twenty-first Edition, Chemical Rubber Company, Cleveland, Ohio, 1973.
- [14] Dworsky, L.N., Modern Transmission Line Theory and Applications, John Wiley & Sons, N.Y., 1979.
- [15] Seshu, S., and Balabanian, N., Linear Network Analysis, John Wiley & Sons, N.Y., 1959.
- [16] Chen, C.T., Introduction to Linear System Theory, Holt, Rinehart, and Winston, Inc., N.Y., 1970.

jammer is of a wider bandwidth than the signal, or at least contains significant energy outside the signal bandwidth of  $\pm 3$  KHz of the center frequency. This also works as the same discriminant that NRL has currently been using (namely frequency separation) although at a somewhat greater frequency difference (3 KHz instead of 1 KHz). The final statistic that drives the array is basically  $\log[(S + I)/I^\gamma]$  where  $\gamma > 1$ . The optimum value of  $\gamma$  is probably between 1.5 and 2.

Zeger-Abrams developed a new model for analysis of a parasitic array, particularly useful for analysis of active terminations and adaptive control. Zeger-Abrams developed active terminations to be used with a compact parasitic array at HF and developed circuitry and an algorithm for their control. Finally, Zeger-Abrams developed an improved PAI circuit to drive an adaptive parasitic array. Possible areas for future development and improvement include: 1) improvements in array stability through improvements in the design of the elements, the terminations, and the algorithm, 2) analytic studies of the array performance that include noise and studies of combining the element outputs in the manner of a conventional array, 3) further improvements in design of a PAI, and 4) the study and design of improved control algorithms.

## 10.0 SUMMARY AND CONCLUSIONS

The parasitic array is a promising method of building an adaptive array in a small package. This is a particularly appealing prospect at HF, where a conventional array would be measured in 100's of feet or even 100's yards.

The theory of an adaptive parasitic array was presented with emphasis on active terminations. Two theoretical models of a parasitic array were discussed, the impedance model and the transmission line model. The array was described in terms of both models and then the relationship between the models was established, should one wish to transform from one model to the other. With this relationship established, we used the transmission line model throughout the remainder of the report.

An explicit solution for the reflectivity values (of the transmission line model) necessary to form nulls on jammers was derived. The issue of stability for an actively terminated array was discussed. The concept of degrees of freedom for the array was introduced. The possibility of using excess degrees of freedom to stabilize the array was demonstrated. Several ideas on how to make the array less likely to go unstable were suggested.

Experimental results obtained in adaptive nulling with a passive reactive parasitic array were reviewed. These results were obtained at HF on the NRL Brandywine Antenna Range with an array about one meter high and a half meter in diameter.

Zeger-Abrams designed and built four active terminations for the NRL array. Preliminary results of using these terminations in the parasitic array were described.

As noted above, an actively terminated array may have stability problems. Zeger-Abrams developed an instability detector (actually a near-instability detector) to be used in conjunction with a control algorithm. A simple modification to use this detector with the current NRL computer control program was described.

Finally, in order to improve the performance of the NRL array, Zeger-Abrams designed an improved performance assessment indicator (PAI) that drives the adaptive control algorithm. This PAI assumes that the



the output of the difference amp is the PAI statistic negated. If  $V_{S+I}$  is the output voltage of the upper log amp and  $V_I$  is the output voltage of the lower log amp, then the true output of the op amp difference amplifier is  $2(\gamma V_I - V_{S+I})$ . The gain of the lower (non-inverting) input is determined by the 10K potentiometer. If the pot is set so there is a short circuit between the log amp output and the non-inverting terminal, then the gain for the non-inverting signal is twice that of the inverting signal,  $\gamma = 1$ . If the pot is set so the non-inverting terminal is shorted to ground, then (quite obviously) the gain for the non-inverting signal is zero,  $\gamma = 0$ . Finally, if it is desired that the PAI be positive going for increasing S/I then one of the excess op amps can be used to invert it.

Several possible performance assessment indicators have been discussed. The recommended PAI has been described in detail. A schematic of the recommended design was presented in Figure 39.

Table 1

Notch Filter Inductors Specifications

| Inductor     | Approximate Number<br>of Windings | Wire Gauge |
|--------------|-----------------------------------|------------|
| 6.41 mH      | 160                               | 32         |
| 5.71 mH      | 150                               | 32         |
| 3.0 mH       | 110                               | 32         |
| 1.85 mH      | 88                                | 32         |
| 1.76 mH      | 75                                | 32         |
| 45 $\mu$ H   | 14                                | 26         |
| 43.6 $\mu$ H | 13                                | 26         |

All cores are Ferroxcube pot cores 1408C-A250-3B7, which require the 1408F1D bobbin and 1408H hardware set each.



more. This is clearly impractical. To get the selectivity desired, it is recommended that the signal at 455 KHz be converted to a lower IF -- in particular 50 KHz. This could be accomplished by mixing with an LO at 505 KHz to produce outputs at 50 KHz and 1.06 MHz (see Figure 39). The 1.06 MHz component is then easily filtered out. The filtering is accomplished with a third order Butterworth lowpass filter with a cutoff at 70 KHz. This filter has less than 1 dB loss at 50 KHz and ideally 70 dB loss at 1.06 MHz. The final concern is the necessary stability of the 505 KHz LO. If the LO is inaccurate then the desired signal is not centered in the notch and some power may leak through the filter. This leak through power may corrupt the PAI measurement and degrade the final achievable S/I. 100 Hz accuracy in the oscillator is felt sufficient to make this degradation negligible. 100 Hz accuracy in a 505 KHz oscillator corresponds to a frequency stability of 200 PPM or 0.02%.

The notch filter is a design previously used by Zeger-Abrams. It had been built and tested and found to work very well. Table 1 gives specifications for the inductors. It is suggested that several extra windings be placed on each inductor and then resonate the inductor with a known capacitance to "tweak" the inductance value.

The signal into the notch filter first goes through a voltage divider. This lowers the input impedance seen by the filter and makes the necessary inductors smaller. There also is a signal attenuation associated with this divider, but the signal-to-noise ratio of the signal is assumed to have been well established by the WJ8718 receiver and this is not deemed a problem. The output op amp provides an infinite output impedance to the filter and restores the gain lost in the input resistor divider.

The output of the notch filter as well as a sample of the input signal are then sent to separate peak detectors. Since the signal levels may be smaller than a diode voltage drop, it was necessary to use ideal peak detectors. The RC network at the output of the op amp sets the fall time constant of the peak detector. This time constant is currently set for 1 ms.

The outputs of the peak detectors go into log amplifiers. The outputs of the amplifiers are then sent into a difference amplifier to form the PAI statistic  $\log[(S + I)/I^\gamma] = \log(S + I) - \gamma \log(I)$ . Note

$\gamma = \text{constant} > 1$

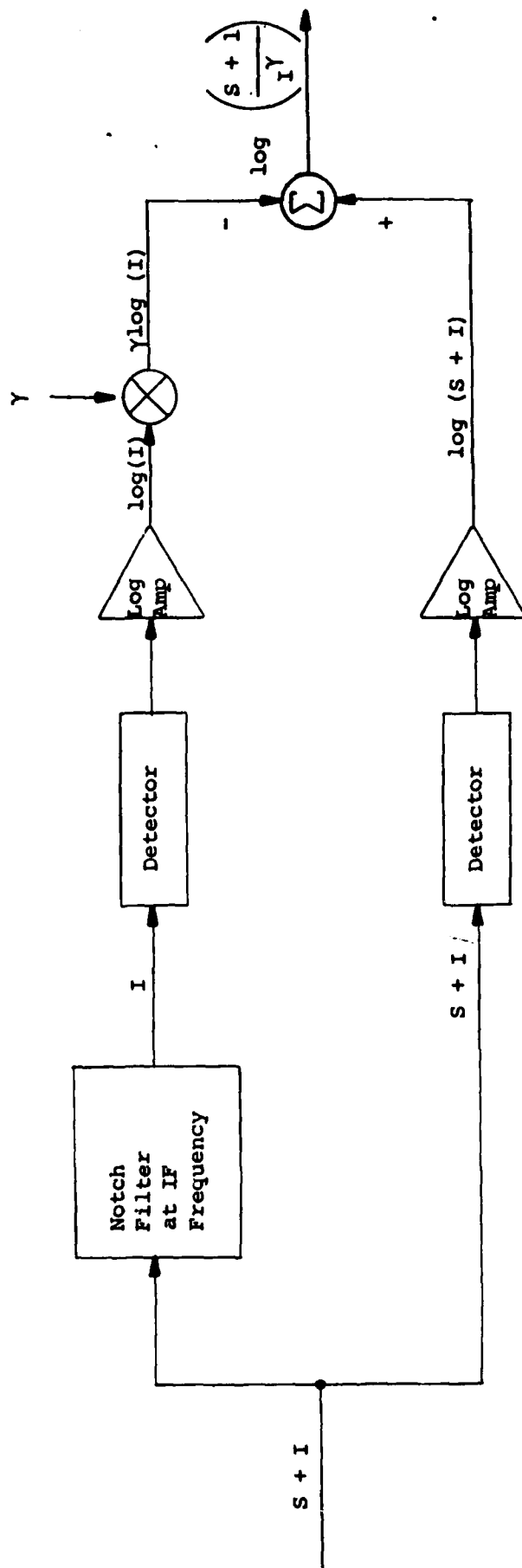


Figure 38 Recommended Signal-Interference Discriminator

Consider, however, the circuit diagramed in Figure 38. The output of this circuit is  $\log[(S + I)/I^\gamma]$ , or equivalently  $\log[(S + I)/I] - (\gamma - 1)\log(I)$ . For large  $I$  this becomes  $-(\gamma - 1)\log(I)$ . Since  $\gamma > 1$ , this term becomes increasingly more negative as  $I$  increases. Thus this circuit will function as a useful PAI. There is a compromise to be made when using this circuit. When  $I > S$ , we would want  $\gamma = 2$  so that the control is driven by  $\approx -\log(I)$ . If  $\gamma$  were less, then we would be reducing the loop gain and increasing the time it would take to reduce a large interference. However when  $S > I$ , we would want  $\gamma \approx 1$  so that the control is driven by  $\approx \log(S/I)$ . For larger  $\gamma$ , the array seeks to reduce  $I$  with a single-mindedness that is counterproductive. It will strive to reduce  $I$  even to the detriment of  $S/I$ . In particular, if  $\gamma = 2$ , the array will reduce  $S/I$  by as much as 1 dB, in order to reduce  $I$  by 1 dB. Note this is better than no desired signal maintainance at all as one would get by using  $-\log(I)$  alone as a PAI. It is thought that the optimum value for  $\gamma$  is between 1.5 and 2. Finally, it may be possible to make  $\gamma$  itself adaptive, although this is not recommended in the initial implementation. One such variable  $\gamma$  might be  $\gamma = 2 - f\{\log[(S + I)/I]\}$  where  $f\{x\} = x$  if  $x \leq 1$  and 1 if  $x > 1$ . Here  $\log[(S + I)/I]$  would be obtained by finding the difference of the log amp outputs before multiplying by  $\gamma$ .

The block diagram in Figure 38 is basically the recommended PAI design. The critical part of the design is the notch filter. Analysis shows that the maximum achievable signal-to-interference ratio out of the array is the ratio of the input to output signal-to-interference ratios of the notch filter, i.e.

$$\max \left( \frac{S}{I} \right)_{\text{array}} = \frac{(S/I)_{\text{filter input}}}{(S/I)_{\text{filter output}}}.$$

Assuming one wants a maximum  $S/I$  output of the array to be at least 30 dB, then one would want the desired signal rejection ratio of the notch filter to be at least 30 dB without significantly reducing the nearby interference.

A notch filter with a 6 KHz 3 dB notch bandwidth at center frequency of 455 KHz and sufficiently steep skirts to satisfy the above requirements was considered. The design, however, required inductors with  $Q$ 's of 800 and

## APPENDIX B

### RELATING S-PARAMETERS TO Z-PARAMETERS

For any N-port network there are two equivalent representations: S (scattering)-parameters and Z (impedance)-parameters. Scattering parameters are defined in Equation (B5) and analyze the system through the forward (incident) and reverse (reflected) voltage traveling waves. Impedance parameters are defined in Equation (B1) and analyze the system through the port currents and voltages. This appendix derives the relationship between these two representations.

Consider the N-port network in Figure B.1, terminated with transmission lines. Let  $Z = [z_{ij}]$  be the open-circuit impedance matrix for the network. The entries of this matrix are defined by

$$z_{ij} = \left. \frac{v_i}{i_j} \right|_{i_k = 0, \text{ for all } k \neq j} \quad (B1)$$

We define the vectors  $\underline{i}$  and  $\underline{v}$

$$\underline{i} = \begin{pmatrix} i_1 \\ \vdots \\ i_N \end{pmatrix}, \quad \underline{v} = \begin{pmatrix} v_1 \\ \vdots \\ v_N \end{pmatrix}.$$

From the definition of Z and superposition we see that

$$\underline{v} = Z \underline{i} \quad (B2)$$

The transmission lines connected to the nth port has a characteristic impedances of  $z_{on}$ .

$$Z_o = \begin{pmatrix} z_{o1} & & 0 \\ & \ddots & \\ 0 & & z_{oN} \end{pmatrix}$$

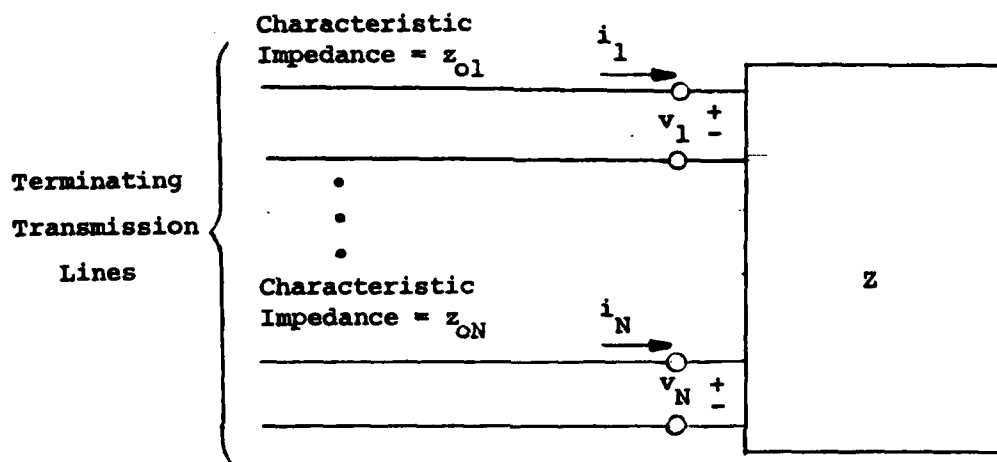


Figure B1 Network Model for Calculating  
Scattering Parameters



The voltage-current telegraph equations for each of the transmission lines can be solved [14, 17, 18] to show that each voltage and current is the sum of two components:

$$\begin{aligned} v_n &= v_{(+ )n} + v_{(- )n} \\ i_n &= i_{(+ )n} + i_{(- )n} \end{aligned} \quad (B3)$$

and in vector form

$$\begin{aligned} \underline{v} &= \underline{v}_{(+)} + \underline{v}_{(-)} \\ \underline{i} &= \underline{i}_{(+)} + \underline{i}_{(-)} \end{aligned} \quad (B4)$$

Here  $v_{(+ )n}$  and  $i_{(+ )n}$  are the forward voltage and current "waves" traveling toward the N-port network and  $v_{(- )n}$  and  $i_{(- )n}$  are the reverse waves traveling away from the N-port. The scattering parameter matrix  $S = [s_{ij}]$  is defined by

$$s_{ij} = \frac{v_{(- )i}}{v_{(+ )j}} \quad v_{(+ )k} = 0, \text{ for all } k \neq j. \quad (B5)$$

From this definition and superposition, we see that

$$\underline{v}_{(-)} = S \underline{v}_{(+)} \quad (B6)$$

It can also be shown from the telegraph equations that these traveling waves are related by the following equations:

$$\frac{v_{(+ )n}}{i_{(+ )n}} = - \frac{v_{(- )n}}{i_{(- )n}} = z_{on} \quad (B7)$$

Substituting Equations B7 into B3 yields:

$$\begin{aligned} v_n &= v_{(+)_n} + v_{(-)_n} \\ i_n &= \frac{v_{(+)_n}}{z_{on}} - \frac{v_{(-)_n}}{z_{on}} \end{aligned} \quad (B8)$$

Upon solving Equation (B8) for  $v_{(+)_n}$  and  $v_{(-)_n}$  we obtain:

$$\begin{aligned} v_{(+)_n} &= \frac{1}{2} (v_n + z_{on} i_n) \\ v_{(-)_n} &= \frac{1}{2} (v_n - z_{on} i_n) \end{aligned} \quad (B9)$$

and in vector form

$$\begin{aligned} \underline{v}_{(+)} &= \frac{1}{2} (\underline{v} + \underline{z}_o \underline{i}) \\ \underline{v}_{(-)} &= \frac{1}{2} (\underline{v} - \underline{z}_o \underline{i}) \end{aligned} \quad (B10)$$

Equation (B2) can be solved for  $\underline{i}$  and substituted into Equation (B10).

$$\underline{v}_{(+)} = \frac{1}{2} (I + \underline{z}_o \underline{z}^{-1}) \underline{v} \quad (B11.a)$$

$$\underline{v}_{(-)} = \frac{1}{2} (I - \underline{z}_o \underline{z}^{-1}) \underline{v} \quad (B11.b)$$

where  $I$  is the matrix identity

Equation (B11.a) can be solved for  $\underline{v}$  and substituted into Equation (B11.b).

$$\underline{v}_{(-)} = (I - \underline{z}_o \underline{z}^{-1}) (I + \underline{z}_o \underline{z}^{-1})^{-1} \underline{v}_{(+)} \quad (B12)$$

By comparing Equation (B12) to (B6), we see that

$$\begin{aligned} S &= (I - \underline{z}_o \underline{z}^{-1}) (I + \underline{z}_o \underline{z}^{-1})^{-1} \\ &= (\underline{z} - \underline{z}_o) \underline{z}^{-1} \underline{z} (\underline{z} + \underline{z}_o)^{-1} \\ &= (\underline{z} - \underline{z}_o) (\underline{z} + \underline{z}_o)^{-1} \end{aligned} \quad (B13)$$

Using the matrix identities A.6 and A.7 of Appendix A, we find the following equivalent forms for S:

$$S = I - 2Z_0 (Z + Z_0)^{-1} \quad (B14)$$

$$= 2Z (Z + Z_0)^{-1} - I \quad (B15)$$

Note if all the  $z_{on}$ 's are the same, then with the fact that Z is symmetric, S must also be symmetric.

Finally, Equation (B13) can be solved for Z in terms of S and  $Z_0$ .

$$S = (Z - Z_0) (Z + Z_0)^{-1}$$

$$S(Z + Z_0) = (Z - Z_0)$$

$$(I + S)Z_0 = (I - S)Z$$

$$Z = (I - S)^{-1} (I + S)Z_0 \quad (B16)$$

## APPENDIX C

### SCATTERING PARAMETERS IN TERMINATED TRANSMISSION LINES

#### C.1 Single Transmission Line

Derivations of the theory used in this appendix are given in [14, 18]. To solve transmission line problems one applies three rules:

- 1)  $v(x) = v_{(+)}(x) + v_{(-)}(x)$ ,  $i(x) = i_{(+)}(x) + i_{(-)}(x)$  and  $z(x) = \frac{v_{(+)}(x)}{i_{(+)}(x)} = -\frac{v_{(-)}(x)}{i_{(-)}(x)}$  are everywhere continuous, where  $x$  is the distance along the transmission line.

- 2)  $z(x) = z_0(x) \frac{1 + s(x)}{1 - s(x)}$  and  $s(x) = \frac{z(x) - z_0(x)}{z(x) + z_0(x)}$

where  $z_0(x)$  is the characteristic impedance at the point  $x$ .

$$z_0(x) = \begin{cases} z_A & x > l \\ z_0 & 0 < x < l \\ z_T & x < 0 \end{cases}$$

$z(x)$  is simply the impedance the transmission line could be terminated with at the point  $x$ , and not change the load as seen by the source.

- 3)  $s(x_1) = e^{j2\beta(x_1 - x_0)} s(x_0)$  where  $\beta = \omega/v_p$  and  $v_p$  is the propagation velocity of the transmission line. This is just the change in phase due to the change in position along the transmission line. Note the change in phase is calculated from twice the change in distance because it is a round trip.

To apply these rules to the transmission line network in Figure C.1, we start at the load,  $z_A$ . Here  $z(l+) = z_A$  and therefore by Rules 1 and 2

$$s(l-) = \frac{z(l-) - z_0}{z(l-) + z_0} = \frac{z_A - z_0}{z_A + z_0} \quad (C1)$$

By Rule 3 we can "move" this reflection coefficient down the transmission line.

$$s(0+) = e^{-j2\beta l} s(l-) \quad (C2)$$

We can now compute  $z(0+)$  from Rule 2.

$$z(0+) = z_0 \frac{1 + e^{-j\beta l} s(l-)}{1 - e^{-j\beta l} s(l-)} \quad (C3)$$

With the continuity of Rule 1, and the second equation of Rule 2 we obtain  $s(0-)$  from Equation (C3).

$$s(0+) = \frac{z(0+) - z_T}{z(0+) + z_T} \quad (C4)$$

We can relate these variables to those used in Section 3.1 of the text.

$$\hat{z}_A = z(0) = z(0+) = z(0-)$$

$$s_A = s(l-)$$

$$\hat{s}_A = s(0+) = m$$

$$s_T = s(0-)$$

In this section of the appendix, we would also like to show  $v_{(+)}(0-) = \frac{1}{2} v_g$ . From the definition of traveling waves and characteristic impedance we have:

$$\begin{aligned} v(0) &= v_{(+)}(0-) + v_{(-)}(0-) \\ i(0) &= i_{(+)}(0-) + i_{(-)}(0-) = \frac{v_{(+)}(0-)}{z_T} - \frac{v_{(-)}(0-)}{z_T} \end{aligned} \quad (C5)$$

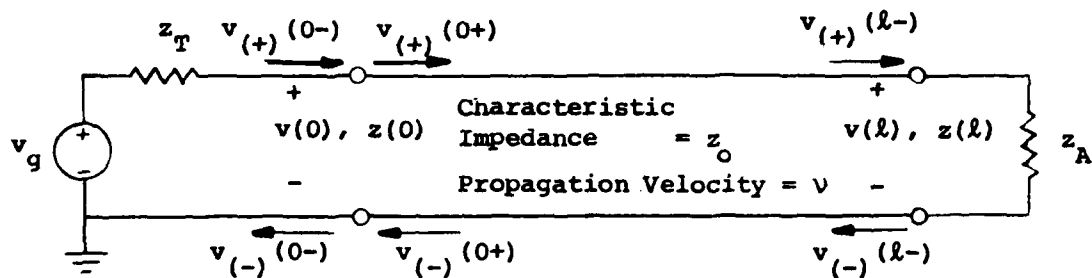


Figure C1 Model for Terminated Transmission Line

But from Figure C.1, we see that

$$\begin{aligned}
 v_g &= z_T i(0) + v(0) \\
 &= v_{(+)}(0-) - v_{(-)}(0-) + v_{(+)}(0-) + v_{(-)}(0-) \\
 &= 2 v_{(+)}(0-)
 \end{aligned} \tag{C6}$$

Finally, we would like to show that the model makes sense as the length of the transmission line approaches zero, i.e., in the absence of any line. In the absence of any transmission line, one would compute the reflection coefficient of the antenna as seen by the source as  $\Gamma = (z_A - z_T)/(z_A + z_T)$ . What needs to be shown is that  $s(0-)$  approaches  $\Gamma$ , as  $\ell$  approaches 0. It is sufficient to show that as  $\ell$  approaches 0, then  $z(0)$  approaches  $z_A$ , for then by Rule 2 and the continuity of  $z(x)$ ,  $s(0-)$  will be  $\Gamma = (z_A - z_T)/(z_A + z_T)$ . As  $\ell$  approaches 0, then  $e^{-j2\beta\ell}$  approaches 1 and from Equation (C3) we can write

$$\lim_{\ell \rightarrow 0} z(0) = z_0 \left[ \frac{1 + s(\ell-)}{1 - s(\ell-)} \right] \tag{C7}$$

Note from Equation (C1) that  $s(\ell-)$  does not depend on  $\ell$ . By combining Equations (C1) and (C7), we find the limit for  $z(0)$  as  $\ell$  approaches 0.

$$\begin{aligned}
 \lim_{\ell \rightarrow 0} z(0) &= z_0 \left[ \frac{1 + \left( \frac{z_A - z_0}{z_A + z_0} \right)}{1 - \left( \frac{z_A - z_0}{z_A + z_0} \right)} \right] \\
 &= z_0 \left[ \frac{z_A + z_0 + z_A - z_0}{z_A + z_0 - z_A + z_0} \right] \\
 &= z_0 \left( \frac{2z_A}{2z_0} \right) \\
 &= z_A
 \end{aligned}$$

## C.2 Multiple Transmission Lines

In this section the results of the previous section are extended for the case of N transmission lines terminated by an N+1 port network (see Figure C.2). First, let us define the following quantities to simplify notation. In keeping with the text, we shall use the indices 0, 1, ..., N.

$$\underline{x} = \begin{pmatrix} x_0 \\ \vdots \\ x_N \end{pmatrix}$$

$$\underline{v}(\underline{x}) = \begin{pmatrix} v_0(x_0) \\ \vdots \\ v_N(x_N) \end{pmatrix}, \quad \underline{v}_{(+)}(\underline{x}) = \begin{pmatrix} v_{0(+)}(x_0) \\ \vdots \\ v_{N(+)}(x_N) \end{pmatrix}, \quad \underline{v}_{(-)}(\underline{x}) = \begin{pmatrix} v_{0(-)}(x_0) \\ \vdots \\ v_{N(-)}(x_N) \end{pmatrix},$$

$$\underline{v}_g = \begin{pmatrix} v_{g0} \\ \vdots \\ v_{gN} \end{pmatrix}, \quad \underline{\ell} = \begin{pmatrix} \ell_0 \\ \vdots \\ \ell_N \end{pmatrix}$$

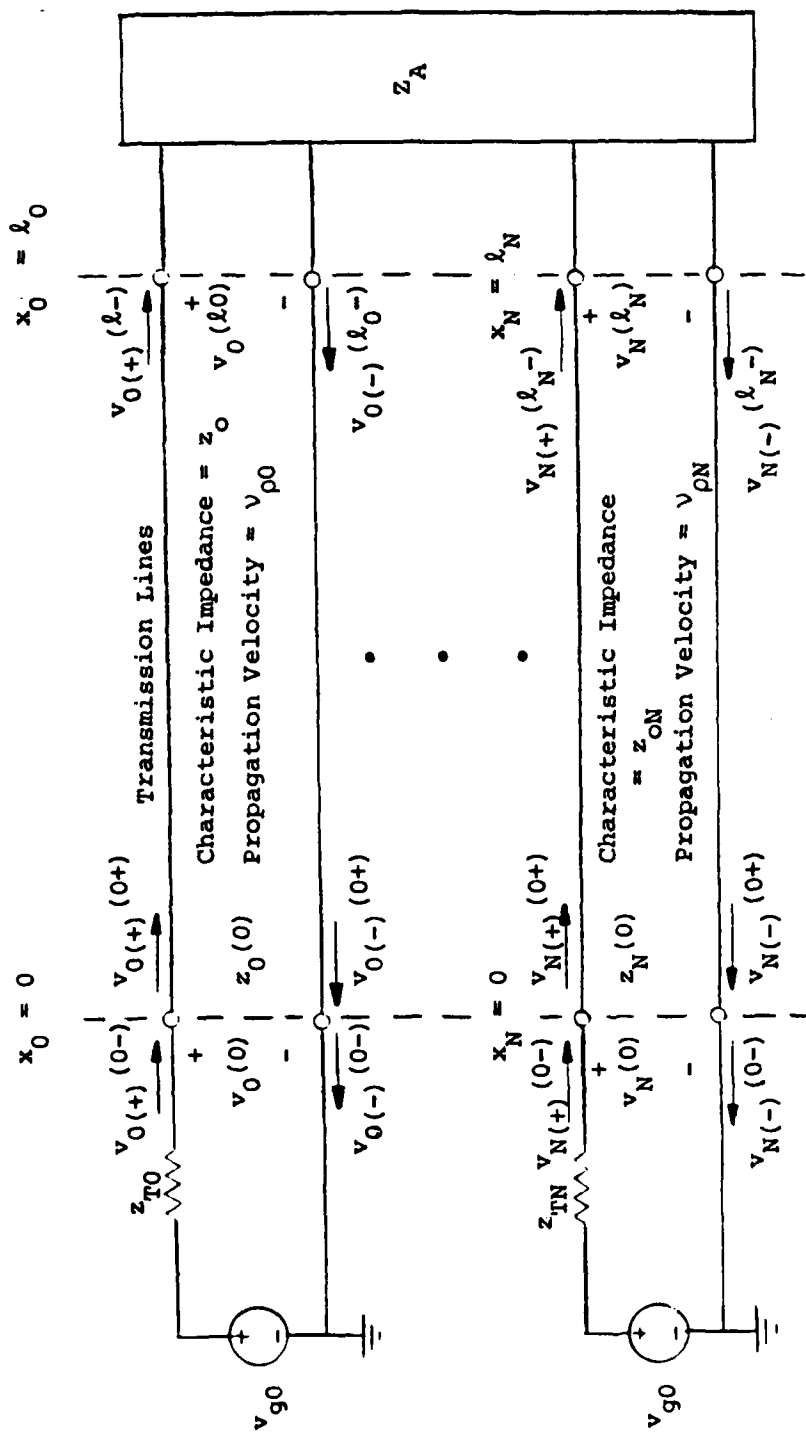
$S(\underline{x})$  matrix of s-parameters relating  $\underline{v}_{(+)}(\underline{x})$  and  $\underline{v}_{(-)}(\underline{x})$

$$Z_O = \begin{pmatrix} z_{o0} & & 0 \\ & \ddots & \\ 0 & & z_{oN} \end{pmatrix}, \quad Z_T = \begin{pmatrix} z_{T0} & & 0 \\ & \ddots & \\ 0 & & z_{TN} \end{pmatrix}$$

The three rules stated in Section C.1 are restated below for multiple transmission lines. (In evaluating these or any following expression, the components of  $\underline{x}$  must be all in the same region, i.e., all in the transmission lines, all in the load  $Z_A$ , or all in the termination.)

- 1)  $\underline{v}(\underline{x})$ ,  $\underline{i}(\underline{x})$  and  $Z(\underline{x})$  are all continuous in  $\underline{x}$ , where  
 $\underline{v}(\underline{x}) = \underline{v}_{(+)}(\underline{x}) + \underline{v}_{(-)}(\underline{x})$ ,  $\underline{i}(\underline{x}) = \underline{i}_{(+)}(\underline{x}) + \underline{i}_{(-)}(\underline{x})$  and  
 $Z(\underline{x})$  is defined by  $\underline{v}_{(+)}(\underline{x}) = Z(\underline{x})\underline{i}_{(+)}(\underline{x})$  and  
 $\underline{v}_{(-)}(\underline{x}) = -Z(\underline{x})\underline{i}_{(-)}(\underline{x})$ .





C-6

Figure C2 Model for Multiple Terminated Transmission Lines

$$2) \quad Z(\underline{x}) = [I - S(\underline{x})]^{-1} [I + S(\underline{x})] Z_0(\underline{x})$$

$$\text{and } S(\underline{x}) = [Z(\underline{x}) - Z_0(\underline{x})][Z(\underline{x}) + Z_0(\underline{x})]^{-1} \text{ where}$$

$$Z_0(\underline{x}) = \begin{cases} Z_A & x_i > l_i \text{ for all } i \\ Z_0 & 0 < x_i < l_i \text{ for all } i \\ Z_T & x_i < 0 \text{ for all } i \end{cases}$$

$$3) \quad S(\underline{x}_1) = D(\underline{x}_1 - \underline{x}_0) S(\underline{x}_0) D(\underline{x}_1 - \underline{x}_0)$$

$$\text{where } D(\underline{x}) = \begin{pmatrix} e^{j\beta_0 x_0} & & 0 \\ & \ddots & \\ 0 & & e^{j\beta_N x_N} \end{pmatrix} \quad 0 \leq x_{1i}, x_{0i} \leq l_i \text{ for all } i,$$

$$\text{and } \beta_i = \frac{\omega}{v_{pi}} \text{ for all } i$$

As in Section C.1, we start at the load  $Z_A$ .

$$Z(l+) = Z_A \quad (C9)$$

Then from Rules 1 and 2 we can compute  $S(l-)$

$$\begin{aligned} S(l-) &= [Z(l-) - Z_0(l)][Z(l-) + Z_0(l)]^{-1} \\ &= [Z_A - Z_0][Z_A + Z_0]^{-1} \end{aligned} \quad (C10)$$

By Rule 3, we can move this scattering matrix down the transmission lines to  $x = 0+$ .

$$S(0+) = D(l) S(l-) D(l) \quad (C11)$$

From  $S(0+)$  and Rule 2, we can compute  $Z(0+)$ .

$$Z(0+) = [I - S(0+)]^{-1} [I + S(0+)] Z_0 \quad (C12)$$

With Rule 2 one can obtain  $S(0-)$  since  $Z(0-) = Z(0+)$  from Rule 1.

$$S(0-) = [Z(0+) - Z_T] [Z(0+) + Z_T]^{-1} \quad (C13)$$

As in Appendix C.1, we can relate these variables to those used in the text in Section 3.3.

$$\hat{Z}_A = Z(0) = Z(0+) = Z(0-) \quad (C14)$$

$$S_A = S(\underline{l}-) \quad (C15)$$

$$\hat{S}_A = S(0+) = M_+ \quad (C16)$$

$$S_T = S(0-) \quad (C17)$$

In the remaining portions of this appendix, several results useful in the text will be derived. First, Equation (C6) of Appendix C.1 will be generalized for the N-port case. We have by definition

$$\begin{aligned} \underline{V}(0) &= \underline{v}_{(+)}(0-) + \underline{v}_{(-)}(0-) \\ \underline{i}(0) &= \underline{i}_{(+)}(0-) + \underline{i}_{(-)}(0-) \end{aligned}$$

By Rule 1, we also have

$$\underline{i}(0) = Z_T^{-1} \underline{v}_{(+)}(0-) + Z_T^{-1} \underline{v}_{(-)}(0-)$$

But from Figure C.2, where  $\underline{v}_g$  is defined, we see that

$$\begin{aligned} \underline{v}_g &= Z_T \underline{i}(0) + \underline{v}(0) \\ &= \underline{v}_{(+)}(0-) - \underline{v}_{(-)}(0-) + \underline{v}_{(+)}(0-) + \underline{v}_{(-)}(0-) \\ &= 2\underline{v}_{(+)}(0-) \end{aligned}$$

Therefore, it can be stated in the general N-port case that

$$\underline{v}_{(+)}(0-) = \frac{1}{2} \underline{v}_g \quad (C18)$$

We would also like to generalize the result shown in Appendix C.1, that in the limit as  $\ell$  (or in the general case  $|\ell|$ ) approaches 0, the model behaves as if no transmission lines were present. Mathematically we need to show that

$$\lim_{|\ell| \rightarrow 0} Z(0) = Z_A.$$

First let us define some normalized quantities. Assuming that  $z_{on} \neq 0$  for any  $n$ , then  $Z_o$  is invertible. In addition, since  $Z_o$  is diagonal, there exists a matrix  $Z_o^{-1/2}$  such that

$$Z_o^{-1/2} = \begin{pmatrix} \sqrt{z_{o0}} & & 0 \\ & \ddots & \\ 0 & & \sqrt{z_{on}} \end{pmatrix}$$

$$Z_o^{-1/2} Z_o^{-1/2} = Z_o^{-1}, \quad (C19)$$

and where  $Z_o^{-1/2} = (Z_o^{-1})^{1/2}$

$$Z_o^{-1/2} Z_o^{-1/2} = Z_o^{-1}. \quad (C20)$$

Now we will define the following normalized values of  $Z_T$  and  $Z_A$ .

$$Z_T' = Z_o^{-1/2} Z_T Z_o^{-1/2} = Z_o^{-1} Z_T = Z_T Z_o^{-1} \quad (C21)$$

since  $Z_T$  is diagonal, and

$$Z_A' = Z_o^{-1/2} Z_A Z_o^{-1/2} \quad (C22)$$

With these normalized quantities, let us rewrite some of the expressions previously derived. First consider  $S(\ell)$  from Equation (C10).

$$\begin{aligned} S(\ell) &= (Z_A - Z_o) (Z_A + Z_o)^{-1} \\ &= (Z_o^{-1/2} Z_A' Z_o^{-1/2} - Z_o^{-1/2} Z_o^{-1/2}) (Z_o^{-1/2} Z_A' Z_o^{-1/2} + Z_o^{-1/2} Z_o^{-1/2})^{-1} \\ &= Z_o^{-1/2} (Z_A' - I) Z_o^{-1/2} (Z_A' + I)^{-1} Z_o^{-1/2} \\ &= Z_o^{-1/2} (Z_A' - I) (Z_A' + I)^{-1} Z_o^{-1/2} \end{aligned} \quad (C23)$$

## APPENDIX G

### GRADIENTS OF PSUEDO-ANALYTIC FUNCTIONS AND APPLICATIONS TO COMPLEX GRADIENT CONTROL

#### Appendix G.1: Theory of Psuedo-Analytic Functions

In the theory of complex variables analyticity is a very useful property of a function. It allows one to treat the function as a real function of a real variable when differentiating.

There are, however, many important functions, e.g. squared magnitude and conjugation of a variable, which are not analytic. In this appendix a property called psuedo-analyticity is defined. Many tools for the study of this property are derived. Finally, with these tools the gradient control law for complex variables is derived.

From single variable complex analysis we know that if a function of a complex variable  $f(z) = u(x,y) + jv(x,y)$  where  $(z = x + jy)$  is analytic, then there is a well defined derivative such that  $f$  and  $z$  follow all the basic rules of differentiation of a real function with respect to a real variable.

$$f'(z) = \frac{df}{dz} = \frac{\partial u}{\partial x} + j \frac{\partial v}{\partial x} = \frac{\partial v}{\partial y} - j \frac{\partial u}{\partial y} \quad (G1)$$

A necessary and sufficient condition for analyticity is that the function satisfy the Cauchy-Riemann equations.

$$\frac{\partial u}{\partial x} = \frac{\partial v}{\partial y} \quad \text{and} \quad -\frac{\partial u}{\partial y} = \frac{\partial v}{\partial x} \quad (G2)$$

These equations can be written more compactly as

$$\frac{\partial f}{\partial x} = -j \frac{\partial f}{\partial y} \quad (G3)$$

Now let  $f$  be a complex scalar function of  $N$  complex variable,  $f(z_1, z_2, \dots, z_N) = u(z_1, \dots, z_N) + jv(z_1, \dots, z_N)$ , where  $z_i = x_i + jy_i$ . Also let  $f$  be analytic with respect to  $z_i$  over the range of all possible values of the other variables. We may then define the complex partial derivative.

The Inequalities (F1 a and b) can be rewritten and combined more conveniently as

$$\left| \operatorname{Re} \left[ \sqrt{m_{22}^2 \rho_2^2 - 4m_{12}^2 \rho_1 \rho_2} \right] \right| < 2 - \operatorname{Re}[m_{22} \rho_2] \quad (\text{F2})$$

Note if  $\operatorname{Re}[m_{22} \rho_2] > 2$ , then the right side of Inequality (F2) is negative and no value of  $\rho_1$  can satisfy the constraint. If, however,  $\operatorname{Re}[m_{22} \rho_2] < 2$  then there exists a range of values that will satisfy the constraint. One such value is

$$\rho_1 = \frac{m_{22}^2 \rho_2^2}{4m_{12}^2}$$

which makes the left side of (F2) equal to zero.

We have shown that an auxiliary with a reflectivity that would normally make it unstable, can sometimes be stabilized by the presence of a second auxiliary antenna.

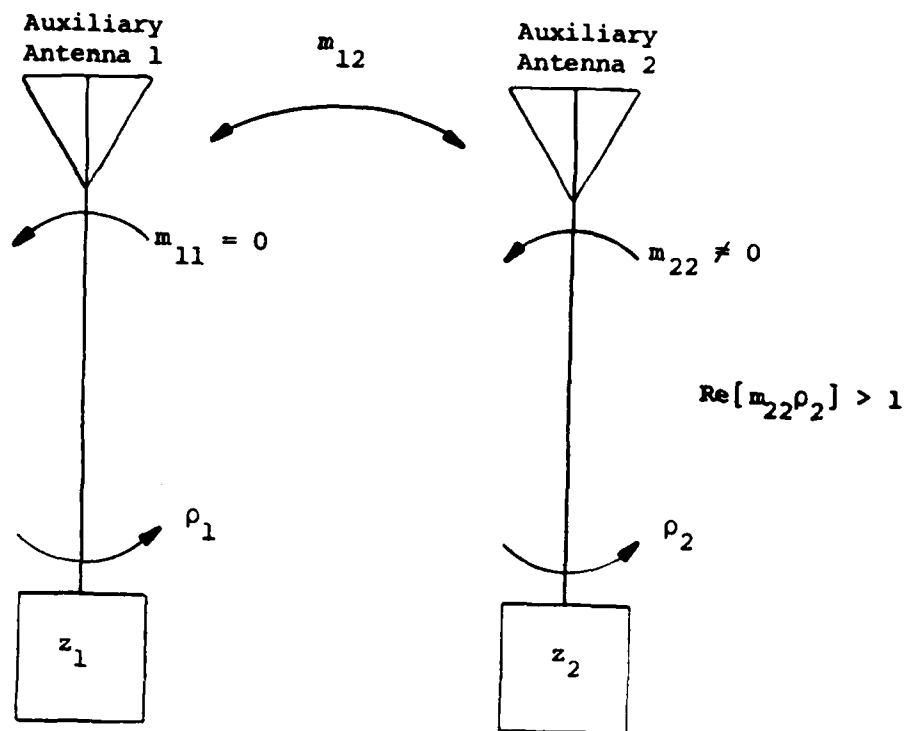


Figure F1 Array with an Unstable Element

## APPENDIX F

### A STABILITY ANALYSIS EXAMPLE

#### Stabilizing An Unstable Element

Consider the 2-element auxiliary array illustrated in Figure F1. It is assumed the self coupling factor, return loss, of the first antenna is zero, the main antenna is absent or has  $\rho_0 = 0$ , and the reflectivities have dominant single stage narrowband filters in the reflectivities so that  $\text{Re}[\text{all eigenvalues}] < 1$  is both necessary and sufficient for stability.

Consider the case  $\text{Re}[m_{22}\rho_2] > 1$ . The second antenna then by itself, or with  $\rho_1 = 0$ , would be unstable. It shall be shown that under certain conditions,  $\text{Re}[m_{22}\rho_2] < 2$ , there are choices for  $\rho_1$  which will stabilize the array.

First we need to find the eigenvalues of MP for this array.

$$MP = \begin{bmatrix} 0 & m_{12} \\ m_{12} & m_{22} \end{bmatrix} \begin{bmatrix} \rho_1 & 0 \\ 0 & \rho_2 \end{bmatrix} = \begin{bmatrix} 0 & m_{12}\rho_2 \\ m_{12}\rho_1 & m_{22}\rho_2 \end{bmatrix}$$

Characteristic Equation =  $\det[sI - MP]$  ...

$$\begin{aligned} &= \det \begin{bmatrix} s & -m_{12}\rho_2 \\ -m_{12}\rho_1 & s - m_{22}\rho_2 \end{bmatrix} \\ &= s^2 - sm_{22}\rho_2 - m_{12}^2\rho_1\rho_2 \end{aligned}$$

The eigenvalues are the roots of the characteristic equation.

$$\text{Eigenvalues} = \frac{m_{22}\rho_2 \pm \sqrt{m_{22}^2\rho_2^2 - 4m_{12}^2\rho_1\rho_2}}{2}$$

The stability constraint applied to these eigenvalues yields two inequalities.

$$\text{Re} \left[ \frac{m_{22}\rho_2 + \sqrt{m_{22}^2\rho_2^2 - 4m_{12}^2\rho_1\rho_2}}{2} \right] < 1 \quad (\text{F1a})$$

and

$$\text{Re} \left[ \frac{m_{22}\rho_2 - \sqrt{m_{22}^2\rho_2^2 - 4m_{12}^2\rho_1\rho_2}}{2} \right] < 1 \quad (\text{F1b})$$



Note the quantity within the brackets is necessarily positive because the term underneath the radical is the sum of two squares,  $r^2 \cos 2\theta - 1$  and  $r^2 \sin 2\theta$ .

Substitute  $\cos \theta = \sqrt{(1 + \cos 2\theta)/2}$  into (E8) and square both sides.

$$\frac{r^2}{2} (1 + \cos 2\theta) > \frac{1}{2} \left[ \sqrt{r^4 + 1 - 2r^2 \cos 2\theta} + r^2 \cos 2\theta - 1 \right]$$

or equivalently

$$1 + r^2 > \sqrt{r^4 + 1 - 2r^2 \cos 2\theta} \quad (\text{E9})$$

Squaring both sides of (E9) now yields

$$1 + 2r^2 + r^4 > r^4 + 1 - 2r^2 \cos 2\theta$$

$$2r^2 > -2r^2 \cos 2\theta$$

$$1 > -\cos 2\theta$$

This will be true if  $\theta \neq \pi/2 + m\pi$  for  $m = 0, \pm 1, \pm 2, \dots$ . But we have the constraint  $|\theta| < \pi/2$ ; therefore, it is always true.

Thus, we have shown for a single stage narrowband filter in the reflectivities the stability constraint  $\text{Re}[\lambda_n] < 1$  is sufficient. Necessity is shown by considering the frequency  $\omega_0$ , where  $f(j\omega_0) = 1$ , and noting that  $\text{Re}[\lambda_n] < 1$  is the necessary constraint derived in Section 4.2.

The roots of (E4) are found from the quadratic equation.

$$\begin{aligned} \text{roots} &= -\frac{b}{2}(1 - \lambda_n) \pm \sqrt{\left[\frac{b}{2}(1 - \lambda_n)\right]^2 - \omega_o^2} \\ &= \omega_o \left[ -\frac{b}{2\omega_o}(1 - \lambda_n) \pm \sqrt{\left(\frac{b}{2\omega_o}\right)^2 (1 - \lambda_n)^2 - 1} \right] \end{aligned} \quad (\text{E5})$$

We want to show the two values of (E5) are in the left half plane if  $\text{Re}[\lambda_n] < 1$ . Let  $x = b(1 - \lambda_n)/2\omega_o$ , then equivalently we can show

$$\text{Re} \left[ -x \pm \sqrt{x^2 - 1} \right] < 0 \quad \text{for } \text{Re}[x] > 0. \quad (\text{E6})$$

(E6) is really two inequalities, one for each choice of the ambiguous sign. These can be combined as in (E7).

$$\text{Re}[x] > |\text{Re}\sqrt{x^2 - 1}| \quad (\text{E7a})$$

Let  $x = re^{j\theta}$ , where  $|\theta| < \pi/2$ . Then (E7a) becomes

$$\begin{aligned} r \cos \theta &> |\text{Re}\sqrt{r^2 e^{j2\theta} - 1}| \\ &> |\text{Re}\sqrt{r^2 \cos 2\theta - 1 + jr^2 \sin 2\theta}| \end{aligned} \quad (\text{E7b})$$

At this stage an identity for complex numbers becomes useful. If  $\sigma = \sigma_R + j\sigma_I$  where  $\sigma_R, \sigma_I$  are real, then

$$\sqrt{\sigma} = \pm \frac{1}{\sqrt{2}} \left[ \sqrt{\mu + \sigma_R} + j\sqrt{\mu - \sigma_R} \right]$$

where  $\mu = \sqrt{\sigma_R^2 + \sigma_I^2}$  and all square roots on the right side are positive.

This identity can be easily verified by squaring. Using the real part of this identity, we can rewrite (E7b)

$$\begin{aligned} r \cos \theta &> \left| \pm \frac{1}{\sqrt{2}} \left[ \sqrt{r^4 \cos^2 2\theta + 1 - 2r^2 \cos 2\theta + r^4 \sin^2 2\theta + r^2 \cos 2\theta - 1} \right] \right| \\ &= \frac{1}{\sqrt{2}} \left[ \sqrt{r^4 + 1 - 2r^2 \cos 2\theta + r^2 \cos 2\theta - 1} \right] \end{aligned} \quad (\text{E8})$$

order term of  $\Lambda(\cdot)$  will vanish. The highest order term will become  $D^{N+1}(s)$ . Since it was assumed that  $D(s)$  and  $N(s)$  had no common factors,  $D^{N+1}(s)$  will not equal zero when  $N(s)$  does.

Thus for any zero of (E1),  $N(s) \neq 0$ . The zeros of (E1) will then be the zeros of  $\Lambda[f^{-1}(s)]$ . The zeros of this factor will be the values of  $s$  for which  $f^{-1}(s)$  equals an eigenvalue of  $M_+P_+$ . Therefore, the array is stable if and only if all zeros of the following  $N + 1$  equations are in the left half plane.

$$f(s) - \frac{1}{\lambda_n} = 0, n = 0, \dots, N \quad (E2)$$

and  $\lambda_n$  is the  $n$ th eigenvalue of  $M_+P_+$

Note the similarity between these equations and that for positive feedback root locus. They are the same if  $f(s)$  is considered the open loop transfer function and  $\lambda_n$  the loop gain. The difference is that in (E2)  $\lambda_n$  is complex instead of positive real.

Finally, it was mentioned earlier that if a single stage narrowband filter is used in the reflectivity, the necessary stability condition,  $\text{Re}[\lambda_n] < 1$ , becomes both necessary and sufficient. This shall now be proved.

What needs to be shown is for  $f(s)$  given in (E3), the equations of (E2) will have no right half plane zeros if  $\text{Re}[\lambda_n] < 1$ .

$$f(s) = \frac{sb}{s^2 + sb + \omega_o^2} = \frac{sb}{\left[s - \frac{b}{2} - j\sqrt{\omega_o^2 - \left(\frac{b}{2}\right)^2}\right]\left[s - \frac{b}{2} + j\sqrt{\omega_o^2 - \left(\frac{b}{2}\right)^2}\right]} \quad (E3)$$

Here  $\omega_o$  is the center frequency of the filter and  $b$  is the 3 dB bandwidth. It is assumed  $\omega_o > b/2$  and indeed  $b$  is small enough that  $M_+(s)$  does not change significantly across the filter passband. The equations of (E2) become

$$\frac{sb}{s^2 + sb + \omega_o^2} - \frac{1}{\lambda_n} = 0$$

or

$$s^2 + sb(1 - \lambda_n) + \omega_o^2 = 0 \quad (E4)$$

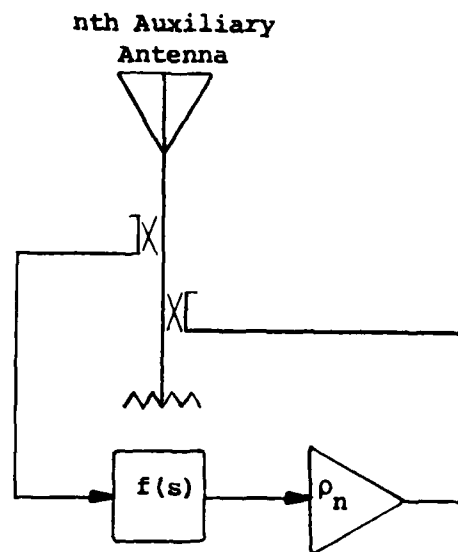


Figure E1 Reflectivity with Narrowband Filter

## APPENDIX E

### SUFFICIENCY OF STABILITY CONDITION WITH NARROWBAND FILTER IN REFLECTIVITIES

Let us apply the general stability criterion of Section 4.2 to the case of narrowband filters within the reflectivities (see Figure E1). It is assumed that the narrowband filter is narrow enough so that  $M_+(s)$  is constant over the passband and is approximated by  $M_+$ . Also assume that the filters within the reflectivities are all the same, so that the  $n$ th entry on the diagonal of  $P_+(s)$  is  $\rho_n f(s)$ . Here  $\rho_n$  is a constant and  $f(s)$  is the same for all reflectivities. Let  $f(s) = N(s)/D(s)$  where  $N(s)$  and  $D(s)$  are polynomials with no common factors. In this case the  $\det[M_+(s)P_+(s)] = \rho_0 \rho_1 \dots \rho_N f^{N+1}(s) \det[M_+]$  is a minor of order  $N + 1$ . Its denominator,  $D^{N+1}$ , is the least common denominator of all the minors. Let  $P_+(s) = P_+ f(s)$ , where  $P_+$  with no argument is the diagonal matrix of the  $\rho_0, \dots, \rho_N$ . Then the system is stable if and only if the following polynomial has no right half plane zeros [16, p.376],

$$\begin{aligned}
 & D^{N+1}(s) \cdot \det[I - M_+ P_+ f(s)] \\
 &= D^{N+1}(s) \cdot f^{N+1}(s) \cdot \det[I \cdot f^{-1}(s) - M_+ P_+] \\
 &= N^{N+1}(s) \cdot \det[I \cdot f^{-1}(s) - M_+ P_+] \\
 &= N^{N+1}(s) \Lambda[f^{-1}(s)] \\
 &= N^{N+1}(s) \Lambda[D(s)/N(s)] \tag{E1}
 \end{aligned}$$

where  $\Lambda(\cdot)$  is the characteristic or eigenvalue equation of  $M_+ P_+$ .

Note this is a polynomial because  $\Lambda(\cdot)$  is a polynomial of order  $N + 1$  and all the  $N(s)$ 's in the denominator of  $f^{-1}(s)$  will be cancelled by the factor  $N^{N+1}(s)$  out front.

Let us first see what happens to the polynomial (E1) at a zero of  $N(s)$ . Because of the preceding factor of  $N^{N+1}(s)$  all but the highest

From the expression for  $P_+$  and Identities A.6 and A.7 of Appendix A, it is seen that

$$(I + P_+) = 2Z_T(Z_T + z_O I)^{-1} \quad (D.4)$$

$$(I - P_+) = 2z_O(Z_T + z_O I)^{-1} \quad (D.5)$$

Substituting Equations (D.4) and (D.5) into Equation (D.3) obtains

$$\begin{aligned} S_T + P_+ &= (Z_T + z_O I) 2Z_T(Z_T + z_O I)^{-1} 2z_O(Z_T + z_O I)^{-1} M_+ \\ &\quad \cdot (I - P_+ M_+)^{-1} (Z_T + z_O I)^{-1} \end{aligned} \quad (D.6)$$

Since  $2z_O$  is a scalar its placement is arbitrary. Also since  $(Z_T + z_O I)$  and  $2Z_T$  are both diagonal, they commute. Therefore, let us rewrite Equation (D.6) as below.

$$\begin{aligned} S_T + P_+ &= 2Z_T(Z_T + z_O I) (Z_T + z_O I)^{-1} (Z_T + z_O I)^{-1} M_+ \\ &\quad \cdot (I - P_+ M_+)^{-1} 2z_O(Z_T + z_O I)^{-1} \\ &= 2Z_T(Z_T + z_O I)^{-1} M_+ (I - P_+ M_+)^{-1} 2z_O(Z_T + z_O I)^{-1} \\ &= (I + P_+) M_+ (I - P_+ M_+)^{-1} (I - P) \end{aligned} \quad (D.7)$$

It only remains to be shown that

$$M_+ (I - P_+ M_+)^{-1} = (I - M_+ P_+)^{-1} M_+$$

and the equivalence of Equations (3.16) and (3.21) will have been proved.

$$\begin{aligned} M_+ (I - P_+ M_+)^{-1} &= \left[ (I - M_+ P_+)^{-1} (I - M_+ P_+) \right] M_+ (I - P_+ M_+)^{-1} \left[ (I - P_+ M_+) (I - P_+ M_+)^{-1} \right] \\ &= (I - M_+ P_+)^{-1} \left[ (I - M_+ P_+) M_+ \right] (I - P_+ M_+)^{-1} \\ &= (I - M_+ P_+)^{-1} (M_+ - M_+ P_+ M_+) (I - P_+ M_+)^{-1} \\ &= (I - M_+ P_+)^{-1} \left[ M_+ (I - P_+ M_+) \right] (I - P_+ M_+)^{-1} \\ &= (I - M_+ P_+)^{-1} M_+ \end{aligned}$$

# APPENDIX D

## EQUIVALENCE OF EQUATIONS (3.16) AND (3.21)

This appendix will show that the two forms for  $S_T$  derived in Section 3.3 are equivalent. These expressions are repeated below.

$$S_T = (Z_T + z_O I) (\hat{S}_A - P_+) (I - P_+ \hat{S}_A)^{-1} (Z_T + z_O I)^{-1} \quad (3.16)$$

and

$$= (I + P_+) (I - M_+ P_+)^{-1} M_+ (I - P_+) - P_+ \quad (3.21)$$

Note that it was shown in the text that  $M_+ = \hat{S}_A$  and by an arbitrary choice we shall use the former expression. It will be convenient to add  $P_+$  to both equations and show the equivalence of the resulting two forms for  $S_T + P_+$ .

$$S_T + P_+ = (Z_T + z_O I) (M_+ - P_+) (I - P_+ M_+)^{-1} (Z_T + z_O I)^{-1} + P_+ \quad (D.1)$$

However, we know from the text that  $P_+ = (Z_T - z_O I) (Z_T + z_O I)^{-1}$ . But since all the matrices in this expression are diagonal, we can also write

$$P_+ = (Z_T + z_O I) P_+ (Z_T + z_O I)^{-1} \quad (D.2)$$

Substituting Equation (D.2) for the last term of (D.1) yields

$$\begin{aligned} S_T + P_+ &= (Z_T + z_O I) (M_+ - P_+) (I - P_+ M_+)^{-1} (Z_T + z_O I)^{-1} \\ &\quad + (Z_T + z_O I) P_+ (Z_T + z_O I)^{-1} \\ &= (Z_T + z_O I) \left[ (M_+ - P_+) (I - P_+ M_+)^{-1} + P_+ \right] (Z_T + z_O I)^{-1} \\ &= (Z_T + z_O I) \left[ (M_+ - P_+) + P_+ (I - P_+ M_+) \right] (I - P_+ M_+)^{-1} (Z_T + z_O I)^{-1} \\ &= (Z_T + z_O I) (I - P_+^2) M_+ (I - P_+ M_+)^{-1} (Z_T + z_O I)^{-1} \\ &= (Z_T + z_O I) (I + P_+) (I - P_+) M_+ (I - P_+ M_+)^{-1} (Z_T + z_O I)^{-1} \quad (D.3) \end{aligned}$$

Now let us determine  $\underline{v}_{(+)}(0+)$  in terms of the source voltages  $\underline{v}_g$ . From Equation (C18) we see that  $\underline{v}_{(+)}(0-) = \frac{1}{2} \underline{v}_g$ .  $\underline{v}_{(+)}(0-)$  is now the traveling voltage wave from the source incident on the termination transmission line interface.  $\underline{v}_{(+)}(0+)$  is composed of the component transmitted through the interface by  $\underline{v}_{(+)}(0-)$ , which is  $(I - P_+) \underline{v}_{(+)}(0-)$ , and by itself first reflected off the antennas and then off the terminations,  $P_+ M_+ \underline{v}_{(+)}(0+)$ . As an equation this becomes

$$\underline{v}_{(+)}(0+) = (I - P_+) \underline{v}_{(+)}(0-) + P_+ M_+ \underline{v}_{(+)}(0+) \quad (C30)$$

Solving Equation (C30) for  $\underline{v}_{(+)}(0+)$  we obtain

$$\begin{aligned} \underline{v}_{(+)}(0+) &= (I - P_+ M_+)^{-1} (I - P_+) \underline{v}_{(+)}(0-) \\ &= \frac{1}{2} (I - P_+ M_+)^{-1} (I - P_+) \underline{v}_g \end{aligned}$$

Finally we may substitute this into Equation (C29).

$$\underline{i}(\underline{\ell}) = \frac{1}{2} Z_0^{-1} (D - D^{-1} M_+) (I - P_+ M_+)^{-1} (I - P_+) \underline{v}_g \quad (C31)$$

If all the transmission lines have the same impedance, then  $Z_0^{-1} = (1/z_0) I$  and  $(I - P_+ M_+) = Q_+^T$ . If the lines are short compared to a wavelength, then  $D = I$ . Under these assumptions the port currents become

$$\underline{i}(\underline{\ell}) = \frac{1}{2z_0} (I - M_+) (Q_+^{-1})^T (I - P_+) \underline{v}_g. \quad (C32)$$



Therefore,  $M_+$  is symmetric if  $S(\underline{l}-)$  is symmetric. From Equation (C8)

$$S(\underline{l}-) = [Z_A - Z_O] [Z_A + Z_O]^{-1}.$$

From Identity A.5 of Appendix A, we see that  $S(\underline{l}-)$  is symmetric if  $Z_A^T Z_O$  is. But  $Z_A$  is symmetric, and if  $z_{on} = z_o$  for all  $n$ , then

$$Z_A^T Z_O = Z_O Z_A$$

which is symmetric. Therefore, if all the  $z_{on}$  are equal, then  $M_+$  is symmetric.

Finally, an expression for the antenna port currents,  $\underline{i}(\underline{l})$ , will be derived in terms of transmission line parameters. By definition and from Rule 1, we obtain an initial expression for  $\underline{i}(\underline{l})$ .

$$\begin{aligned} \underline{i}(\underline{l}) &= \underline{i}_{(+)}(\underline{l}-) + \underline{i}_{(-)}(\underline{l}-) \\ &= Z_O^{-1} \underline{v}_{(+)}(\underline{l}-) - Z_O^{-1} \underline{v}_{(-)}(\underline{l}-) \end{aligned} \quad (C27)$$

For simplicity of notation let the delay matrix  $D(\underline{l})$  be denoted as  $D$ . Noticing that

$$\underline{v}_{(+)}(\underline{l}-) = D \underline{v}_{(+)}(0+)$$

and

$$\underline{v}_{(-)}(\underline{l}-) = D^{-1} \underline{v}_{(-)}(0+)$$

Equation (C27) can be rewritten as below.

$$\underline{i}(\underline{l}) = Z_O^{-1} D \underline{v}_{(+)}(0+) - D^{-1} \underline{v}_{(-)}(0+) \quad (C28)$$

But we also know that  $\underline{v}_{(-)}(0+) = M_+ \underline{v}_{(+)}(0+)$  from the definition of  $S(0+)$  and Equation (C16). This can be substituted into Equation (C28) to obtain

$$\underline{i}(\underline{l}) = Z_O^{-1} (D - D^{-1} M_+) \underline{v}_{(+)}(0+). \quad (C29)$$

Using Identity A.3 of Appendix A, we can put Equation (C23) into a form that will turn out to be more convenient. (It was the use of this identity that required the normalization procedure.

$$S(\underline{\ell}-) = Z_0^{\frac{1}{2}} (Z_A' + I)^{-1} (Z_A' - I) Z_0^{\frac{1}{2}} \quad (C24)$$

However, as  $|\underline{\ell}|$  approaches,  $D(\underline{\ell})$  approaches  $I$ . Therefore, from Equation (C11)

$$\begin{aligned} \lim_{|\underline{\ell}| \rightarrow 0} S(0+) &= S(\underline{\ell}-) \\ &= Z_0^{\frac{1}{2}} (Z_A' + I)^{-1} (Z_A' - I) Z_0^{-\frac{1}{2}} \end{aligned} \quad (C25)$$

We can now show the limit as  $|\underline{\ell}|$  approaches 0 of  $Z(0)$  is  $Z_A$ . From Equation (C12) and noting that  $Z(0) = Z(0+)$ , we obtain

$$\begin{aligned} \lim_{|\underline{\ell}| \rightarrow 0} Z(0) &= \lim_{|\underline{\ell}| \rightarrow 0} [I - S(0+)]^{-1} [I + S(0+)] Z_0 \\ &= [I - Z_0^{\frac{1}{2}} (Z_A' + I)^{-1} (Z_A' - I) Z_0^{-\frac{1}{2}}]^{-1} [I + Z_0^{\frac{1}{2}} (Z_A' + I)^{-1} (Z_A' - I) Z_0^{\frac{1}{2}}] Z_0 \\ &= Z_0^{\frac{1}{2}} [I - (Z_A' + I)^{-1} (Z_A' - I)]^{-1} Z_0^{-\frac{1}{2}} Z_0^{\frac{1}{2}} [I + (Z_A' + I)^{-1} (Z_A' - I)] Z_0^{-\frac{1}{2}} Z_0 \\ &= Z_0^{\frac{1}{2}} [Z_A' + I - Z_A' + I]^{-1} (Z_A' + I) (Z_A' + I)^{-1} [Z_A' + I + Z_A' - I] Z_0^{\frac{1}{2}} \\ &= Z_0^{\frac{1}{2}} (2I)^{-1} (2Z_A') Z_0^{\frac{1}{2}} \\ &= Z_A \end{aligned} \quad (C26)$$

Now it will be shown that if all the transmission lines are of the same characteristic impedance, then  $M_+ = \hat{S}_A = S(0+)$  is symmetric, i.e.,  $M_+^T = M_+$ .

$$\begin{aligned} M_+ &= S(0+) = D(\underline{\ell}) S(\underline{\ell}-) D(\underline{\ell}) \\ &= D^T(\underline{\ell}) S(\underline{\ell}-) D(\underline{\ell}) \end{aligned}$$

because  $D(x)$  is diagonal and hence symmetric.

$$\frac{\partial f}{\partial z_i} = \frac{\partial u}{\partial x_i} + j \frac{\partial v}{\partial x_i} = \frac{\partial v}{\partial y_i} - j \frac{\partial u}{\partial y_i} \quad (G4)$$

If  $f$  is analytic for all the variables  $z_1, \dots, z_N$ , then one can define a complex gradient

$$\nabla f = \begin{pmatrix} \frac{\partial f}{\partial z_1} \\ \vdots \\ \frac{\partial f}{\partial z_n} \end{pmatrix} \quad (G5)$$

Consider a function  $g(z) = r(x,y) + jq(x,y)$ , which is not analytic, but whose real partials  $\partial r/\partial x$ ,  $\partial q/\partial x$ ,  $\partial r/\partial y$  and  $\partial q/\partial y$  exist throughout the region of interest. Such a function is defined to be psuedo-analytic. For such a function it is useful to define the psuedo-derivative  $\hat{g}'(z)$  as in (G6).

$$\hat{g}' = \frac{\partial g}{\partial z} = \frac{\partial g}{\partial x} + j \frac{\partial g}{\partial y} = \frac{\partial r}{\partial x} + j \frac{\partial q}{\partial x} + j \frac{\partial r}{\partial y} - \frac{\partial q}{\partial y} \quad (G6)$$

Note from (G3) we see that the psuedo-derivative of an analytic function is zero. The computation of the psuedo-derivative can be a test for analyticity.

Psuedo-analyticity can be extended to multivariate functions as analyticity was. Consider a complex scalar function of  $N$  complex variables  $g(z_1, \dots, z_N) = r(z_1, \dots, z_N) + jq(z_1, \dots, z_N)$ . If the partial derivatives  $\partial r/\partial x_i$ ,  $\partial r/\partial y_i$ ,  $\partial q/\partial x_i$  and  $\partial q/\partial y_i$  exist for all possible values of the other variables, then  $g$  is said to be psuedo-analytic in  $z_i$  and one can define the psuedo-partial derivative as in (G7).

$$\hat{\frac{\partial g}{\partial z_i}} = \frac{\partial g}{\partial x_i} + j \frac{\partial g}{\partial y_i} = \frac{\partial r}{\partial x_i} + j \frac{\partial q}{\partial x_i} - \frac{\partial q}{\partial y_i} + \frac{\partial r}{\partial y_i} \quad (G7)$$

Similarly, if  $g$  is psuedo-analytic for all the variables  $z_1, \dots, z_N$ , then one can define the psuedo-gradient as in (G8).

$$\hat{\nabla}g = \begin{pmatrix} \frac{\partial g}{\partial z_1} \\ \vdots \\ \frac{\partial g}{\partial z_N} \end{pmatrix} = \begin{pmatrix} \frac{\partial g}{\partial x_1} \\ \vdots \\ \frac{\partial g}{\partial x_N} \end{pmatrix} + j \begin{pmatrix} \frac{\partial g}{\partial y_1} \\ \vdots \\ \frac{\partial g}{\partial y_N} \end{pmatrix} \quad (G8)$$

Again, note for an analytic function  $f$ ,  $\hat{\nabla}f = 0$ .

To ease the cumbersome notation, let us define the operators  $\nabla_x(\cdot)$  and  $\nabla_y(\cdot)$ .

$$\nabla_x(\cdot) = \begin{pmatrix} \frac{\partial(\cdot)}{\partial x_1} \\ \vdots \\ \frac{\partial(\cdot)}{\partial x_N} \end{pmatrix} \quad \text{and} \quad \nabla_y(\cdot) = \begin{pmatrix} \frac{\partial(\cdot)}{\partial y_1} \\ \vdots \\ \frac{\partial(\cdot)}{\partial y_N} \end{pmatrix} \quad (G9)$$

With these operators Equation (G8) can be rewritten.

$$\begin{aligned} \hat{\nabla}g &= \nabla_x g + j \nabla_y g \\ &= \nabla_x r + j \nabla_x q - \nabla_y q + j \nabla_y r \end{aligned} \quad (G10)$$

Note  $\nabla_x(g^*) = \nabla_x r - j \nabla_x q = (\nabla_x g)^*$  where  $(\cdot)^*$  denotes conjugation. Similarly,  $\nabla_y(g^*) = (\nabla_y g)^*$ . From Equation (G3), we see the gradient for an analytic function  $f$  is easily written as in (G11).

$$\nabla f = \nabla_x f = -j \nabla_y f \quad (G11)$$

Finally, we define the operator  $\hat{\nabla}^*$ , the conjugate psuedo-gradient, in (G12).

$$\hat{\nabla}^* g = \nabla_x g - j \nabla_y g \quad (G12)$$

Note for an analytic function  $f$ , the conjugate psuedo-gradient is not zero but twice the analytic gradient.

$$\hat{\nabla}^* f = \nabla_x f - j \nabla_y f = 2 \nabla f \quad (G13)$$

We will prove three theorems useful when working with psuedo-gradients.

Theorem 1: The conjugate of the psuedo-gradient is the conjugate psuedo-gradient of the conjugate, i.e.,

$$(\hat{\nabla}g)^* = \hat{\nabla}^*g^* \quad . \quad (G14)$$

$$\begin{aligned} \text{proof: } (\hat{\nabla}g)^* &= (\nabla_x g + j\nabla_y g)^* \\ &= (\nabla_x r + j\nabla_x q - \nabla_y q + j\nabla_y r)^* \\ &= \nabla_x r - j\nabla_x q - \nabla_y q - j\nabla_y r \\ &= \nabla_x g^* - j\nabla_y g^* \\ &= \hat{\nabla}^*g^* \end{aligned}$$

Theorem 2: For two psuedo-analytic functions of N variables,  $g_1$  and  $g_2$ , the product rule of derivatives holds, i.e.,

$$\hat{\nabla}(g_1 g_2) = g_1 \hat{\nabla}g_2 + g_2 \hat{\nabla}g_1 \quad . \quad (G15)$$

$$\begin{aligned} \text{proof: } \hat{\nabla}(g_1 g_2) &= \nabla_x(g_1 g_2) + j\nabla_y(g_1 g_2) \\ &= g_1 \nabla_x g_2 + g_2 \nabla_x g_1 + jg_1 \nabla_y g_2 + jg_2 \nabla_y g_1 \\ &= g_1 \hat{\nabla}g_2 + g_2 \hat{\nabla}g_1 \end{aligned}$$

Theorem 3: For an analytic function  $f$ ,

$$\hat{\nabla}|f|^2 = 2f(\nabla f)^* \quad (G16)$$

proof:  $\hat{\nabla}|f|^2 = \hat{\nabla}(ff^*)$

$$= f\hat{\nabla}f^* + f^*\hat{\nabla}f, \quad \text{from (G15)}$$

$$= f(\hat{\nabla}f^*) + 0, \quad \text{from note after (G8)}$$

$$= f(\hat{\nabla}^* f)^*, \quad \text{from (G14)}$$

$$= f(2\nabla f)^*, \quad \text{from (G13)}$$

$$= 2f(\nabla f)^*$$

## Appendix G.2: Complex Gradient Control

Consider a system (e.g. a parasitic array) that is controlled by  $N$  complex state variables  $z_1, \dots, z_N$  (e.g. the reflectivities). It is desired to minimize some positive definite scalar quantity,  $V(\underline{z})$  (e.g. power received at the main antenna). A function is positive definite if it is nonnegative real for all values of its argument and is zero only for an argument of zero. Note that  $V(\underline{z})$  is not analytic in any of its state variables. If, however,  $V(\underline{z})$  is psuedo-analytic in all of its state variables, one can employ the complex gradient control algorithm defined by (G17).

$$\dot{\underline{z}} = -k \hat{\nabla} V(\underline{z}), \quad \text{where } k > 0, \quad \underline{z} = \begin{pmatrix} z_1 \\ \vdots \\ z_N \end{pmatrix} \quad (G17)$$

and  $\hat{\nabla}$  is the psuedo-gradient defined in the previous section.

In applying this control law one equates real and imaginary components of both sides. Let  $\underline{z} = \underline{x} + jy$  where  $\underline{x}$  and  $\underline{y}$  are real vectors. Then (G17) implies the following two real control laws.

$$\dot{\underline{x}} = -k \operatorname{Re} [\hat{\nabla} V(\underline{z})] \quad (G18)$$

$$\dot{\underline{y}} = -k \operatorname{IM} [\hat{\nabla} V(\underline{z})] \quad (G19)$$

From Equation (G10), we can rewrite (G18) and (G19).

$$\begin{aligned}\dot{\underline{x}} &= -k \operatorname{Re} \left[ \nabla_{\underline{x}} V(\underline{x}, \underline{y}) + j \nabla_{\underline{y}} V(\underline{x}, \underline{y}) \right] \\ &= -k \nabla_{\underline{x}} V(\underline{x}, \underline{y})\end{aligned}\tag{G20}$$

$$\begin{aligned}\dot{\underline{y}} &= -k \operatorname{Im} \left[ \nabla_{\underline{x}} V(\underline{x}, \underline{y}) + j \nabla_{\underline{y}} V(\underline{x}, \underline{y}) \right] \\ &= -k \nabla_{\underline{y}} V(\underline{x}, \underline{y})\end{aligned}\tag{G21}$$

The quantity  $\hat{\nabla} V(\underline{x}, \underline{y})$  separates into real and imaginary components as above because  $\nabla_{\underline{x}} V$  and  $\nabla_{\underline{y}} V$  are purely real since  $V$  is positive definite.

But Equations (G20) and (G21) simply represent the familiar real gradient control law for the  $2N$  real variables  $x_1, \dots, x_N, y_1, \dots, y_N$ . The complex control law of (G17) is just a compact way of writing this for complex variables.

Let us now compute  $dV/dt$  from the real multivariate chain rule.

$$\begin{aligned}\frac{dV}{dt} &= (\nabla_{\underline{x}} V)^T \dot{\underline{x}} + (\nabla_{\underline{y}} V)^T \dot{\underline{y}} \\ &= \operatorname{Re} \left[ (\nabla_{\underline{x}} V + j \nabla_{\underline{y}} V)^{*T} (\dot{\underline{x}} + j \dot{\underline{y}}) \right] \\ &= \operatorname{Re} \left[ (\hat{\nabla} V)^{*T} \dot{\underline{z}} \right] \\ &= \operatorname{Re} \left[ (\hat{\nabla} V)^{*T} (-k \hat{\nabla} V) \right] \\ &= -k |\hat{\nabla} V|^2\end{aligned}\tag{G22}$$

We see that  $dV/dt$  is always nonpositive. Thus the system is stable in a control sense. This property of  $dV/dt$  is negative semi-definiteness. If  $dV/dt$  or equivalently  $|\hat{\nabla} V|^2$  is zero only when  $\underline{z} = 0$ , then  $dV/dt$  would be negative definite and the system would be asymptotically stable in a control sense. This means there are no nonzero local minimum of  $V$  for the control law to get trapped in and it will always drive  $V$  to zero.

A useful special case is when  $V(\underline{z}) = |f(\underline{z})|^2$  where  $f(\underline{z})$  is an analytic function over all the state variables. We can then apply Theorem 3 of the previous section to Equation (G17).

$$\dot{\underline{z}} = -2k f(\underline{z})^* \tag{G23}$$

This is the form of the complex gradient law we shall find most useful in our analysis.

Lastly, consider the example of a conventional adaptive array, as in Figure 1 of the text. The array output is given by (G24).

$$\epsilon = y_0 + \underline{y}^T \underline{w} \quad (G24)$$

where  $y_0$  is the signal at the main antenna,  $\underline{y}$  is the vector of signals at the auxiliary antennas and  $\underline{w}$  is the vector of the adaptive weights. It is desired to minimize  $|\epsilon|^2$ . We can apply (G23).

$$\begin{aligned} \underline{w} &= -2k \epsilon (\nabla \epsilon)^* \\ &= -2k \epsilon \underline{y}^* \quad \text{from Identity A.17} \end{aligned} \quad (G25)$$

This is the well known least mean square (LMS) algorithm.

#### Appendix G.3: Gradient Control of Active Complex Parasitic Terminations

Let us apply this theory to the adaptive control of parasitic elements. Consider Equation (G17). Our positive definite function is  $|y_0|^2$ , the power incident on the termination of the main antenna. To apply (G17) we need state control variables which are zero when  $|y_0|^2$  is. Let these variables be  $z_n = \rho_n - \rho_{n0}$ , where  $\rho_n$  is the nth reflectivity and  $\rho_{n0}$  is the value of this reflectivity necessary for a null. From Chapter 2, we know  $|y_0|^2$  as a function of the reflectivities  $\rho_n$ . Let us signify this by  $|y_0(\underline{\rho})|^2 = |y_0(\underline{z} + \underline{\rho}_0)|^2$  where  $\underline{\rho}$ ,  $\underline{z}$ , and  $\underline{\rho}_0$  are respectively vectors of the  $\rho_n$ ,  $z_n$ , and  $\rho_{n0}$ . Lastly, let  $\hat{\nabla}_{\rho}(\ )$  represent the gradient with respect to the  $\rho_n$  and  $\nabla_z(\ )$  and  $\hat{\nabla}_z(\ )$  be the gradient and psuedo-gradient with respect to the  $z_n$ . Equation (G17) now becomes (G26).

$$\begin{aligned} \dot{\underline{z}} &= \dot{\underline{\rho}} = -k \hat{\nabla}_z |y_0(\underline{z} + \underline{\rho}_0)|^2 \\ &= -2k y_0(\underline{z} + \underline{\rho}_0) \left[ \nabla_z y_0(\underline{z} + \underline{\rho}_0) \right]^* \end{aligned} \quad (G26)$$

Note with the notation of Appendix A,

$$\nabla_z y_0(\underline{z} + \underline{\rho}_0) = \partial y_0 / \partial \underline{z} = (\partial y_0 / \partial \underline{z}^T)^T$$



We can apply the chain rule of A.20 and obtain (G27).

$$\begin{aligned}\nabla_{\underline{z}} y_0(\underline{z} + \underline{\rho}_0) &= (\partial y_0 / \partial \underline{z}^T)^T \\ &= \left[ (\partial y_0 / \partial \underline{\rho}^T) (\partial \underline{\rho} / \partial \underline{z}^T) \right]^T\end{aligned}\quad (G27)$$

But  $\partial \underline{\rho} / \partial \underline{z}^T$  is the identity matrix. Equation (G27) then becomes

$$\begin{aligned}\nabla_{\underline{z}} y_0(\underline{z} + \underline{\rho}_0) &= (\partial y_0 / \partial \underline{\rho}^T)^T \\ &= \partial y_0 / \partial \underline{\rho} \\ &= \nabla_{\underline{\rho}} y_0(\underline{\rho})\end{aligned}\quad (G28)$$

This has simply been an application of the chain rule to the set of translated variables  $\underline{z}_n = \underline{\rho}_n - \underline{\rho}_{n0}$ . The result allows us to state the control law in terms of the reflectivities without the need to know the values necessary for nulls.

$$\dot{\underline{\rho}} = -2k y_0(\underline{\rho}) \left[ \nabla_{\underline{\rho}} y_0(\underline{\rho}) \right]^* \quad (G29)$$

The vector  $\underline{\rho}$  is not used in computation, but the reflectivities are arranged into the diagonal matrix  $P$ . To use Equation (G29) we must separate it into  $N$  equations of the form.

$$\dot{\rho}_n = -2k y_0 \left( \frac{\partial y_0}{\partial \rho_n} \right)^*, \quad n = 1, \dots, N \quad (G30)$$

We must now compute  $\partial y_0 / \partial \rho_n$ . The relationship of  $y_0$  and  $\rho_n$  is expressed by Equation (2.3).

$$\begin{aligned}y_0 &= y_{s0} + \rho_0 \underline{m}_{00} y_0 + \underline{m}_0^T P \underline{y} \\ \underline{y} &= \underline{y}_s + \rho_0 \underline{m}_0 y_0 + M P \underline{y}\end{aligned}\quad (2.3)$$

Let us differentiate both sides of these equations using differentiation formulae A.16 and A.17.

$$\frac{\partial y_0}{\partial \rho_n} = \rho_0 m_{00} \frac{\partial y_0}{\partial \rho_n} + m_0^T \left( E_{nn} y + P \frac{\partial y}{\partial \rho_n} \right) \quad (G31a)$$

$$\frac{\partial y}{\partial \rho_n} = \rho_0 m_0 \frac{\partial y_0}{\partial \rho_n} + M \left( E_{nn} y + P \frac{\partial y}{\partial \rho_n} \right) \quad (G31b)$$

$$\text{where } E_{nm} = \begin{bmatrix} \delta_{i-n, j-m} \end{bmatrix}$$

Solve (G31b) for  $\frac{\partial y}{\partial \rho_n}$  and substitute into (G31a).

$$\begin{aligned} \frac{\partial y_0}{\partial \rho_n} &= \rho_0 m_{00} \frac{\partial y_0}{\partial \rho_n} + m_0^T \left[ E_{nn} y + P Q^{-1} \left( \rho_0 m_0 \frac{\partial y_0}{\partial \rho_n} + M E_{nn} y \right) \right] \\ &= \rho_0 \left( m_{00} + m_0^T P Q^{-1} m_0 \right) \frac{\partial y_0}{\partial \rho_n} + m_0^T \left( I + P Q^{-1} M \right) E_{nn} y \end{aligned} \quad (G32)$$

$$\text{where } Q = I - MP$$

Note the existence of  $Q^{-1}$  is necessary for RF stability. Using matrix identity A.8 with  $B = I$ ,  $V = M$ ,  $U = P$ , and realizing  $MP = (PM)^T$ , one can show  $(I + P Q^{-1} M) = (Q^{-1})^T$ . Lastly, define  $e_n$  = vector of all zeros except the  $n$ th element which is 1. Then  $E_{nn} = \frac{e_n e_n^T}{n-n}$ , and  $E_{nn} y = \frac{e_n y_n}{n-n}$ . We can now solve (G32) for  $\partial y_0 / \partial \rho_n$ .

$$\begin{aligned} \frac{\partial y_0}{\partial \rho_n} &= \frac{m_0^T (Q^{-1})^T e_n}{1 - \rho_0 \left( m_{00} + m_0^T P Q^{-1} m_0 \right)} y_n \\ &= \frac{e_n^T Q^{-1} m_0}{1 - \rho_0 \left( m_{00} + m_0^T P Q^{-1} m_0 \right)} y_n \\ &= \alpha_n y_n, \text{ where this defines } \alpha_n. \end{aligned} \quad (G33)$$

Equation (G33) can be substituted into the control law of (G30).

$$\rho_n = -2k y_0 (\alpha_n y_n)^* \quad (G34)$$

Compare this expression to the LMS control law for a conventional adaptive array in (G25). They are the same except for the factor  $\alpha_n^*$ , where  $\rho_n$  corresponds to  $w_n$ ,  $y_0$  to  $\epsilon$  and  $y_n$  to the signal at the  $n$ th antenna. The physical significance of  $\alpha_n$  is discussed in the test.

## APPENDIX H

### DERIVATION OF GRADIENT CONTROL WITH PILOT

From Appendix G, Equations (G30) and (G31) state the gradient control law for an adaptive parasitic array.

$$\dot{\rho}_n = -2ky_0(\alpha_n y_n)^* \quad , \quad \text{for } k > 0 \quad (G31)$$

$$\text{where } \alpha_n = \frac{\underline{e}_n^T \underline{Q}^{-1} \underline{m}_0}{1 - \rho_0 (\underline{m}_{00} + \underline{m}_0^T \underline{PQ}^{-1} \underline{m}_0)} \quad \text{and } \underline{e}_n = \begin{pmatrix} 0 \\ \vdots \\ 0 \\ 1 \\ 0 \\ \vdots \\ 0 \end{pmatrix} \text{ nth element} \quad (G30)$$

In implementing gradient control it will be necessary to estimate the factor  $\alpha_n$ . It will be shown in this appendix that a pilot signal sent up the main antenna will be received at the nth auxiliary antenna multiplied by the factor  $\alpha_n$ , under the condition  $\rho_0 = 0$ .

From the expression for  $\alpha_n$  above, we see that  $\alpha_n = \underline{e}_n^T \underline{Q}^{-1} \underline{m}_0$ . Now consider a pilot signal,  $y_{p0}$ , injected upward at the main antenna (see Figure H1). This upward voltage traveling wave couples to the N auxiliaries with the coupling factors of  $\underline{m}_0$ . This creates an initial downward vector of traveling waves of  $\underline{m}_0 y_{p0}$ . From Equation (2.5b) the final vector of downward traveling voltages,  $y_p$ , is found to be  $\underline{Q}^{-1} \underline{m}_0 y_{p0}$ , when  $\rho_0 = 0$ . The voltage traveling downward at the nth antenna,  $y_{pn}$ , is  $\underline{e}_n^T \underline{Q}^{-1} \underline{m}_0 y_{p0}$ .

$$\frac{y_{pn}}{y_{p0}} = \underline{e}_n^T \underline{Q}^{-1} \underline{m}_0 = \alpha_n \quad (H1)$$

$$\text{given } \rho_0 = 0$$

It can be shown for the case  $\rho_0 \neq 0$ , through Equations (2.3 a and b), that the ratio  $y_{pn}/y_{p0}$  is in general given by (H2).

$$\frac{y_{pn}}{y_{p0}} = \left[ \frac{1}{1 - \underline{m}_{00} \rho_0} \right] \underline{e}_n^T \left[ \underline{Q} + \left( \frac{\rho_0}{1 - \underline{m}_{00} \rho_0} \right) \underline{m}_0 \underline{m}_0^T \underline{P} \right]^{-1} \underline{m}_0 \quad (H2)$$

This does not equal  $\alpha_n$ . Thus the constraint  $\rho_0 = 0$  is clearly needed.

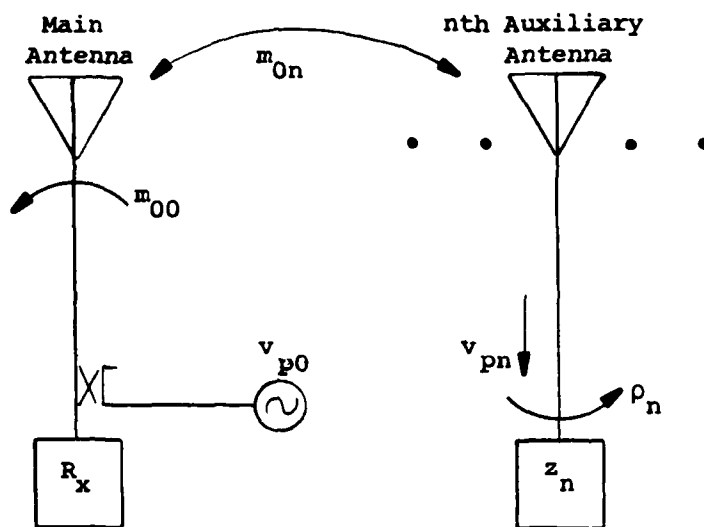


Figure H1 Pilot Signal Injection

**END**

**FILMED**

**5-85**

**DTIC**